THESE de DOCTORAT de L'UNIVERSITE PARIS 6
Spécialité:
Chimie Physique et Chimie Analytique
présentée

par M. Ingo Köper
pour obtenir le grade de DOCTEUR de l'UNIVERSITE PARIS 6
Sujet de la thèse:

Influence du tréhalose sur la dynamique de la C-phycocyanine; une étude par diffusion quasiélastique de neutrons

soutenue le 01.07.2002

devant le jury composé de:

Mme M.-C. Bellissent-Funel
M. G. Kneller (Rapporteur)
M. R. Lechner (Rapporteur)
M. W. Petry
M. P. Turq
Mme J. Yaniv-Rouviere

Biologie wird im 21. Jahrhundert
den heutigen Rang von
Chemie und Physik einnehmen.
*John Naisbitt(*1930)*

A good scientific theory
should be explicable to a barmaid.
Ernest Rutherford (1871-1937)

Ce travail a été effectué dans le groupe "Biologie" du Laboratoire Léon Brillouin et dans le groupe "E13" du département de physique de la Technische Universität München. Je remercie Charles Henri de Novion, José Teixeira ainsi que Pierre Monseau et Michel Alba de m'avoir acceuilli et LLB.

J'exprime ma profonde et sincère reconnaissance à Marie-Claire Bellissent-Funel et Winfried Petry qui ont dirigé cette thèse. Je les remercie de m'avoir guidé avec leur esprit enthousiaste.

Pierre Turq m'a fait l'honneur de présider le jury de cette thèse. Je suis heureux de lui témoigner ici ma gratitude. Je remercie tout particulièrement Ruep Lechner et Gerald Kneller d'avoir accepté d'être les rapporteurs de cette thèse. J'associe à ces remerciements Josette Yaniv-Rouviere qui a également accepté d'être membre de jury de cette thèse.

Je suis particulièrement reconnaissant à Stéphane Longeville, avec qui j'ai partagé la charge du spectromètre MUSES et qui m'a beaucoup appris sur la technique de diffusion de neutrons et la technique à écho de spin en particulier.

Je remercie également Nadine Leygues du L.A.D.I.R. (Thiais), qui a mené avec grand interêt le projet de la deutération du tréhalose. Ce fut un grand plaisir de travailler avec elle.

Mes remerciements vont aussi a Andrew Gall, avec qui j'ai pu decouvrir lors d'intéressants discussions les mystères de la biologie et de la biochimie. Je tiens à remercier Xavier Agostini pour toute son aide lors des plusieures réparations de cryogénie.

Je remercie également Claude Pfister, qui m'a chaleureusement acceuilli à Grenoble lors de mes expériences. Mes remerciements vont aussi à Roland Gähler et à Markus Bleuel, qui m'ont fait participer à leur enthousiasme envers la technique d'écho de spin par résonance.

Je souhaite remercier chaleureusement Camille Loupiac et Giulia Fadda pour tous ce bons moments que nous avons passé ensemble. Elles vont me manquer. Je remercie également Jean-Marc Zanotti et Serge Dellerue pour leur précieux conseils et leur amitié. Que Noémie, Cécile, Raphaël et Julian Oberdisse, soient assuré de mon amitié sincère.

Enfin, je tiens à remercier tout l'ensemble du personnel du troisième étage, surtout Abdeslam, Bouchra, Bruno, Caroline, Daniéla, Didier, Fabrice, Francesco, Géraldine, Guillaume, Lazlo, Marie-Sousai, Olga, Sandra et Stéphanie.

... danke ...

Contents

Abstract

Trehalose is a well known disaccharide that shows in nature interesting bioprotecting properties. It is produced by organisms such as certain plants, spores or fungi that are able to survive hostile external conditions such as high or low temperatures. They can pass through these periods in a state of *anhydrobiosis*, a phase of suspended animation, without suffering damage. Trehalose shows also a high efficiency in preserving biomaterial in *in vitro* experiments; trehalose is more efficient than other bioprotecting materials. Despite several investigations in this field, the protective mechanism at an atomic or molecular scale remains still unclear. There exist two models to describe the interaction between the sugar molecules and the biomaterial. One predicts direct interactions between trehalose and the biomolecules while the other one suggests a slowing-down mechanism via viscosity effects. The trehalose would from a glassy state in which the biomolecule gets embedded and thus protected from denaturation.
We studied a model system with regard to these models. The C-phycocyanin (CPC) is a globular protein, that is involved in the light harvesting process of cyanobacteria. Recently dynamics of this protein have been studied by neutron scattering techniques. We compare these results with data obtained on trehalose coated protein samples.

In a first step, dynamics of trehalose in aqueous solution were investigated using neutron time-of-flight and neutron spin-echo techniques. The temperature dependence of the diffusive motions have been described. Furthermore we studied dynamics of trehalose in dilute aqueous CPC solution. No evidence for direct interactions between the protein and the sugar could be detected.

Afterwards, we performed neutron scattering experiments to study the influence of trehalose on the dynamics of the CPC protein. Hydrated powder samples were used to study the internal dynamics of the protein. Using different neutron scattering techniques we observed dynamics from 0.1 ps up to some nanoseconds in a Q-range up to 4 Å^{-1}. Fast dynamics were studied by neutron time-of-flight techniques, longer time scales were visible performing neutron spin-echo experiments. Also backscattering techniques were used, especially to investigate rather high values of momentum transfer.
Using different sample compositions with deuterated or protonated compounds we were able to study only selected motions e.g. from the protein by masking contributions from trehalose and hydration water.
The relaxational process in the observed time range could be described by a stretched exponential decay. The obtained relaxation times increase by a factor of 100 when comparing protein dynamics with and without trehalose.
The geometry of motion has been described using a simple model of a particle diffus-

ing inside a sphere. The analysis of time-of-flight and backscattering data revealed no change in the geometry of the protein movements when trehalose is added to the sample.

On the whole the obtained results favour the following image of the interactions between trehalose and the CPC protein:
In the presence of trehalose the dynamics of the protein is hindered due to an increase of the viscosity of the hydration shell. Being placed in a more viscous medium, protein movements are slowed down, the geometry of motion remains nevertheless unchanged. These facts correspond to the model, that proposed a protective mechanism via embedding the biomaterial into a glassy trehalose structure.

Résumé

Le tréhalose est un disaccharide qui est connu pour ses propriétés bioprotectrices. Il existe un certain nombre d'organismes ou de plantes, qui sont capable de survivre dans des conditions hostiles comme des températures très élevées ou très basses. Ces organismes passent alors dans un état qu'on appelle *anhydrobiosis* où ils vivent avec une activité réduite. Une fois réhydratés, ils reprennent leur même cycle de vie. Le tréhalose a également démontré son efficacité comme protecteur des matériaux biologiques dans des expériences *in vitro*. Ce sucre est notamment plus efficace que d'autres produits ayant des propriétés similaires.
Malgré un certain nombre d'études dans ce domaine, le mécanisme de protection à l'échelle atomique ou moléculaire n'est toujours pas clair. Il existe dans la littérature deux modèles pour décrire les interactions entre le tréhalose et les biomolécules. Un modèle propose un mécanisme qui est basé sur des interactions directes entre le sucre et le biomateriau. L'autre modèle suggère que les biomolécules sont protégées contre la dénaturation, parce que le tréhalose forme un état vitreux autour d'elles et empêche de cette manière la dégradation.
Nous avons étudié un système modèle afin de vérifier la validité de ces deux hypothèses. La C-phycocyanine (CPC) est une protéine globulaire qui joue un rôle dans le cycle photosynthétique des cyanobactéries. Récemment, la dynamique de cette protéine a été étudiée par des techniques de diffusion de neutrons. Nous utilisons ces résultats pour les comparer avec des donnés obtenues sur des échantillons contenant de la CPC en présence du tréhalose.

Dans une première étape nous avons étudié la dynamique du tréhalose en utilisant les techniques de temps de vol et de l'écho de spin des neutrons. Nous avons décrit la dépendance en température des mouvements diffusifs du tréhalose dans des solutions aqueuses. L'étude de la dynamique du tréhalose dans une solution diluée

de CPC n'a donné aucune indication quant à l'existence d'interactions directes entre le tréhalose et la protéine.

Dans une deuxième étape, nous avons analysé, grâce à des expériences de diffusion de neutrons, l'influence du tréhalose sur la dynamique de la C-phycocyanine. Nous avons utilisé des échantillons sous forme de poudres hydratées pour pouvoir accéder a la dynamique interne de la protéine. Par différentes techniques, nous avons pu examiner la dynamique dans une gamme de temps entre 0.1 ps et quelques ns et dans une gamme en Q jusqu'à 4 $Å^{-1}$. La dynamique rapide est accessible par des techniques de temps de vol de neutrons, tandis que la dynamique lente est observée à l'aide des techniques par écho de spin des neutrons. Nous avons utilisé aussi des techniques de rétrodiffusion, pour accéder en particulier à de grandes valeurs de Q. Grâce à l'utilisation d'échantillons avec des parties protonées ou deutériées, choisies soigneusement, nous avons eu seulement accès à la dynamique de certaines parties de l'échantillon. Par exemple, nous avons étudié la dynamique de la protéine (protonée), tandis que les contributions du tréhalose et de l'eau d'hydratation, etaient masquées.
Nous avons pu décrire le processus de relaxation à l'aide d'une fonction de type "exponentielle étirée". Le temps de relaxation que nous avons pu attribuer aux mouvements de la protéine augmente de deux ordres de grandeur quand la protéine se trouve en présence du tréhalose.
A l'aide d'un modèle simple, qui décrit la diffusion d'une particule dans une sphère, nous avons décrit la géométrie des mouvement des résidus de la protéine. L'analyse des expériences en temps de vol et en rétrodiffusion a montré que cette géométrie ne change pas sous l'influence du tréhalose.

L'ensemble des résultats obtenus nous conduit à l'image suivante des interactions entre les molécules de tréhalose et de la CPC:
En présence du tréhalose les mouvements de la protéine sont modifiés. La viscosité de la couche d'hydratation augmente. Dans cet environnement plus visqueux, les mouvements de la protéine sont ralentis, mais la géométrie de ces mouvements est conservée. Ce type d'interaction correspond au modèle, qui propose un mécanisme de protection par l'inclusion des biomatériaux dans une forme vitreuse de tréhalose.

Zusammenfassung

Trehalose ist ein weit verbreitetes Disaccharid, das in der Natur eine interessante schützende Funktion hat. Zahlreiche Organismen wie niedere Pflanzen, Sporen oder Pilze, die diesen Zucker produzieren, können extremen äußeren Bedingungen standhalten. Beispielsweise gibt es Pflanzen, die völlig austrocknen können. Einmal wieder rehydriert, können sie ihren normalen Lebenszyklus wieder aufnehmen. Sie

überleben in einem Stadium reduzierter Aktivität, auch *anhydrobiosis* genannt, ohne nennenswerte Beschädigungen aufzuweisen. Auch in *in vitro* Experimenten zeigt Trehalose die Fähigkeit, Biomaterial zu schützen. Gegenüber ähnlichen Materialien ist Trehalose deutlich effizienter.
Trotz zahlreicher Untersuchungen auf diesem Gebiet ist der Schutzmechanismus von Trehalose auf atomarer oder molekularer Ebene weiterhin unklar. In der Literatur wurden zwei Modelle vorgestellt, um die Wechselwirkungen zwischen Trehalose-Molekülen und dem Biomaterial zu beschreiben. Ein Modell sagt direkte Wechselwirkungen zwischen dem Zucker und den Biomolekülen vorher, während das andere Viskositätseffekte zu Grunde legt. Das Biomaterial würde demnach vor Denaturierung geschützt, indem es in einer glasartigen Trehalose Struktur eingebettet wird.
Wir haben ein Modell System im Hinblick auf diese beiden Modelle untersucht. Das C-Phycocyanin (CPC) ist ein globulares Protein, das eine Rolle im photosynthetischen Zyklus der Cyanobakterien spielt. Neuere Arbeiten haben die Dynamik dieses Proteins mit Hilfe von Neutronenstreutechniken untersucht. Wir können die dort gewonnenen Ergebnisse mit unseren Experimenten an Proben vergleichen, die sowohl das CPC Protein als auch Trehalose-Moleküle enthalten.

In einem ersten Schritt haben wir die Dynamik von Trehalose in wässrigen Lösungen untersucht. Wir konnten die Abhängigkeit der diffusen Bewegungen von der Temperatur beschreiben. Eine Untersuchung der Trehalosedynamik in verdünnter CPC-Lösung konnte keine Hinweise auf direkte Zucker-Protein-Wechselwirkungen liefern.

Danach haben wir mit Hilfe von Neutronenstreuexperimenten den Einfluss von Trehalose auf die Dynamik des CPC-Proteins untersucht. Wir haben hydratisierte Puderproben verwendet, um die interne Dynamik des Proteins zu studieren. Mit Hilfe verschiedener Neutronenstreutechniken konnten wir Bewegungen in einem Zeitfenster von 0.1 ps bis zu einigen Nanosekunden untersuchen und in einem Q-Bereich bis zu 4Å^{-1}. Schnelle Dynamik konnte mit Flugzeitmessungen, längere Zeitskalen mit Neutronen Spin-Echo Experimenten beobachtet werden. Vor allem im hohen Q-Bereich führten wir weiterhin Rückstreumessungen durch.
Mit Hilfe unterschiedlicher Probenzusammensetzungen aus protonierten und deuterierten Produkten konnten wir den Kontrast variieren und beispielsweise nur die Proteindynamik untersuchen, während Beiträge zum Streusignal von Trehalose und Wasser-Molekülen maskiert sind.
Die Relaxationsprozesse konnten im untersuchten Zeitfenster mit einer gestreckten Exponentialfunktion beschrieben werden. Die Relaxationszeit ist für eine Probe mit Trehalose um einen Faktor von bis zu 100 höher als für eine Probe ohne Trehalose. Die Geometrie der beobachteten Molekülbewegungen konnte mit einem einfachen Modell eines Teilchens, das innerhalb einer sphärischen Umgebung diffundiert, beschrieben werden. Die Analyse der Flugzeit- und Rückstreudaten zeigte, dass die

Geometrie der Proteinbewegungen durch die Anwesenheit von Trehalose-Molekülen nicht verändert wurde.

Zusammenfassend ergeben die erhaltenen Ergebnisse das folgende Bild der Wechselwirkungen zwischen Trehalose und dem CPC Protein:
In Anwesenheit von Trehalose werden die Proteinbewegungen behindert und verlangsamt. Der Grund hierfür ist eine Zunahme der Viskosität der Hydrathülle des Proteins. In einer viskoseren Umgebung wird die Proteindynamik verlangsamt, die Geometrie der Bewegungen bleibt jedoch erhalten. Dieses Bild entspricht dem in der Literatur beschriebenen Modell eines Schutzmechanismus, bei dem das Biomaterial in ein Trehaloseglas eingebettet wird.

I Introduction

Le tréhalose est un di-saccharide que l'on peut trouver dans certaines plantes et certaines organismes qui sont capable de résister à des environnements hostiles dus à des températures extrêmes ou à des périodes de sécheresse [1, 2]. Parmi les molécules ayant des propriétés protectrices similaires, le tréhalose semble être le plus efficace [3, 4]. Les propriétés protectrices du tréhalose sont connues depuis 50 ans [5]. Cependant le mécanisme de protection à l'échelle moléculaire reste toutefois mal connu.
Il existe déjà une large gamme d'applications du tréhalose, en particulier en pharmacie, en médecine et dans l'industrie agro-allimentaire. Il y a quelques mois, la commission européenne a admis l'utilisation du tréhalose comme ingrédient dans les denrées alimentaires [6][1]. Le sucre peut être utilisé comme un additif qui a un goût moins intense que le sucrose et est de plus moins calorique. Un chewing-gum, par exemple, où l'on remplace le sucrose par le tréhalose ne résiste pas seulement mieux contre l'humidité, mais il est aussi plus blanc et moins agressif pour les dents. Dans les produits de boulangerie et dans les pâtisseries le tréhalose peut modifier le goût sucré et il peut remplacer les matières grasses.
Le tréhalose a des applications en médicine. On a inventé un système qui permet de déterminer rapidement le groupe sanguin d'un patient a été inventé [7]. En lyophilisant des anticorps en présence de tréhalose on préserve leur fonctionalité pendent le stockage. Le tréhalose est également utilisé pour empêcher la dénaturation des molécules dans divers médicaments.
Il existe mème une série de produits cosmétiques où le tréhalose devrait jouer un rôle de prévention contre les rides [2]. Récemment, on a envisagé d'utiliser le tréhalose pour conserver des documents.

Nous ne nous sommes pas seulement intéressés aux effets ou aux mécanismes de protection du tréhalose, à l'échelle macroscopique, mais aussi aux effets à l'echelle microscopique. On a peu d'informations sur les interactions au niveau moléculaire entre des molécules de tréhalose et des biomolécules, par exemple des protéines, des anticorps ou des membranes. Dans la littérature, deux modèles ont été présentés et

[1] http://www.trehalose.co.uk
[2] http://www.trehalose.it

discutés pour décrire ces interactions. Le premier prévoit des interactions directes entre les molécules de sucre et le biomatériau [1] tandis que l'autre modèle décrit la protection par une encapsulation des biomolécules dans une forme vitreuse d'une solution aqueuse de tréhalose [8].

Nous avons étudié un système modèle et interprété les résultats dans le contexte de ces deux modèles. La C-phycocyanine(CPC) est une petite protéine globulaire qui peut être isolée des cyanobactéries, *synechoccoccus lividus*. Elle fait partie du cycle photosynthétique de ces bactéries. Nous avons la chance de posséder une forme complètement deuteriée de cette protéine [9]. Nous avons étudié l'influence du tréhalose sur la dynamique de cette protéine grâce à des expériences de diffusion de neutrons. Nous comparons les données obtenues sur des échantillons contenant la CPC hydratée en présence de tréhalose avec des expériences faites sur la protéine en absence de tréhalose [10, 11].

Dans les systèmes biologiques, les processus ont lieu à diverses échelles de temps, depuis la femtoseconde (vibrations atomiques) jusqu'à la microseconde où ont lieu des processus de repliement des protéines [12]. La synthèse d'une protéine dans une cellule peut même durer quelques secondes. Il existe également une large gamme en échelle spatiale: les liaisons atomiques sont de l'ordre de quelques angstrœm, les dimensions d'une protein sont de quelques nanomètres, celles d'une cellule entière de quelques micromètres.
Il n'existe pas de technique unique pour couvrir expérimentalement toute cette gamme en temps en en espace. En utilisant la technique de diffusion de neutrons qui permet de combiner différents types de spectromètres, nous pouvons accéder à des gammes en temps entre la femtoseconde et la nanoseconde. La longeur d'onde typique des neutrons est de quelques angstrœm. Nous pouvons donc sonder à l'aide de la diffusion de neutrons des domaines dans l'espace entre quelques angstrœms et des micromètres.

On s'intéresse à la dynamique des protéines car ces molécules ont des fonctions essentielles dans les organismes vivants. Elles peuvent remplir une grand varieté de fonctions, qui dépendent souvent de leur structure et de leur conformation tridimensionelle ainsi que des modifications de celle-ci au cours du temps. Des protéines interagissent dans le transport des ions dans des cellules. Elles peuvent aussi être essentielles dans la formation et la conformation des structures biologiques, comme par exemple des membranes. La C-phycocyanine, que nous avons utilisée, joue son rôle de collectrice de lumière dans les cyanobactéries. Au cours des différentes fonctions les interactions entre la proteine et son environnement, la plupart du temps une solution aqueuse, sont d'une grande importance.

Lorsque l'on étudie un système biologique avec des méthodes physiques, on se

heurte à des difficultés techniques et à des problèmes d'analyse des données, mais on se doit de convaincre les physiciens de l'intérêt de son sujet et, d'expliquer aux biologistes l'avantage d'utiliser les méthodes physiques. De plus il faut toujours veiller à ne négliger, ni l'aspect biologique, ni l'aspect physique du sujet posé.
Le tréhalose est un di-saccharide qui présente des propriétés biologiques très intéressantes. Il fait déjà l'objet de nombreuses études. La plupart des expériences utilise plutôt des méthodes biologiques et porte sur les propriétés biologique, par exemple l'influence du tréhalose sur l'activité d'une enzyme. D'autre part, il existe des expériences qui conduisent à déterminer des grandeurs physiques, comme la viscocité ou la température de transition vitreuse du tréhalose. Pendant mon travail de thèse, qui est à l'interface physique - biologie, j'ai essayé de tenir compte des deux aspects évoqués précédemment. Quand j'ai utilisé la technique de diffusion de neutrons, ou plus exactement la diffusion quasiélastique de neutrons, un outil qui est performant pour étudier la dynamique des systèmes biologiques, j'ai toujours essayé de ne pas perdre de vue la nature biologique du problème. J'ai essayé d'analyser les données expérimentales en utilisant des modèles simples.

La difficulté majeure des expériences de diffusion de neutrons est, que dans la plupart des cas, les résultats de ces expériences ne donnent pas des informations directes aux questions posées. Il faut donc utiliser un modèle pour les interpréter. Ce modèle doit dans notre cas tenir compte en même temps des aspects physiques et des aspects biologiques du problème. Il faut tenir compte de ce que l'on peut observer avec la technique utilisée et ce que signifie cette observation pour l'échantillon. Il faut aussir tenir compte de la qualité des données expérimentales et adapter le modèle à cette qualité. Il ne me semble guère utile d'utiliser un modèle très sophistiqué pour interpréter des données ayant une qualité moyenne. J'ai essayé de garder en mémoire ces points lors de l'analyse et de la discussion des résultats obtenus.

Nous avons étudié dans un premier temps la dynamique du tréhalose dans des solution aqueuses. Avec la combinaison des techniques de temps-de vol et à écho de spin nous avons pu observer des mouvements sur une grande gamme de temps. Pour des temps rapides, la diffusion des molécules de tréhalose peut être décrite par un modèle simple de diffusion. Si l'on considère des mouvements plus lents, ce modèle n'est plus valable, les processus de diffusion deviennent plus compliqués.

Dynamique du tréhalose en solution aqueuse[3]

Si l'on veut comprendre les interactions entre le tréhalose et une protéine, il est nécessaire d'étudier dans un premier temps la dynamique du tréhalose en solution aqueuse. Nous avons sondé les mouvements diffusifs du tréhalose dans des solutions concentrées. Nous avons utilisé les techniques de temps-de-vol et à écho de spin de neutrons. La première technique donne accès aux temps rapides jusqu'à quelques ps, la deuxième couvre une gamme temporelle jusqu'à la nanoseconde. Nous avons pu décrire la dynamique à temps courts par une diffusion simple. Les coefficients de diffusion du tréhalose en fonction de la température ont été déterminés. Aux temps les plus longs, les mouvements diffusifs deviennent plus compliqués et nous avons dû introduire une relaxation de type "étirée".
Nous avons pu mettre en évidence que les caractéristiques des mouvements étaient indépendants de la température. Les données obtenues, à différentes températures, ont été décrites par une seule courbe maîtresse.
Nous avons pu mettre en évidence que les temps de relaxation, en fonction de la température suivaient le même comportement que la viscosité de la solution.

[3]soumis à Physical Rewiev Letters

Dynamics in aqueous trehalose solutions

I.Köper, M.-C. Bellissent-Funel, W. Petry

We present a study on the dynamical behavior of trehalose in concentrated aueous solutions. Experiments were performed using neutron tiem-of-flight and neutron spin-echo techniques. Fast dynamics could be described using a simple diffusional model, while dynamical processes at longer times show a more complex behavour and have to been described by a stretched exponential decay. One observes when performing temperature depending experiments a good accord with data from viscosity measurements.

Introduction

Trehalose is a well known disaccharide with bioprotecting properties. It has been isolated from algae, bacteria, fungi, insects, invertebrates and yeasts as well as from lower vascular plants and a few flowering plants [1]. It has been found even in some mammalian systems. One of the most interesting facts of this non-reducing glucosides is that it has been found in large quantities in organisms that are able to survive extreme external stresses such as high or very low temperatures or periods of complete drought [2–6]. Two models have been proposed to describe the protective effect on a molecular lenght scale. The first one, proposed by Green and Angell [7] is based on the very high glass transition temperature of trehalose solutions. Following this model the protected biomolecule is placed in a glassy trehalose structure and thus the formation of ice crystals would be hindered. The structure of the biomaterial would be conserved and life and decay processes would be suspended [8].
The other main hypothesis, the so-called 'water-replacement theory' was proposed by Crowe *et al.* [9]. It tries to find evidence for direct interactions between the protected biomaterial and the trehalose molecules.
We performed a series of neutron scattering experiments in order to describe the behaviour of trehalose in aqueous solution. The system trehalose/water is already quite well investigated. One can find in literature several experimental as well as theoretical work to describe the behaviour of this system, often in comparison with other saccharide/water systems.
Duda and Stevens found by chiroptical measurements, that the linkage geometry of trehalose in solution is relatively inflexible [10], a fact that has been confirmed by molecular dynamics simulations [11, 12].
Kawai *et al.* [13] and Magazu *et al.* [14] showed by NMR and ultrasonic measurements respectively, that trehalose has a very high ability to bind water. The hydration number varies as a function of temperature between 10 and 12 water molecules per trehalose molecule [14]. These authors found also that at high concentrations the two rings of the disaccharide should somehow overfold forming intermolecular hydrogen bridged bonds. A fact that was confirmed by Elias and Elias [15].
Akao *et al.* showed by infrared spectroscopic studies, that a cluster of a trehalose molecule and its bound water molecules behaves like a small water cluster. They called this effect "water-camouflage effect", explaining, that trehalose molecules could play the role of water on a membrane or protein surface. This corresponds to the so called 'water-replacement theory' from Crowe *et al.* [9].
Dynamics of trehalose in water have been studied by NMR-techniques [16–20], photon correlation spectroscopy [21, 22] and neutron spectroscopy [21, 23].

Materials and methods

Dynamics of trehalose molecules in aqueous solutions were investigated using the neutron time-of-flight techniques with the spectrometer MIBEMOL. Neutron spin-echo experiments were performed on the spectrometer MUSES, both of the Laboratoire Léon Brillouin.
Time-of-flight experiments give access to the dynamic structure factor $S(Q, \omega)$. This is correlated to the intermediate scattering function I(Q,t), that is obtained in spin-echo experiments via a Fourier transformation:

$$I(Q,t) = \int S(Q,\omega)\exp(i\omega t)d\omega \qquad (1)$$

We used samples of trehalose in water at rather high concentrations. Time-of-flight measurements were performed on the protonated form of the sugar, only labile protons were exchanged against deuterons. Spin-echo experiments were performed on sampoles containind deuterated trehalose in heavy water. Deuterated trehalose is commercially not available. It can be obtained by catalytic exchange reactions following a procedure of Koch *et al* [24, 25]. Details will be published elsewere.

Time-of-flight experiments

We were able to investigate both the effect of the concentration as well as the temperature dependence of the dynamics of trehalose in aqueous solution.
Measurements were performed at a temperature of 298 K for a solution of 50 w% trehalose in heavy water and at temperatures between 270 K and 311 K for a solution containing 30 w% trehalose in D_2O. In time-of-flight experiments one investigates the incoherent scattering from a sample. We used samples of protonated trehalose in heavy water. The obtained signal is so mainly due to scattering from the non-exchanged protons of the trehalose molecules.
Experiments were performed at 6Å neutron wavelength, corresponding to an energy resolution of 96 μeV (FWHM).
Two types of sample containers were used for the different experiments. A flat aluminium container of 1 mm thickness that was placed in the neutron beam with an angle of about 45 degree with respect to the incident beam. The second type was an aluminium hollow cylinder with a 21 mm outer diameter and a sample layer of about 0.5 mm thickness. Nominal transmissions are 87 % for the 50 w% sample and 89% for the 30 w% sample.
Data were collected for about 8 h, corrected for empty cell contributions and normalised to a standard vanadium scatterer. The obtained signal is mainly due to the incoherent scattering cross sections of the protons of the trehalose molecules. Nevertheless one has to take into account the contribution from the solution, in our case from heavy water.
To subtract this contribution we measured a sample of pure D_2O, using the same sample container as for the trehalose solution. The obtained signal can be described by a single Lorentzian line.
The dynamic structure factor of the trehalose solutions is now analysed using two Lorentzian lines, each of them folded by the measured resolution of the spectrometer and fixing the width of one of them to values obtained from the analysis of the pure water sample. Using this way of analysis we take into account the contributions from the buffer solution. The second Lorentzian line will describe the contributions due to the scattering of the trehalose molecules.

Neutron spin-echo experiments

All the spin-echo experiments we present were performed on the resonance spin-echo spectrometer MUSES. We performed experiments investigating the coherent scattering of a sample containing 50 w% deuterated trehalose in heavy water.
The solution was placed in a flat aluminium cell of 1 mm thickness that was closed by an indium seal. The cell was oriented with an angle of 45 degrees with respect to the incident beam. We used wavelengths of 4 and 4.8 Å. The resolution function of the instrument was measured using a quartz crystal.
We performed experiments at different temperatures and different Q-values around the maximum in the structure factor of about Q=1.9 $Å^{-1}$. Data were collected for about 10 hours per temperature. Each data point is the result of the fit of an echo-point, determined by eight points.

Data analysis and results

Time-of-flight experiments

In figure 1 examples of the scattering function are given. The data can be described very well by the sum of the two Lorentzian functions. One can see,

T/K	D(50 w%, 6 Å)	D(30 w%, 6Å)
270		$0.50 \cdot 10^{-6} cm^2 s^{-1}$
293		$1.75 \cdot 10^{-6} cm^2 s^{-1}$
298 / 300	$1.1 \cdot 10^{-6} cm^2 s^{-1}$	$2.20 \cdot 10^{-6} cm^2 s^{-1}$
311		$2.80 \cdot 10^{-6} cm^2 s^{-1}$

Table 1: Diffusion coefficients for aqueous solutions of trehalose obtained by neutron time-of-flight experiments.

that the contribution from the heavy water to the scattering signal is very small. Nevertheless it is worth to say, that fit using only one Lorentzian line was not possible.

The temperature dependence of the diffusion coefficient as well as the effect of a change in concentration is shown in figure 2. The width Γ (FWHM) of the Lorentzian line that describes the trehalose dynamics as a function of the wavevector can be described by a DQ^2-law, where D is the diffusion coefficient. Deviation at small Q from this law might be due to multiple scattering effects.
Data obtained using 6 Å neutrons on a sample of 50 w% Trehalose in D_2O at 298 K are compared to those of a sample containing 30 w% trehalose at different temperatures. When varying the concentration the diffusion coefficient changes from $1.1 \cdot 10^{-6} cm^2 s^{-1}$ for the 50 w% sample to $2.2 \cdot 10^{-6} cm^2 s^{-1}$ for the 30 w% sample. Numerical values are listed in table 1.

spin-echo experiments

In figure 3 one can see the obtained intermediate scattering function at Q=1.7 Å. Experiments were performed in a temperature range between 250 K and 300 K. The data at Q=1.7Å and T=290 K have been extended to short times by adding data from time-of-flight experiments. The intermediate scattering function can be obtained by a Fourier transformation of the dynamic structure factor, obtained in the time-of-flight analysis, according to

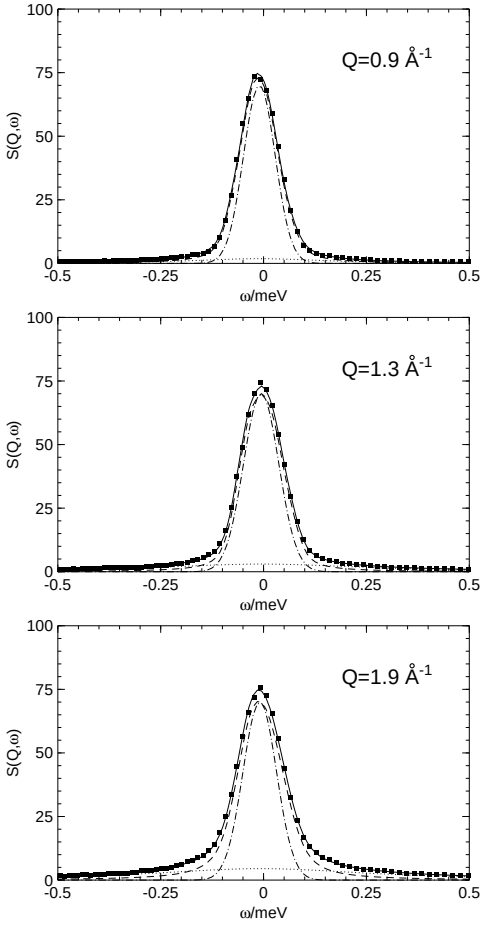

Figure 1: Quasielastic scattering for a 50 w% trehalose/D_2O mixture at 298 K at different Q-values. Solid lines represent best results using two Lorentzian lines. The dashed line shows the trehalose contribution, the dotted lines shows the contribution from the buffer. Also included is the experimental resolution function.

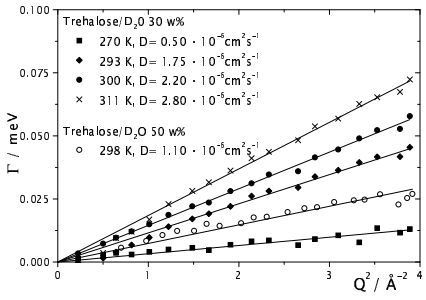

Figure 2: Width of the Lorentzian lines describing the dynamics of trehalose as a function of Q^2: influence of the temperature, experiments performed at 6Å. Solid lines represent fits according to a DQ^2-law, numerical values for the diffusion coefficients are shown in the figures.

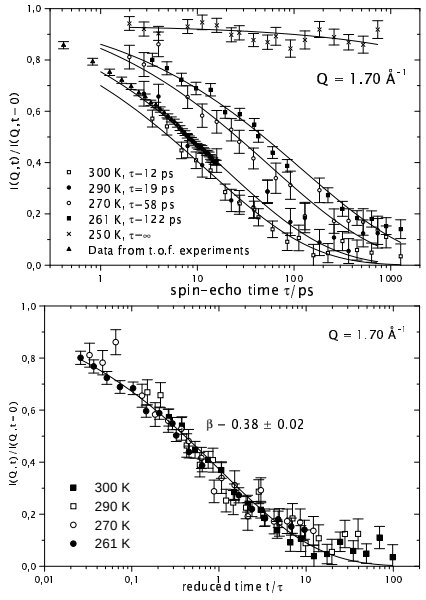

Figure 3: left: Intermediate scattering functions for a sample containing 50 w% trehalose in D_2O at different temperatures and at two Q-values. Solid lines represent refinements according to equation 2. right:Master curve representation of the data shown in figure 3. On a reduced time scale experimental data for temperatures >261 K can be described by a single stretched exponential function.

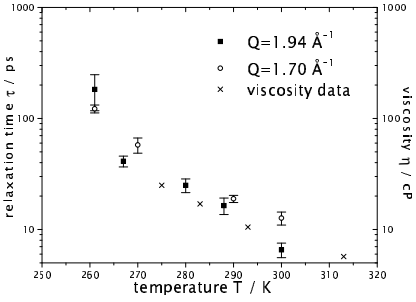

Figure 4: Relaxation times τ of the refinements shown in figure 3. We included viscosity data from [26] obtained for a sample containing 0.487 w% trehalose in H_2O.

equation 1. [1]
At 250 K the sample was probably already crystallized. We suppose, that also the fluctuations in the spin-echo signal at T=261 K could be attributed to an at least partially crystallized sample.

All the experimental curves can be described using a stretched exponential function of the Kohlrausch-Williams-Watt type:

$$I(Q,t) = A \cdot \exp\left(-\frac{t}{\tau(Q)}\right)^{\beta(Q)} \qquad (2)$$

This type of analysis, often used in the description of glass forming liquids corresponds to a distribution of relaxation times, present in the system. β describes the width of this distribution. The obtained relaxation times are shown in table 2.

Data for all temperatures can be plotted on a master-curve where the spin-echo time is divided

[1] We show here in fact results obtained from different scattering processes. In the time-of-flight experiment we probe the incoherent scattering mainly from the trehalose molecules, while the spin-echo data describe the coherent scattering from the trehalose molecules and the water. Nevertheless, the observed dynamics should be similar as it can be seen by the good overlap of the two curves. Nevertheless we do not fit the combined data. The shown curve results by fitting only the spin-echo data.

Q/Å^{-1}	T/K	τ/ps	β
1.7	300	12 ± 1.7	0.38 ± 0.03
1.7	290	19 ± 1.4	0.38 ± 0.02
1.7	270	58 ± 9.0	0.38 ± 0.02
1.7	261	122 ± 10	0.38 ± 0.04
1.7	250	∞	-

Table 2: Parameters of the curves shown in figure 3. The relaxations times are shown as a function of temperature in figure 4.

by the obtained relaxation time. In figure 3 one can see that all the data points can be described by a common master curve according to equation 2 obtaining a value for β of about 0.38. [2]

In figure 4 the evolution of the relaxation time τ as a function of temperature can be seen. It increases nearly exponentially when decreasing the temperature. We observe an increase in the relaxation times by an order of magnitude when decreasing the temperature from 300 K to 260 K. This is in quite good agreement with findings from viscosity measurements [26, 27]. They showed that the viscosity of aqueous trehalose solutions increases by about a factor of 7, when the temperature is reduced from T=330 K to T=250 K. As one can see from figure 4 the viscosity for a similar sample shows the same temperature dependence as our relaxation times. When we suppose, that the protein motions are correlated to the viscosity of its hydration shell, an increase in the viscosity should lead to a slowing down of the protein dynamics.

Discussion and conclusion

We analysed the diffusional behaviour of trehalose in concentrated aqueous solution. With time-of-flight experiments we investigate dynamics at low resolution. In this dynamical window trehalose motions could be described by a simple diffusional law. We neglected rotational motions of the trehalose molecules. An introduction of an additional Q-independent Lorentzian line that would correspond to a rotational phenomenon did not succeeded. We concider, that rotational motions should be too fast to be detected.
Using neutron spin-echo experiments one investigates dyanmics on a time-scale up to some nanoseconds. The intermediate scattering function obtained by the spin-echo technique corresponds to coherent scattering contributions from all atoms in the sample. We observe thus dynamics of the trehalose molecules as well as from the water molecules.
The spin-echo data show a more complex decay that can no longer be described by a simple exponential function. We concider a stretched exponential behaviour. The obtained relaxation times coincide perfectely with findings from viscosity measurements.
One could argue that dynamics on the time-of-flight scale should also show a stretched exponential behaviour. In fact the Fourier transformed data overlap very well with spin-echo data. Nevertheless it remains difficult to describe the time-of-flight data separately by a stretche exponential deacy. To perform such an adjustment and to obtain reasonable values for the parameter β the experimental data does cover a dynamic scale too small. One should fix the value for β for example from spin-echo measurements; unfortunately we could not perform experiments as a function of Q due to low scattering intensities. In fact experiments were only possible arround the maximum in the structure factor at about Q=1.9 Å^{-1}.

[2] In fact we performed an iterative fitting procedure. The data for the different temperature were first fitted individually. With the obtained relaxation times we obtain a master curve. Here we get the parameter β that can now be reintroduced to re-fit the relaxation times.

References

[1] A. Elbein, "The metabolism of α,α-trehalose", *Adv.Carbohydr.Chem.Biochem.*, **30**, 227–256, (1974).

[2] R. Payen, "Variations des teneurs en glycogene et en trehalose pendant le sechage de la levure", *Can.J Res.*, **27B**, 749–756, (1949).

[3] J. Clegg and M. Filosa, "Trehalose in the cellar slime mould dictyostelium mucoroides", *Nature*, **192**, Nr:4807, 1077–1078, (1981).

[4] K. Madin and J. Crowe, "Anhydrobiosis in nematodes: carbohydrate and lipid metabolism during dehydration", *J.Exp.Zool.*, **193**, 335–342, (1975).

[5] S. Loomis, S. O'Dell and J. Crowe, "Anhydrobiosis in nematodes: control of the synthesis of trehalose during induction", *J.Exp.Zool.*, **221**, 321–330, (1980).

[6] K. Fox, "Putting proteins under glass", *Science*, **267**, 1922–1923, (1995).

[7] J. Green and C. Angell, "Phase relations and vitrification in saccharide-water solutions and the trehalose anomaly", *J.Phys.Chem.*, **93**, Nr:8, 2880–2882, (1989).

[8] J. Crowe, M. Whittam, D. Chapman and L. Crowe, "Interactions of phospholipid monolayers with carbohydrates", *Biochim.Biophys.Acta*, **769**, 151–159, (1984).

[9] J. Crowe, L. Crowe and D. Chapman, "Infrared spectroscopic studies on interactions of water and carbohydrates with a biological membrane", *Arch.Biochem.Biophys.*, **232**, Nr:1, 400–407, (1984).

[10] C. Duda and E. Stevens, "Trehalose conformation in aqueous solution from optical rotation", *J.Am.Chem.Soc.*, **112**, 7406–7407, (1990).

[11] M. Sakurai, M. Murata, Y. Inoue, A. Hino and S. Kobayashi, "Molecular-dynamics study of aqueous solution of trehalose and maltose: Implication for the biological function of trehalose", *Bull.Chem.Soc.Jpn.*, **70**, 847–858, (1997).

[12] G. Bonanno, R. Noto and S. Fornili, "Water interaction with α-α-trehalose : molecular dynamics simulation", *J.Chem.Soc.,Faraday Trans.*, **94**, 2755–2762, (1998).

[13] H. Kawai, M. Sakurai, Y. inoue, R. Chujo and S. Kobayashi, "Hydration of oligosaccharides : anomalous hydration ability of trehalose", *Cryobiology*, **29**, 599–606, (1992).

[14] S. Magazu, P. Migliardo, A. Musolino and M. Sciotino, "α,α-trehalose-water solutions. 1. Hydration phenomena and anomalies in the acoustic properties", *J.Phys.Chem.B*, **101**, 2348–2351, (1997).

[15] M. Elias and A. Elias, "Trehalose+water fragile system : properties and glass transition", *J.Mol.Liquids*, **83**, 303–310, (1999).

[16] N. Karger and H.-D. Lüdemann, "Temperature dependence of the rotational mobility of the sugar and water molecules in concentrated aqueous trehalose and sucrose solutions", *Z. Naturforsch.*, **46c**, 313–317, (1991).

[17] G. Batta, K. Köver, K. Gervay, M. Hornyak and G. Rpberts, "Temperature dependence of molecular conformation, dynamics, and chemical shift anisotropy of α,α-trehalose in D_2O by NMR-relaxation", *J.Am.Chem.Soc.*, **119**, 1336–1345, (1997).

[18] S. Magazu, G. Maisano, P. Migliardo, E. Tettamanti and V. Villari, "Transport phenomena and anomalous glass-forming behaviour in α,α-trehalose aqueous solutions", *Mol. Physics*, **96**, Nr:3, 381–387, (1999).

[19] C. Branca, S. Magazu, G. Maisano, P. Migliardo and E. Tettamanti, "On the bioprotective effectiveness of trehalose: ultrasonic technique, Raman scattering and NMR investigations", *J. Mol. Structure*, **481-481**, 133–140, (1999).

[20] E. Iannilli, E. Tettamanti, L. Galantini and S. Magazu, "An intagrated quasi-elastic light-scattering, pulse-gradient-spin-echo study on the transport properties of α, α-trehalose, sucrose and maltose deuterium oxide solutions", *J.Phys.Chem*, **105**, 12143–12149, (2001).

[21] S. Magazu, G. Maisano, D. Majolino, P. Migliardo, A. Musolino and V. Villari, "Diffusive properties of α,α-trehalose-water solutions", *Prog. Theor. Ph. Supplement*, **126**, 195–200, (1997).

[22] S. Magazu, G. Maisano, P. Migliardo and V. Villari, "Experimental simulation of macromolecules in trehalose aqueous solutions : A photon correlation spectroscopy study", *J. Chem.Phys.*, **111**, Nr:19, 9086–9092, (1999).

[23] S. Magazu, D. Majolino, H. Middendorf, P. Migliardo, A. Musolino, M. Scortino and U. Wanderlingh. "α,α-trehalose-water solutions: an important bioprotective liquid system. Diffusive motions as probed by dynamic light scattering and IQENS". In S. Cusack, Editor, *Biological Macromolecular Dynamics*, 155–159. Adenine Press, (1997).

[24] H. Koch and R. Stuart, "A novel method for specific laballing of carbohydrates with deuterium by catalytic exchange", *Carbohydrate Res.*, **59**, C1–C6, (1977).

[25] H. Koch and R. Stuart, "The catalytic C-deuteration of some carbohydrate derivatives", *Carbohydrate Res.*, **67**, 341–348, (1978).

[26] C. Branca, S. Magazu, G. Maisano, P. Migliardo, V. Villari and A. Sokolov, "The fragile character and structure-breaker role of α,α-trehalose: viscosity and Raman scattering findings", *J.Phys.: Condens.Matter*, **11**, 3823–3832, (1999).

[27] S. Magazu, G. Maisano, H. Middendorf, P. Migliardo, A. Musolino and V. Villari, "α,α-trehalose-water solutions. II. Influence of hydrogen bond connectivity on transport properties", *J.Phys.Chem.B*, **102**, 2060–2063, (1998).

Dynamique à haute résolution d'une protéine en présence de tréhalose[4]

Le spectromètre à rétrodiffusion IN13, à l'Institut Laue-Langevin offre la possibilité d'étudier des mouvement locaux avec une haute résolution en énergie de 10 μeV (largeur à mi-hauteur). Il permet d'accéder à une grande gamme en Q.
Nous avons utilisé deux configurations différentes. Les scans élastiques donnent accès au déplacement carré moyen des atomes. Nous avons mesuré, en fonction de la température, l'intensité diffusée pour un transfert d'énergie égal à 0. L'analyse des données en fonction de Q^2 a été réalisée avec un modèle linéaire. Pour un mélange protéine sèche/tréhalose, les déplacements carrés moyens ont un comportement harmonique dans toute la gamme de température explorée. Dans le cas des échantillons hydratés, on peut observer une transition dynamique autour de 200 K. Cette transition a été déjà décrite pour d'autres systèmes. Toutefois, nous avons trouvé le même comportement pour plusieurs échantillons avec des rapports -protéine hydratée/sucre- différents entre la protéine hydratée et le sucre.

L'analyse du signal quasiélastique permet d'étudier la dynamique de ces systèmes. Pour des échantillons contenant de la protéine dans sa forme protonée en présence de tréhalose deutérié, et hydratée avec de l'eau lourde, le facteur de structure dynamique correspond aux mouvements des protons de la protéine. Ces mouvements peuvent être décrits avec le modèle d'une particule qui diffuse dans une sphère. L'élargissement quasiélastique en fonction de Q montre un comportement typique d'une telle diffusion: une partie constante à petit Q, suivie d'une croissance linéaire. Le niveau du plateau est proportionnel au coefficient de diffusion. Nous avons pu mettre en évidence que la présence du tréhalose ralentit fortement les mouvements de la protéine. Nous avons remarqué également, que la contribution élastique du signal augmentait pour les échantillons contenant du tréhalose. Une partie des mouvements, visible avec des échantillons sans tréhalose, devient trop lente pour être détectée, avec la résolution instrumentale.
L'analyse du facteur de structure incohérent élastique (EISF) nous a donné des informations sur les dimensions de la sphère utilisée dans notre modèle. Nous avons observé, que le diamètre de la sphère n'était pas modifié par la présence du tréhalose. Nous concluons que l'ensemble des observations conforte le modèle de Green et Angell dans sa description des interactions entre le tréhalose et les biomolécules. L'augmentation de la viscosité de la couche d'hydratation par le tréhlalose, puis la formation d'un état vitreux autour de la protéine conduisent aux mêmes informations que nos expériences. D'un autre côté, des interactions directes comme dans le modèle de Crowe devraient modifier la géométrie des mouvements, mais l'analyse de nos données expérimentales ne conduit pas à cette observation.

[4]soumis à Biophysical Journal

Dynamics in trehalose coated protein at high resolution

I.Köper, M.-C. Bellissent-Funel, W. Petry

We performed elastic and quasielastic neutron scattering experiments using the backscattering spectrimeter IN13 in order to investoigate interactions between trehalose, a well know bioprotector and the C-phycocyanin protein. Elastic scattering scans giving information about the atomic mean square displacements revealed a nearly identical behavior for samples containing hydrated protein powders both with and without trehalose. At the same times quasielastic scattering experiments show a clear slowing down of protein motions. The geometry of motion of the protein dynamics could be described using a simple model.

Introduction

Trehalose is a well known disaccharide with bioprotecting properties. It has been isolated from algae, bacteria, fungi, insects, invertebrates and yeasts as well as from lower vascular plants and a few flowering plants [1]. It has been found even in some mammalian systems. One of the most interesting facts of this non-reducing glucosides is that it has been found in large quantities in organisms that are able to survive extreme external stresses such as high or very low temperatures or periods of complete drought [2–6]. Two models have been proposed to describe the protective effect on a molecular lenght scale. The first one, proposed by Green and Angell [7] is based on the very high glass transition temperature of trehalose solutions. Following this model the protected biomolecule is placed in a glassy trehalose structure and thus the formation of ice crystals would be hindered. The structure of the biomaterial would be conserved and life and decay processes would be suspended [8].
The other main hypothesis, the so-called 'water-replacement theory' was proposed by Crowe *et al.* [9]. It tries to find evidence for direct interactions between the protected biomaterial and the trehalose molecules.

We performed a series of neutron scattering experiments in order to describe the interactions between trehalose and a protein, the C-phycocyanin, a protein that takes place in the photosynthetic cycle of cyanobacteria.

Materials and methods

We used the C-phycocyanin extracted from the cyanobacteria *synecchoccus lividus*. It was furnished by H.L. Crespi [10]. Recently S. Dellerue studied extensively the dynamics of the CPC protein by neutron scattering techniques and combined and explained the obtained results with data from molecular dynamics simulations [11, 12].
We performed experiments on hydrated powder samples. Trehalose was used in its deuterated form. Details on the deuteration will be published elsewere. Labile protons of the sugar and the protein were exchanged against deuterons by successive dialysis. A solution of CPC and trehalose was co-lyophilized to obtain a homogeneous powder of the mixture. The powder was hydrated in an rectangular alluminium cell in a heavy water atmosphere. The level of hydration was checked by wheight. The cell was finally closed by an indium seal.

The backscattering spectrometer IN13 of the ILL, Grenoble has the advantage to give access to a large Q-range up to values of about 5 $Å^{-1}$. We used this instrument to measure the incoherent scattering function. Due to the sample composition, we investigate mainly motions of the protein. With an incident wavelength of 2.3 Å one obtains a resolution of 10 μeV (FWHM).
We performed two types of experiments. In the elastic scan mode one investigates the scattering without energy transfer. Thus one has access to the Debeye Waller factor. When analysing the data as a function of the scattering vector Q, one obtains the mean square displacement of the scattering particles. In the quasielastic mode one measures the dynamic structure factor $S(Q,\omega)$.

Elastic scattering

We performed experiments on different samples containing trehalose coated CPC protein in different ratios and with different levels of hydration. Cordone *et al.* performed a quite similar experiment on trehalose coated dry myoglobin [13]. They found that a dynamical transition present in hydrated myoglobin [14] cannot be detected in dry trehalose coated protein. We can confirm these results for the CPC protein. But we also investigated the effect of trehalose coating in hydrated powder samples.

We performed elastic neutron scattering scans in a temperature range from 40 K up to 330 K, counting 90 minutes per temperature. Data were corrected for empty cell contributions and normalised to a standard vanadium scatterer using standard programs of the ILL. The intensity of the scattered signal is proportional to:

$$S(Q,\omega=0) \propto exp\left(-\frac{Q^2 \cdot \langle u^2 \rangle}{3}\right) \qquad (1)$$

For each temperature we can analyse the data over a Q-range up to Q=4 $Å^{-1}$ using equation 1. Some examples are shown in figure 1. The slope of the solid lines corresponds to the mean square displacements. The mean square displacement for different samples as a function of temperature is shown in figure 2.
To normalise the data from different experiments to a common scale, the harmonic region at low temperature was assumed to be linear. Data were extrapolated and normalised to be 0 at T=0K.
Figure 2 shows the mean square displacements for the following samples: a dry sample of trehalose coated CPC (1 g trehalose per g CPC), a sample containing hydrated CPC protein (0.5 g D_2O per gram protein) and two samples of hydrated trehalose coated CPC with 0.75 g trehalose and 0.75 g D_2O and 0.3 g trehalose and 0.7 g D_2O per gram protein respectively. At low temperature up to about 200 K all samples show a classical harmonic behavior. For the dry sample this behavior continues even at highest temperatures, a fact that is consistent with findings from Cordone *et al.* on trehalose coated myoglobin. When hydrating the samples a dynamical transition can be observed at temperatures higher than 200 K. Furthermore, the mean square displacements are more or less independent from the sample composition, even if the values for the trehalose free sample seem to be a little bit higher than that of the trehalose coated ones. Furthermore the values for the samples containing less trehalose (0.3 g trehalose and 0.7 g D_2O per g protein) are slightly higher than for the sample containing a large amount of trehalose and a similar degree of hydration (0.75 g trehalose and 0.75 g D_2O per g protein), especially at highest temperatures.

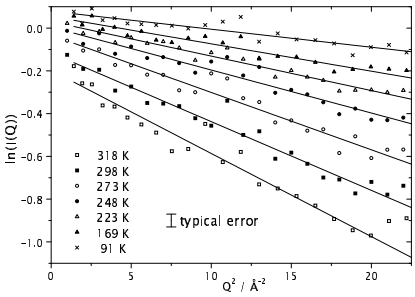

Figure 1: Analysis of the elastic scattering data at several temperatures for a sample containing 0.75 g trehalose and 0.75 g D_20 per gram protein. The scattering intensity is plotted versus the scattering wavevector. Using a linear model and according to equation 1, the slope of the straight lines corresponds to the mean square displacements. Experiments performed on the spectrometer IN13 using an experimental resolution of FWHM=10 μeV.

Quasielastic scattering

We used hydrated powder samples of CPC protein in oder to avoid contribution from long range diffusive motion of the whole protein. We observe only dynamics on a small amplitude. To describe these motions we use a model proposed by Volino and Dianoux in 1980 [15]. They developed a formalism describing the diffusive motion of a particle confined inside a spheric environment.
In time-of-flight and backscattering experiments one measures the dynamical structure factor S(Q,ω). In

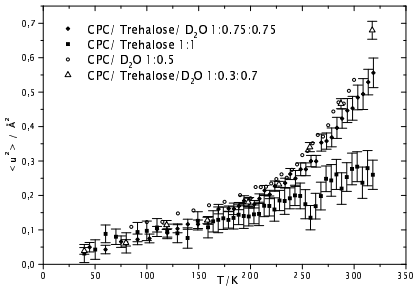

Figure 2: Mean square displacements $<u^2>$ as a function of temperature for samples of different composition of CPC protein, trehalose and heavy water. Experiments performed on the IN13 spectrometer using an experimental resolution of FWHM=10 μeV.

our case it can be described using the sum of an elastic and a broadening term according to:

$$S(Q,\omega) = DW \cdot [A_0(Q) \cdot \delta(\omega) + (1 - A_0(Q)) \cdot L(Q,\omega)] \quad (2)$$

Here $DW \sim exp(-Q^2 < u >^2)$ is the Debeye Waller factor and $L(Q,\omega) = \frac{1}{\pi} \cdot \frac{\Gamma(Q)}{\Gamma(Q)^2+\omega^2}$ a Lorentzian line of the width (FWHM) Γ.

The length scale of the observed motions is inverse proportional to Q. At small Q values a system as described above would show a behavior independent of Q up to a value Q_0, that corresponds to the size of the sphere. For larger Q one should observe classic diffusion according to a DQ^2 law, with D being the diffusion coefficient.
The signal obtained from such a system should have, at least at small Q, a large elastic contribution. One can introduce the elastic scattering factor, which is the contribution of the elastic scattering to the total scattering. In the case of incoherent scattering it is called elastic incoherent structure factor (EISF). Volino and Dianoux described its behavior as a function of Q for a particle diffusing inside a sphere. One would expect a behavior for the EISF according to

$$A_0(Q) = \left(\frac{3j_1(Qa)}{Qa}\right)^2, \quad (3)$$

with $j_1(x) = (sin(x) - x \cdot cos(x))/x^2$, a Bessel function of the first order and a the radius of the sphere.

Experimental data always depend on instrumental resolution. It limits the time window in which motion can be detected. Dynamics that are to fast for the dynamical scale will contribute to the background signal, slower motions to the elastic scattering signal. In this case the EISF function does not achieve zero values in the experimental range. To take into account this effect we introduce a fraction p of immobile protons. This fraction of scatterer is thus invisible to the experimental conditions.

$$EISF = p + (1 - p) \cdot A_0(Q) \quad (4)$$

The analysis of the quasielastic scattering is quite difficult. As the neutron flux on the instrument is not very high and as one single scan over an energy range from -110 to 100 μeV takes 10 hours, data collection times were of about three days per sample to obtain sufficient statistics. Even after this time the quality of the spectra is not very satisfying, partially due to the highly elastic signal with only little quasielastic contributions. In figure 3 the dynamic structure factors at different Q-values are shown for a sample containing 0.75 g deuterated trehalose and 0.75 g heavy water per gram protonated CPC protein.

We performed experiments at different sample composition and at different temperatures. To be able to compare our results to previous results of a sample containing hydrated CPC powders [16], one of the chosen temperatures was 280 K, where the signal of our trehalose coated samples showed only a small broadening of the scattered signal.
The scattered signal can be described using the sum of an elastic and a quasielastic term, as shown in equation 2. We analyse the results in the same way as described for the time-of-flight data.

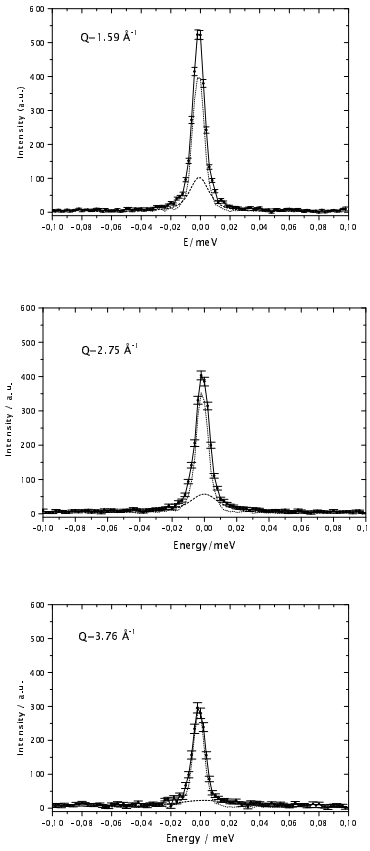

Figure 3: Dynamic structure factors for a sample containing 0.75 g deuterated trehalose and 0.75 g heavy water per gram protonated CPC protein measured at 280 K. The solid line describes the fit according to equation 2. The dotted lines shows the elastic contribution, the dashed one the quasielastic contribution. Experiments performed on the IN13 spectrometer with a resolution of 10 μeV.

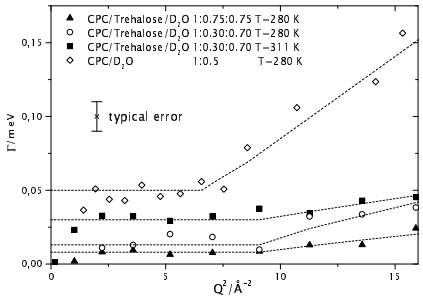

Figure 4: Half width at half maximum Γ of the Lorentzian line describing the broadening of the scattered signal, as a function of the momentum transfer vector. Dashed lines are guides to the eyes to demonstrate the two different regions according to the model of Dianoux and Volino [15]. Experiments performed on the spectrometer IN13 with a resolution of 10 μeV (FWHM).

Figure 4 shows the half width at half maximum Γ of the Lorentzian term in equation 2. One can see the typical behavior of a confined diffusion: a first region with a constant value for Γ is followed by a region with a linear dependence of Γ as a function of the momentum transfer. The value of the plateau at small Q depends on the diffusion coefficient. The Q-value, that marks the point, where the behavior changes, is proportional to the radius of the sphere. Due to the large errors we only present a qualitative analysis of these parameters.
In figure 5 the elastic incoherent structure factors for different sample compositions are shown. The curves can be described using equation 3 and 4.

We will discuss two effects. The influence of trehalose on the dynamics of the system as well as its temperature dependence. From figure 4 one can see a clear slowing down of the protein motions due to the addition of trehalose. The difference in the plateau value, directly proportional to the diffusion coefficient is of about one order of magnitude when comparing a sample containing hydrated CPC protein (h=0.5) with a sample containing trehalose coated hydrated CPC protein (0.75 g trehalose per

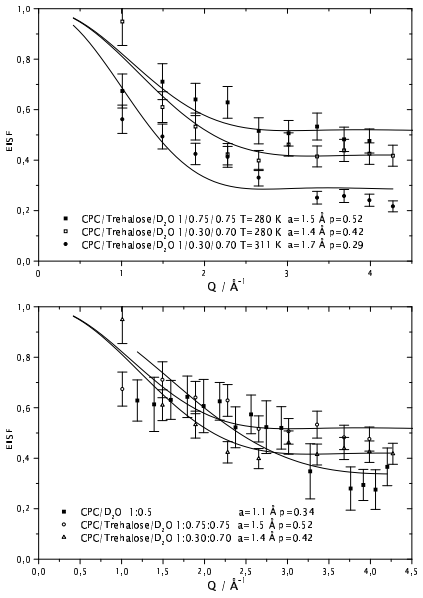

Figure 5: Elastic incoherent structure factors for samples containing trehalose coated, hydrated CPC powders. up: influence of the temperature, down: influence of the sample composition. Solid lines represent adjustments according to the model of a particle diffusing inside a sphere. Experiments performed on the spectrometer IN13 with a resolution of 10 μeV (FWHM).

g protein, h=0.75). The difference between the samples with different contents of trehalose, 0.75 and 0.3 g trehalose per gram protein, is less pronounced. The effect of a change in temperature is evident and quite straightforward. We performed the quasielastic measurement on a sample containing 0.3 g trehalose per gram protein, hydrated to 0.7 g heavy water per gram protein at 280 K and 311K. As one could expect, the diffusive motion at the higher temperature is faster by a factor of about 5.

The same effect can be seen in the elastic incoherent structure factors in figure 5. The parameter p is correlated to the number of protons, contributing to the signal. The higher p, the more elastic is the signal, the less protons are visible to the instrumental resolution. For the sample containing the highest amount of trehalose (0.75 g per gram protein) only 50 % of all protons contribute to the signal, while in the sample without trehalose only about 35 % of the protons contribute to the elastic scattering signal. For the sample containing 0.3 g trehalose the proportion is still about 42 %. One has to keep in mind, that the samples containing trehalose are hydrated to a higher level of hydration than the sample without trehalose. The pure protein sample was hydrated to h=0.5 while we used hydration levels of h=0.75 and h=0.1 for the trehalose coated samples. The signal of the trehalose coated samples would become even more elastic at a lower level of hydration. When rising the temperature from 280 K to 311 K the amount of invisible protons decreases from 42 % to 29 %, as one would expect. We obtain here values different to those obtained in the time-of-flight experiments due to the fact, that the dynamic range in both experiment is different. Thus we do not probe the same motions.
The determination of the radius a of the sphere is quite uncertain due to the considerable statistical error of the data. The following trends can be observed: the fit for the sample without trehalose gives the smallest value for a, followed by the samples containing trehalose at 280 K. The highest value for a is obtained for the experiment at 311 K.

Conclusion

We performed elastic and quasielastic eutron scattering experiment on trehalose coated hydrated protein samples in order to sudy the influence of the treahlose molecules on the protein motions. The analysis of the quasielastic scattering signal reveals a clear slowing down of the protein dynamics due to the presence of the trehalose molecules. The elastic incoherent structure factor shows also an increase of the elastic scattering contribution, indicating the slowing down of certain parts of protein dynamics below experimental resolution.
At the same time the analysis of the geometry of motion as well as the analysis of the mean square displacements by elastic scattering scans showed that the geometry should be the same with and without trehalose. When comparing these facts to the two

models proposed by Crowe and Green respectively, we would favour the latter one. One could expect, that in the case of direct interactions between trehalose and protein molecules, the geometry of motion of the protein molecules should be modified. On the other hand, an increase of the viscosity of the hydration shell, as proposed by Green and Angell whould result similar to our observations.

References

[1] A. Elbein, "The metabolism of α,α-trehalose", *Adv.Carbohydr.Chem.Biochem.*, **30**, 227–256, (1974).

[2] R. Payen, "Variations des teneurs en glycogene et en trehalose pendant le sechage de la levure", *Can.J Res.*, **27B**, 749–756, (1949).

[3] J. Clegg and M. Filosa, "Trehalose in the cellar slime mould dictyostelium mucoroides", *Nature*, **192**, Nr:4807, 1077–1078, (1981).

[4] K. Madin and J. Crowe, "Anhydrobiosis in nematodes: carbohydrate and lipid metabolism during dehydration", *J.Exp.Zool.*, **193**, 335–342, (1975).

[5] S. Loomis, S. O'Dell and J. Crowe, "Anhydrobiosis in nematodes: control of the synthesis of trehalose during induction", *J.Exp.Zool.*, **221**, 321–330, (1980).

[6] K. Fox, "Putting proteins under glass", *Science*, **267**, 1922–1923, (1995).

[7] J. Green and C. Angell, "Phase relations and vitrification in saccharide-water solutions and the trehalose anomaly", *J.Phys.Chem.*, **93**, Nr:8, 2880–2882, (1989).

[8] J. Crowe, M. Whittam, D. Chapman and L. Crowe, "Interactions of phospholipid monolayers with carbohydrates", *Biochim.Biophys.Acta*, **769**, 151–159, (1984).

[9] J. Crowe, L. Crowe and D. Chapman, "Infrared spectroscopic studies on interactions of water and carbohydrates with a biological membrane", *Arch.Biochem.Biophys.*, **232**, Nr:1, 400–407, (1984).

[10] K. Bradley, Chen.S.H., M.-C. Bellissent-Funel and H. Crespi, "The observation of structural transitions of a single protein molecule", *Biophys. Chemistry*, **53**, 37–44, (1994).

[11] S. Dellerue, A. Petrescu, J. Smith, A. Longeville and M.-C. Bellissent-Funel, "Collective dynamics of a photosynthetic protein probed by neutron spin-echo spectroscopy and molecular dynamics simulation", *Physica B*, **276-278**, 514–515, (2000).

[12] S. Dellerue and M.-C. Bellissent-Funel, "Relaxational dynamics of water molecules at protein surface", *Chem.Phys.*, **258**, 315–325, (2000).

[13] L. Cordone, P. Galajda, E. Vitrano, A. Gassmann, A. Ostermann and F. Parak, "A reduction of protein specific motions in co-ligated myoglobin embedded in a trehalose glass", *Eur. Biophys.J.*, **27**, 173–176, (1998).

[14] W. Doster, S. Cusack and W. Petry, "Dynamical transition of myoglobin revealed by inelastic neutron scattering", *Nature*, **337**, 754–756, (1989).

[15] F. Volino and A. Dianoux, "Neutron incoherent scattering law for diffusion in a potential of spherical symmetry: general formalism and application to diffusion inside a sphere", *Mol.Phys.*, **41**, Nr:2, 271–279, (1980).

[16] S. Dellerue. *Structure er dynamique de protéines photosynthtiques étudiées par diffusion de neutrons et simulation par dynamique moléculaire.* PhD Thesis, Université de Paris-Sud, (2000).

Dynamique "gênée" d'une protéine en présence du tréhalose[5]

Nous avons étudié des mélanges de tréhalose et de protéine C-phycocyanine, sous forme de poudres hydratées, avec les techniques de temps-de-vol et à écho de spin de neutrons. La comparaison des résultats obtenus sur des échantillons avec et sans tréhalose permet de décrire l'éffet du tréhalose sur la dynamique de la protéine. La technique à écho de spin de neutrons offre une large gamme de temps d'observation. On mesure la fonction intermédiaire de diffusion entre 3 ps et 4 ns. Des temps plus rapides sont accessibles avec la technique de temps-de-vol.
Pour un échantillon contenant de la CPC sous forme de poudre hydratée, les résultats des expériences par écho de spin combinés avec ceux des simulations numériques montrent un signal qui décroît avec un temps de relaxation de τ=1 ps. En présence de tréhalose, cette relaxation est ralentie de deux ordres de grandeur.

Les expériences en temps-de-vol donnent également accès au facteur de structure élastique incohérent. Nous avons analysé cette fonction avec un modèle simple de diffusion d'une particule dans une sphère. Ainsi nous avons pu décrire la géométrie des mouvements de la protéine. La présence du tréhalose semble n'avoir aucun effet sur la géométrie de ces mouvements.

[5]acepté dans Applied Physics

Applied Physics A manuscript No.
(will be inserted by the editor)

Hindered protein dynamics in the presence of a cryoprotecting agent

Ingo Köper[1,2], Marie-Claire Bellissent-Funel[1], Winfried Petry[2]

[1] Laboratoire Leon Brillouin, CEA Saclay, F-91191 Gif-sur-Yvette
[2] Physikdepartment E13, TU München, D-85747 Garching

Received: date / Revised version: date

Abstract We present a study of the influence of trehalose, a well known cryoprotecting disaccharide on the dynamics of a protein, the C-phycocyanin. Dynamics is investigated in a time range from some pico to several nanoseconds using different neutron scattering techniques. Data obtained on samples containing hydrated powders of the protein in presence of trehalose are compared to that of the protein alone, studied by neutron scattering techniques as well as by molecular dynamics simulations.
The analysis of time-of-flight data gives access to the geometry of the observed motions. These motions can be described via a model of a particle diffusing inside a sphere.
We observe a slowing down of the movements of the protein due to the presence of trehalose of one to two orders of magnitude, while the geometry of motions is conserved.

PACS: 87.14.Ee, 87.15.Kg

1 Introduction

Anhydrobiosis is a wide spread phenomenon in nature. Several organisms such as plants, spores, fungi or higher microorganisms are known to be able to survive extreme external stresses such as high or low temperatures or periods of drought by passing in a state of suspended animation. Once being rehydrated they recover their normal active metabolism, often within minutes [1–3].
The mechanisms involved in this protection have been studied for a long time. Several molecules have been found to be able to stabilise and protect biomaterial against denaturation caused by external stresses. Beneath all this protecting agents the disaccharide trehalose shows the highest effectiveness [4,5]. Trehalose is the general name for the D-glucosyl-D-glucosides. Neither the way trehalose or other types of protecting agents prevent biomolecules from denaturation nor the reason for the higher effectiveness of trehalose seem to be clear. Two main hypotheses have been proposed. The first one describes the protecting mechanism via direct interactions between trehalose and the biomolecule. Thus the sugar would replace the water normally present at the surface of the biomaterial and conserve its structure [6]. The other hypothesis focuses on the fact, that trehalose easily forms amorphous phases with very high glass transition temperatures [7]. The proposed mechanism consists in conserving the structure by embedding the biomaterial in a glassy structure of trehalose. Depending on the nature of the sample and the kind of applicated stress, especially freezing and freeze-drying, examples for both theories have been found.
In our work we try to investigate the interactions between trehalose and a protein. We do not examine the difference between trehalose and other bioprotecting molecules.
We study the dynamics of the C-phycocyanin (CPC), a small light-harvesting protein, extracted from the cyanobacteria *synechoccus lividus*. Recently dynamics of this protein has been studied by neutron scattering techniques and molecular dynamics simulations [8,9].
A somehow similar study has been published in 1999 by Cordone *et al* [10]. They compared the mean square displacements of hydrated myoglobin with that of trehalose coated dry myoglobin. A dynamical transition observed in the pure protein sample could not be detected in the presence of trehalose.
Our approach is different, as we use hydrated samples both of the protein alone and of the trehalose coated protein.

Send offprint requests to: ikoper@cea.fr, FAX:+33.1.69.08.82.61

2 Materials and Methods

CPC protein was provided by H.L. Crespi [11]. We possess a protonated as well as a deuterated form of the protein.
Deuterated trehalose is commercially not available. We succeeded in obtaining a 80% deuterated form of the disaccharide modifying a procedure of Koch and Stuart [12]. Details will be published elsewhere.
We investigated samples in form of hydrated powders. Labile protons of the protein and of the sugar were exchanged against deuterons, protein and sugar are co-lyophilized in a determined mixture and the dry powder is hydrated in a heavy water atmosphere. The level of hydration was determined by the change of the weight of the powder.
Neutron scattering experiments were performed on the time-of-flight spectrometer MIBEMOL and on the neutron spin-echo spectrometer MUSES of the Laboratoire Léon Brillouin, Saclay. For the time-of-flight measurements the sample contained protonated protein and deuterated trehalose, while for spin-echo measurements completely deuterated samples were used.
On a time-of-flight spectrometer one measures the dynamic structure factor $S(Q,\omega)$. This is in fact the Fourier transform of the intermediate scattering function $I(Q,t)$, directly investigated in spin-echo experiments. When transforming time-of-flight date one can combine results from both techniques on a common time scale.
The intermediate scattering function is time dependent, so it can be analysed in terms of correlations times. We use a stretched exponential function to describe the decay of the signal.

$$I(Q,t) = A \cdot exp - \left(\frac{t}{\tau}\right)^{\beta} + C(Q) \qquad (1)$$

The stretching exponent β gives information about the width of the distribution. C(Q) takes into account for contributions at long times.
Time-of-flight experiments using an energy resolution of 96 μeV gives access to dynamics on a time scale up to 10 ps. In this short time range we analyse the incoherent structure factor on an energy scale with the sum of an elastic and a Lorentzian term. This corresponds to an analysis on a time scale by a stretching exponent β=1. In this case C(Q) corresponds to the elastic incoherent structure factor (EISF),which is the ratio of the elastic to the total scattering.

$$EISF = A_0(Q) \qquad (2)$$

Experimental data depend always on instrumental resolution. It limits the time window in which motions still can be detected. Faster dynamics will contribute to the background signal, slower motions to the elastic scattering signal. In this case the EISF function does not achieve zero values in the experimental range. To take into account this effect we introduce a fraction p of immobile protons. This fraction of scatterers is thus invisible to the experimental conditions.

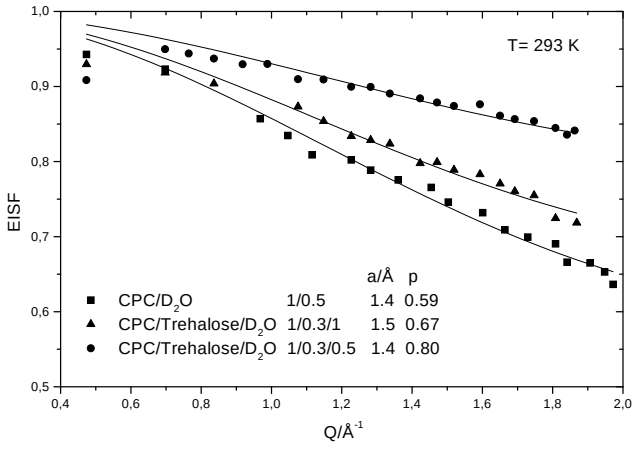

Fig. 1 Elastic incoherent structure factors (EISF) for three different samples containing hydrated powders of CPC protein and trehalose. The measurements were performed at a temperature of 293 K on the time-of-flight spectrometer MIBEMOL, using an incident wavelength of 6 Å. Solid lines represent fits according to equation 3 and 4. Note that the origin of the y-axis is set to 0.5 and not to 0.

$$EISF = p + (1-p) \cdot A_0(Q) \qquad (3)$$

We use a model proposed by Volino and Dianoux to describe the form of the curve. A particle diffusing inside a sphere should follow a law depending on a radius a of the sphere [13],

$$A_0(Q) = \left(\frac{3j_1(Qa)}{Qa}\right)^2, \qquad (4)$$

where $j_1(x) = (sin(x) - x \cdot cos(x))/x^2$ is a Bessel function of the first order.
A similar approach has been used and validated in the study of the dynamics of paravalbumin [14] and of C-phycocyanin [15,16].

3 Results and Discussion

In figure 1 we present the elastic incoherent structure factor (EISF) for three samples of different compositions. The curves can be analysed using the model described above. We obtain similar values of the radius a of the sphere of about 1.4 Å to 1.5 Å for all investigated samples. The content of trehalose influences the fraction p of immobile protons. This value describes the fraction of protons that is not detectable with the instrumental resolution. For a hydrated CPC sample this value is of about 0.59, while it is 0.67 and 0.80 for samples containing 0.3 g trehalose and respectively 0.5 g and 1.0 g D_2O per g protein.

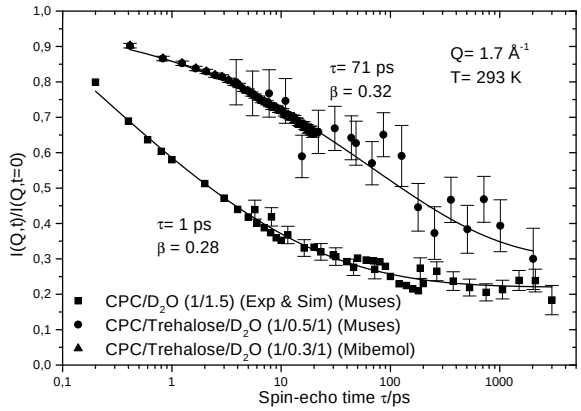

Fig. 2 Intermediate scattering function combining different instruments and techniques. Results obtained for a scattering vector of 1.7 Å at 293 K for samples containing hydrated powders of CPC protein and trehalose. Solid lines present results of fitting data points with stretched exponential functions according to equation 1.

Data obtained by time-of-flight experiments give access only to fast motions up to 10 ps. In order to cover a longer time scale we performed neutron spin-echo experiments.

In figure 2 we present data from time-of-flight and neutron spin-echo experiments on samples containing hydrated CPC/ trehalose powders. These date are compared with results obtained from neutron spin-echo experiments and molecular dynamics simulations on hydrated CPC powders. As the neutron spin-echo experiments give access to slower times we can no longer describe the evolution of the function by a single relaxation time. As more and more relaxational processes influence the protein the stretching parameter β becomes different from 1. The obtained relaxation times for the samples vary from 1 ps to 71 ps when hydration water is partially replaced by trehalose. The values for β, that correspond to the distribution of relaxation times are given in the figure.

4 Conclusions

We describe here the influence of the well known cryoprotecting disaccharide trehalose on the dynamics of the protein C-phycocyanin. Combined neutron time-of-flight and neutron spin-echo experiments as well as results from molecular dynamics simulations showed a relaxational behaviour in the time range from few pico to several nanoseconds.
Comparison between samples with and without trehalose showed a clear slowing down of dynamics in the observed time window. In neutron spin-echo experiments one investigates collective dynamics of the whole sample via the coherent scattering. In our samples we investigate thus the collective dynamics of the protein, the trehalose molecules and the hydration water at the same time. An analysis of the data from molecular dynamics simulations on the hydrated CPC sample showed, that the dynamics at times longer than 10 ps is dominated by protein motions, while the relaxation at shorter times is mainly due to water dynamics [16].
The analysis of the elastic incoherent structure factor in terms of a model describing the diffusion of a particle inside a sphere showed, that the size of the sphere is hardly affected. This model is certainly a simple one and one could argue, that it is quite optimistic to propose a model with only one parameter. In reality one should expect at least a distribution of spheres, when considering that the space explored by a proton is spherical. To our opinion the data obtained in our experiments do not provide enough information to apply a more sophisticated model. Furthermore in neutron scattering experiments one obtains only mean values over all processes in the sample. S. Dellerue found from molecular dynamics simulations of the CPC protein that the dynamics of the protein can be described using a distribution of spheres with a mean value of about 1.6Å.
From our point of view the slowing down of the protein dynamics is due to the increase of the viscosity of the hydration shell when trehalose is added. If one was dealing with direct interactions between trehalose and protein molecules the geometry of the movements would have been affected. The presented results show, that this is not the fact, as demonstrated by a value for the radius a of the sphere that is almost independent from the sample composition.

References

1. Payen,R., Can.J.Res. **27B** 749 (1949)
2. Clegg,J.S. and Filosa,M.F., Nature **192** 1077 (1961)
3. Fox,K.C., Science **267** 1922 (1995)
4. Bieganski,R.M., Fowler,A., Morgan,J.R. and Toner,T., Biotechnol. Prog. **14** 615 (1998)
5. Sola-Penna,M. and Meyer-Fernandes,J.R., Arch.Biochem.Biophys. **360** 10 (1998)
6. Crowe,J.H., Crowe,L.M. and Chapman,D., Science **223** 701 (1984)
7. Green,J.L. and Angell,C.A., J.Phys.Chem. **93** 2880 (1989)
8. Dellerue,S., Petrescu,A., Smith,J.C., Longeville,S. and Bellissent-Funel,M.C. Physica B **276-278** 514 (2000)
9. Dellerue,S. and Bellissent-Funel,M.C. Chem.Phys. **258** 315 (2000)
10. Cordone,L. and Ferrand,M. and Vitrano,E. and Zaccai,G. Biophys.J. **76** 1043 (1999)
11. Crespi,H.L., IAEA Vienna, 111 (1977)
12. Koch,H.J. and Stuart,R.S., Carbohydrate Res. **59** C1 (1977)
13. Volino,F. and Dinaoux,A.J. Mol.Phys. **41** 271 (1980)
14. Zanotti,J.M., Bellissent-Funel,M.C. and Parello,J., Biophys.J. **76** 2390 (1999)
15. Dellerue,S., PhD-Thesis, Orsay (2000)
16. Dellerue,S., Petrescu,A.-J., Smitch,J.C. and Bellissent-Funel,M.-C., Biophys.J. accepted for publication

II Résumé et perspectives

II.1 Vue d'ensemble

La C-phycocyanine en présence de tréhalose, est un système complexe. Nous avons étudié la dynamique de cette protéine à l'aide de différents instruments de diffusion de neutrons pour accéder à différentes résolutions en énergie (ou en temps). La dynamique rapide, jusqu'à 10 ps, a été observée au cours des expériences de type temps-de-vol. La technique de rétrodiffusion a permis de couvrir une gamme en temps jusqu'à 100 ps. Avec la technique à écho de spin de neutrons, nous avons pu étudier la dynamique entre 3 ps et 4 ns. Nous avons mené des expériences à des valeurs de Q plutôt élevées ce qui nous a permis d'étudier des mouvements internes locaux. L'utilisation d'échantillons sous forme de poudres hydratées nous a permis de négliger les processus de diffusion à longue distance et nous avons pu sonder, du moins dans la gamme de la ps à la ns, les mouvements des chaînes latérales et du squelette de la protéine.
S. Dellerue *et al.* ont analysé une simulation de dynamique moléculaire de la CPC hydratée [11]. Ils ont trouvé que les processus de relaxation du squelette ont lieu pour des valeurs de Q inférieures à 2Å^{-1}, entre 10 et 100 ps. La dynamique des chaînes latérales a lieu entre 20 et 500 ps. Ces valeurs sont des valeurs moyennes sur les parties concernées de la protéine. L'analyse des données de simulation avec une fonction de type exponentielle étirée conduit à des valeurs de l'exposant β compris entre 0.3 et 0.4. Nous présentons sur la figure II.1, l'évolution du temps de relaxation τ et de l'exposant β en fonction de Q, respectivement pour le squelette et pour les chaînes latérales.

Les expériences de temps-de-vol et les expériences de rétrodiffusion permettent de mesurer le facteur de structure dynamique $S(Q,\omega)$. Les expérience à écho de spin permettent d'accéder à la fonction intermédiare de diffusion $I(Q,t)$. Ces deux gandeurs sont reliées par une transformation de Fourier:

$$I(Q,t) = \int S(Q,\omega) \cdot exp(i\omega t) d\omega \tag{II.1}$$

Nous avons transformé les résultat obtenus par des expériences de temps-de-vol afin de les comparer à ceux obtenus par écho de spin car ces deux fonctions ont un

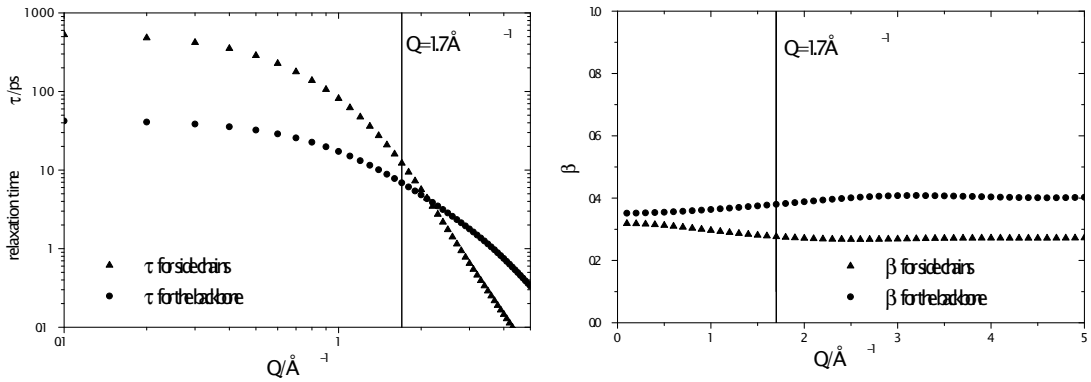

Figure II.1: Analyse d'une simulation MD de la CPC hydratée. Séparation des mouvements des chaînes latérales et du squelette. Les processus de relaxation ont été décrits par une exponentielle étirée [11].

intervalle de temps commun. Pour étudier l'influence du tréhalose sur la dynamique de la CPC, nous comparons nos résultats expérimentaux ainsi combinés avec ceux de S. Dellerue pour la CPC hydratée. Dans ce derniers cas, les resultats de diffusion de neutrons ont été comparés à ceux de la simulation MD. Les différentes techniques conduisent à observer différentes contributions. La technique de temps-de-vol donne la contribution incohérente de tous les atomes de l'échantillon. Dans un échantillon qui est composé d'une protéine protonée, de tréhalose deuterié et d'eau lourde, ces contributions sont en majorité dues aux protons de la protéine.
Dans le cas des expériences à écho de spin, nous avons utilisé, soit des échantillons complètement protonés, soit complètement deutériés. Le signal obtenu contient les contributions de tous les atomes de l'échantillon et cela proportionnellement à leur concentration.
Dans le tableau II.1, nous présentons les sections efficaces calculées cohérentes et incohérentes pour les différentes compositions des échantillons que nous avons utilisés. Une séparation entre les contributions de la protéine, du tréhalose et de l'eau est faite. Selon les différentes compositions, le signal de diffusion est dominé par différentes contributions.

La figure II.2 montre un résumé des données obtenues à Q=1.7 $Å^{-1}$ et à T=298 K.

Le processus de relaxation obtenu pour un échantillon contenant la CPC hydratée peut être décrit par une exponentielle étirée avec un temps de relaxation de 1 ps et un exposant β=0.27. Cette relaxation plutôt rapide est liée à une forte contribution de l'eau d'hydratation au signal de diffusion. La dynamique de la protéine contribue aux temps les plus longs à un plateau ayant une valeur égale à 0.21.
Nous comparons cette relaxation avec les résultats obtenus pour des échantillons contenant des mélanges hydratés de CPC/tréhalose. Nous avons utilisé des compo-

	h-CPC	d-CPC	h-trehalose	d-trehalose	H_2O	D_2O
temps-de-vol, rétrodiffusion						
rapport / g	1			0.3		1
rapport moléculaire	1			30		1800
σ_{coh} relative	0.10			0.03		0.12
σ_{inc} relative	0.67			0.05		0.03
écho de spin, incohérent						
rapport / g	1		0.3		1	
rapport moléculaire	1		32		1970	
σ_{coh} relative	0.03		0.01		0.03	
σ_{inc} relative	0.32		0.09		0.52	
écho de spin, cohérent						
rapport / g		1		0.5		1
rapport moléculaire		1		53		1900
σ_{coh} relative		0.28		0.11		0.29
σ_{inc} relative		0.05		0.18		0.08

Table II.1: Contributions relatives calculées pour les échantillons utilisés.

sitions de 0.5 g de tréhalose et 1 g de D_2O par gramme de protéine, dans les expériences à écho de spin et de 0.5 g de tréhalose et 1 g de D_2O dans les expériences de temps-de-vol. Les fonctions de diffusion contiennent différentes contributions. Les résultats des expériences de temps-de-vol contiennent une contribution prédominante de la protéine.
Les données obtenues avec les expériences à écho de spin peuvent être décrites à l'aide d'une exponentielle étirée, avec un temps de relaxation τ =110 ps et un exposant β=0.3. Les données obtenues avec les expériences à temps-de-vol permettent d'étendre l'exponentielle décroissante vers les temps plus courts, avec un bon raccordement. Il est important de remarquer qu'un ajustement des données obtenues en combinant des données de temps-de-vol et d'écho de spin ne change pas le paramètre de l'ajustement des données d'écho de spin, prises séparément.
Nous remarquons la présence d'un plateau à temps long également obtenue pour la protéine hydratée. Le valeur du plateau est égale à 0.29 ce qui montre que le signal contient une contribution élastique plus élevée. Une partie plus importante des mouvements n'a pas pu être résolue, quand nous étudions la dynamique de la protéine en présence de tréhalose.
Sur la figure II.2 nous présentons aussi les données obtenues avec une solution aqueuse de tréhalose avec une concentration de 50 % en masse. Nous montrons ici une combinaison des données des expériences en temps-de-vol et en écho de spin. La fonction intermédiaire de diffusion peut être décrite par une loi de type exponen-

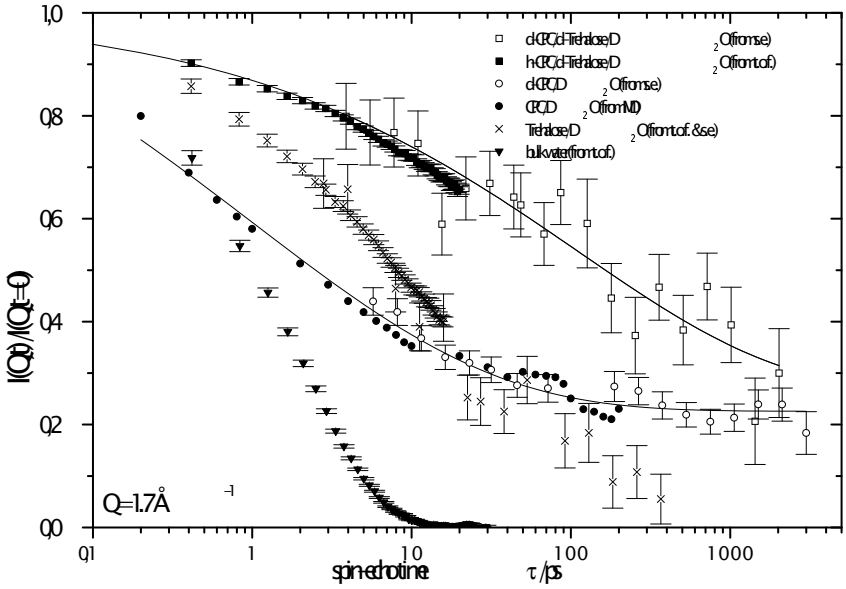

Figure II.2: Fonctions intermédiaires de diffusion pour différents échantillons et différentes techniques: temps-de-vol (t.o.F.), écho de spin (s.e.) et simulation numérique (MD). Nous comparons des échantillons contenant des poudres hydratées de protéine avec (□) et sans (○) tréhalose. Nous montrons aussi les résultats pour une solution aqueuse de tréhalose (x) et pour l'eau pure (+). Toutes les expériences ont été réalisées à Q=1.7Å^{-1} et à T=298 K.

tielle étirée avec un temps de relaxation τ=19 ps et un exposant β=0.38. La courbe décroit vers 0 dans la fenêtre du spectromètre.
A titre de comparaison, nous montrons aussi la décroissance exponentielle pour un échantillon d'eau pure. On obtient un temps de relaxation τ=1 ps. Les processus dynamiques ont lieu jusqu'à 10 ps. Il n'y a pas de mouvements pour des temps supérieurs à cette valeur.

La comparaison des données présentées dans la figure II.2 pour différentes échantillons nous conduit à la conclusion suivante:
Les mouvements de la protéine sont ralentis lorsque le tréhalose est présent. Il est difficile de quantifier exactement l'effet parce que les fonctions de diffuson sont composées de différents contributions provenant de la protéine, du tréhalose et de l'eau d'hydratation. Ces contributions sont proportionelles à la section efficace et à la concentration de chaque espèce, mais des prédictions quantitatives à partir de ces valeurs restent difficiles et incertaines. On peut avoir une idée des contributions indiviuelles en réalisant des expériences en faisant varier d'une manière systématique les concentration relatives de la protéine, du tréhalose et de l'eau d'hydratation. La contribution de l'eau est relativement importante dans l'échantillon hydraté sans

tréhalose. Le temps de relaxation de la protéine est du même ordre de grandeur que le temps de relaxation de l'eau pure. Cependant le phénomène de relaxation du système doit être décrit par une exponentielle étirée; aux temps les plus longs le signal correspond à la contribution de la protéine.

Les expériences avec des solutions aqueuses de tréhalose donnent des informations sur le comportement diffusif du sucre. La relaxation du système tréhalose /eau est plus rapide que dans le mélange protéine hydratée. Le signal contient aussi la contribution du tréhalose, mais aux temps longs, la décroissance est liée aux mouvements de la protéine.
Le temps de relaxation augmente de deux ordres de grandeur quand le tréhalose est présent dans l'échantillon. De plus,la valeur du plateau aux temps les plus longs, qui correspond aux contributions élastiques et donc aux mouvement non-résolus, augmente aussi, quand nous ajoutons du tréhalose à la protéine hydratée.
Il nous semple intéressant que l'exposant β soit le même pour les échantillons avec et sans tréhalose. Une telle décroissanc décrite avec une fonction de type exponentielle étirée peut être interprétée comme une distribution de "décroissances" avec différents temps de relaxation. Le temps de relaxation que nous extrayons de notre analyse est donc une valeur moyenne de cette distribution. Le paramètre β correspond dans cette description à la largeur de la distribution. Cette largeur est donc la même pour ces deux échantillons différents.

Nous avons obtenu des informations sur la géométrie des mouvements en analysant le facteur de structure élastique incohérent (EISF) avec le modèle de Dianoux et Volino [13]. Ce modèle décrit la diffusion d'une particule, à l'intérieur d'une sphère. Quand on analyse le signal quasiélastique d'une protéine, on obtient des valeurs moyennes sur tous les atomes de l'échantillon. On peut imaginer, que la trajectoire complexe explorée au cours des mouvement internes d'une protéine peut être décrite par une enveloppe sphérique. Une stratégie similaire a été déjà utilisée dans l'étude de la dynamique de la paravalbumine [14]. Carpentier *et al.* ont appliqué ce modèle à la dynamique des chaînes alkyls. Pour des chaînes partiellement deutériées le rayon obtenu à partir de l'EISF, dépend du degré de deutériation [15]. Quand le nombre des protons de la chaîne augmente, le rayon de la sphère augmente.
Nos résultats montrent que les dimensions de la sphère dépendent fortement du degré d'hydratation. Cette observation indique que les mouvements de la protéine ne sont possible, que s'il existe une certaine quantité d'eau d'hydratation autour de la molécule. Cela confirme les traveaux de Rupley et Careri [16] et est en accord avec les résultats présentés par Rector *et al.* Ces derniers auteurs ont trouvé une forte corrélation entre la viscosité de la couche d'hydratation et les fluctuations atomiques à la surface de la myoglobine [17]. En absence d'eau d'hydratation, on ne peut plus observer de mouvements, au moins dans la gamme de temps de nos expériences. Cela a été également démontré par Cordone *et al.* avec des échantillons contenant

du tréhalose et de la myoglobine sèche, par diffusion élastique de neutrons [18]. Nous avons pu reproduire ces résultats avec nos échantillons. L'évolution du déplacement carré moyen est harmonique dans toute la gamme de températures considérées.

Lorsque nous ajoutons du tréhalose à la protéine, la partie élastique du signal de diffusion augmente, parce que certains mouvements sont ralentis de telle sorte qu'ils ne sont plus observables avec la résolution instrumentale. Dans les courbes de l'EISF ceci se traduit par une augmentation du plateau à grand Q. Mais la géométrie reste toujours la même pour les échantillons avec et sans tréhalose. Même les dimensions de la sphère ne sont pas influencées par la présence du tréhalose. Les déplacements carré moyens sont également presque identiques pour les différents échantillons.

II.2 Conclusion

La dynamique des systèmes biologiques a lieu dans une vaste gamme temporelle et spaciale. A ce jour, il n'existe pas de moyen expérimental unique pour étudier tous ces processus dynamiques. A l'aide des expériences de diffusion de neutrons thermiques nous pouvons accéder aux processus qui ont lieu dans une fenêtre temporelle, entre la pico- et la nanoseconde. Nous pouvons observer des mouvements à une échelle atomique en réalisant des expériences dans une gamme en Q jusqu'à 5 $Å^{-1}$.
Nous avons réalisé des expériences élastique et quasiélastique de diffusion de neutrons pour étudier l'influence du tréhalose sur la dynamique interne de la protéine CPC. Le tréhalose est un disaccharide ($C_{12}H_{22}O_{11}$) qui est connu pour posséder des propriétés protectrices des biomolécules contre des conditions externes hostiles comme la sécheresse ou des températures extrêmes. Il existe deux hypothèses pour décrire l'effect protecteur à une échelle moléculaire. Crowe *et al.* ont proposé un mécanisme qui met en évidence des interactions directes entre le sucre et les biomolécules [4]. Green et Angell expliquent la protection par la formation d'un état vitreux de la solution aqueuse de tréhalose autour des biomolécules ce qui empêcherait la dénaturation de ces dernières [8].
Nous avons étudié un système modèle dans le contexte de ces deux hypothèses. La C-phycocyanine est une protéine globulaire qui contribue au cycle photosynthétique des cyanobactéries. La dynamique de cette protéine a été étudiée récemment par des expériences de diffusion quasiélastique de neutrons et par des simulations de dynamique moléculaire. Nous avons comparé ces derniers résultats avec des données obtenues avec des échantillons contenant de la CPC en présence de tréhalose. Nous avons utilisé des échantillons sous forme de poudres hydratées afin d'étudier la dynamique interne de la protéine. Nous avons pu observer des mouvements entre la pico-et la nansoseconde grâce à la combinaison de différents types d'expériences de diffusion de neutrons.

La technique de diffusion de neutrons est sensible aux sections efficace cohérente et incohérente de chaque atome présent dans l'échantillon. Le facteur de sutructure dynamique est obtenu en mesurant la contribution incohérente avec les techniques de temps-de-vol et de rétrodiffusion. Nous pouvons sélectionner certaines parties d'un échantillon, en utilisant la différence entre les sections efficaces de l'hydrogène et du deutérium. Nous avons réussi à synthétiser une forme de tréhalose deuteriée à 80 % afin de minimiser la contribution du sucre dans des mélanges avec la protéine. Dans des échantillons qui contiennent la CPC en présence de tréhalose et de l'eau lourde le signal obtenu est en majorité dû à la protéine. Dans des expériences à écho de spin nous pouvons, soit étudier la contribution cohérente des échantillons complètement deutériés, soit étudier la contribution incohérente des échantillons complètement protonés.

Nous avons mené une étude des solutions aqueuses concentrées de tréhalose avec les techniques de temps-de-vol et à écho de spin de neutrons. Aux temps courts nous avons pu décrire la dynamique du système par une loi de diffusion simple. Pour des temps plus longs, le comportement devient plus complexe. Nous avons décrit les résultats obtenus par la technique à écho de spin sur l'échelle de temps de la nanoseconde par une fonction de type éxponentielle étirée. Nous avons également étudié l'influence de la température sur la relaxation du système. Nous avons mis en évidence que pour toutes les températures étudiées un seul paramètre β pouvait décrire les différentes courbes, et nous avons pu introduire une courbe maîtresse.

Pour étudier les interactions entre le tréhalose et la CPC, nous avons réalisé des expériences sur des échantillons sous forme de poudres hydratées comme des mélanges sucre/protéine. En utilisant des poudres, nous avons pu négliger les contributions dues à la diffusion à longue distance. Nous observons plutôt des mouvements internes de la protéine, notamment des mouvements des chaînes latérales et du squelette. Nous avons comparé la dynamique de la protéine en présence du tréhalose, à la dynamique de la protéine sans tréhalose.
L'utilisation des échantillons sous forme de poudre montre que le signal contient une forte contribution élastique et un faible élargissement quasiélastique ce qui rend l'analyse des données expérimentales assez difficile.
Nous avons pu décrire les mouvements à temps court avec un modèle simple de diffusion localisée. Pour décrire la géométrie de ces mouvements, nous avons utilisé le modèle de diffusion d'une particule à l'intérieur d'une sphère. Nous n'avons pas pu mettre en évidence que la présence du tréhalose changeait la géométrie des mouvements de la protéine. Le diamètre de la sphère n'est pas influencé par le sucre. Nous avons également réalisé des expérience de diffusion élastique de neutrons. Nous avons ansi obtenu des informations sur le déplacement carré moyen des atomes de la protéine, une grandeur dont le comportement en fonction de la température est

pratiquement indépentant de la composition de l'échantillon.

L'analyse de l'élargissement quasiélastique des spectres montre un ralentissement important de la dynamique de la protéine en présence de tréhalose, surtout à l'échelle de la nanoseconde, accessible avec la technique à écho de spin.
Dans la littérature deux modèles ont été proposés pour décrire l'effect protecteur du tréhalose. Nos résultats favorisent le modèle de Green et Angell [8]. Celui-ci propose que le biomatériau est inclus dans une forme vitreuse de tréhalose. De cette manière la structure de la biomolécule doit être conservée et les processus de vie et de dégradation suspendus.
Quand on compare les résultats expérimentaux avec les deux modèles, on doit toujours considérer que les phénomènes observés dépendent fortement des conditions expérimentales et des conditions de préparation des échantillons. Par exemple, on a mis en évidence que le tréhalose formait des liaisons directes avec des chaînes polipeptidiques quond on séchait des membranes en présence de sucre [19].
Notre système contenait une protéine globulaire. Dans la plupart des expériences la protéine était hydratée avec une ou plusieurs couches d'eau. Pour cette raison notre stratégie est différente des études menées sur des échantillons complètement désséchés. Nos travaux méritent d'être plutôt comparées à ceux qui s'intéressent aux phénomènes de cryoprotection et à l'effet du tréhalose, à basses températures [20,21]. Dans ce cas, l'eau d'hydratation reste dans le biomatériau et le tréhalose empêche la dénaturation et la destruction du matériel cellulaire ce qui peut avoir lieu après la formation de cristaux de glace. Dans ce cas, le mécanisme protecteur pourrait être similaire aux phénomènes que nous avons observés dans notre système. La température de transition vitreuse très élévée du tréhalose [8, 22] et la capacité du tréhalose à garder jusqu'à 11 molécules d'eau à sa surface [23] devraient favoriser la formation d'un état vitreux autour de la biomolécule.
Nous avons mis en évidence que pour les échantillons utilisés et dans nos conditions expérimentales, les mouvements de la protéine sont fortement ralentis parce que la présence du tréhalose dans la couche d'hydratation augmentait la viscosité de celle-ci. Nous n'avons pas pu trouver d'indice pour des interactions directes entre le sucre et la molécule de CPC.

Nous avons analysé le facteur de structure dynamique pour obtenir le facteur de structure élastique incohérent (EISF). Il serait intéressant d'étudier également la dépendance en Q du signal observé à temps long avec la technique à écho de spin. Une analyse similaire à l'analyse de l'EISF devrait donner des informations sur la géométrie des mouvements dans ce domaine de temps. S. Dellerue a pu faire cette analyse avec des données des simulations de dynamique moléculaire [10]. Malheureusement une telle expérience serait très longue à réaliser et nécessiterait beaucoup de temps. A l'heure actuelle, le spectromètre MUSES est équipé d'un seul détecteur. Mais il y a un projet d'implanter un multidétecteur ce que devrait

faciliter largement des expériences de ce type.

L'étude des mouvements individuels de certaines parties d'une protéine, par example de certains résidus, nécessite la deutériation spécifique de certains acides aminés bien choisis de la protéine. Il est aujourd'hui possible de mener la synthèse complète d'une protéine à partir des acides aminés comme élements de construction. Une telle synthèse est cependant très onéreuse car on a besoin pour les expériences de diffusion de neutrons d'une certaine quantité de biomatériau afin d'obtenir un rapport signal/bruit raisonnable.

Nos expériences ne permettent pas d'expliquer pourquoi le tréhalose possède de telles propriétés de protection, ni comment le tréhalose est produit et utilisé dans la nature, voire dans les organismes vivants. Nous avons étudié comment le tréhalose modifie la dynamique de la C-phycocyanine dans des échantillons sous forme de poudres hydratées. La CPC est une petite protéine globulaire. Des interactions entre le tréhalose et d'autres protéines du mème type devraient être similaires parce que nous n'avons pas trouvé d'indice pour des liaison préférentielles entre le sucre et la protéine. Ces informations pourraient être intéressantes surtout dans le domaine de la pharmacie et de la préparation des médicaments. Des solutions de tréhalose sont déjà utilisées pour protéger et garder des médicaments à base de protéines. Les informations sur les interactions entre les molécules de tréhalose et les protéines devraient aider à l'amélioration de ces applications.

Nous avons utilisé la technique de diffusion de neutrons pour étudier le système complexe CPC/tréhalose/eau. Les neutrons ont l'avantage de permettre de regarder d'une manière non-destructive au sein d'un échantillon. Nous avons pu décrire les interactions entre les molécules de tréhalose et de CPC dans le contexte de deux modèles décrits dans la littérature. Nos résultats favorisent le modèle de Green et Angell. Ils décrivent l'éffet protecteur du tréhalose par l'encapsulation du biomatériau protégé dans une solution aqueuse vitreuse de tréhalose.

THESE de DOCTORAT de L'UNIVERSITE PARIS 6
Spécialité:
Chimie Physique et Chimie Analytique
présentée

par M. Ingo Köper
pour obtenir le grade de DOCTEUR de l'UNIVERSITE PARIS 6
Sujet de la thèse:

Influence of trehalose on the dynamics of the C-phycocyanin protein; a quasielastic neutron scattering study

Introduction

Trehalose is a non-reducing disaccharide. It occurs naturally in plants and organisms that are able to survive under hostile external conditions such as extreme temperatures or periods of drought [1, 2]. Among other molecules with similar protective effects, trehalose seems to be the most effective one [3, 4]. Even if the protective properties of trehalose have been know for about 50 years [5], the mechanism on a molecular or atomic length scale that leads to these properties remains unclear.
Nevertheless, trehalose has found already a wide field of applications, in particular in pharmacy, health care and food science. So, some month ago, the European Commission has approved the use of trehalose as a novel food in the European Union [6][1]. It can be used as additive, it is half as sweet as sucrose and comes with a lower cariogenity. For example a chewing gum containing trehalose at the place of sucrose resists not only better against moisture uptake, it is even whiter and less aggressive to teeth. Trehalose moderates the sweetness in bakery and confectionery products, can replace fat and control moisture migration in baked goods.
In medicine a dry blood typing plate has been developed to determine quickly the blood group of a patient [7]. Monoclonal antibodies are dried in the presence of trehalose and thus during storage no altering of their functionality occurs. Antibiotics for skin application were included in vesicles, that contained trehalose to prevent denaturation of the drug molecules.
There exist even a cosmetic product series, where trehalose is supposed to assist in the prevention of skin-aging processes[2]. Recent projects try to invent trehalose based products to prevent documents from aging.

We did not investigate the macroscopic effects or mechanisms of the protective use of trehalose. We studied rather effects on a microscopic length scale where only little is known about molecular interactions between trehalose molecules and the protected biomaterial, for example proteins, antibodies or membranes. Two different models have been proposed in literature to describe these interactions. One of them predicts direct interactions between trehalose and the biomaterial [1], while for the other one the biomaterial is protected by being embedded in a glassy trehalose

[1] see http://www.trehalose.co.uk
[2] see http://www.trehalose.it

structure [8].

We have studied a model system with regard to these two models. The C-phycocyanin is a small globular protein, isolated from the cyanobacteria *synechoccoccus lividus*. It contributes to the photosyntetic cycle of the bacteria. We have investigated the influence of trehalose on the dynamics of this protein by neutron spectroscopy experiments. Results obtained on samples containing trehalose coated protein are compared to data from pure protein samples [10, 11].

Dynamics in biological system cover time scales from several femtoseconds, where vibrational motions take place, up to microseconds for protein folding processes [12]. Protein synthesis takes even some seconds. There exist also a large range in space. Atomic bounds have a length of some Ångstroem, a protein has a size of some nanometers, a whole cell measures some micrometers.
There exist no single experience to cover this whole range in time and space. Using neutron spectroscopy and combining different types of spectrometer one can access to time scales from femto- to nanoseconds. Typical neutron wavelength are in the order of some Ångstroem. Neutrons therefore probe space domains from some picometers to several micrometers.
Protein dynamics is of special interest, as proteins play a crucial role in any living organism. They cover a large variety of different functions, often depending on their three dimensional structure and its changes in time. Proteins can play a role in the transport of electrons, they can be necessary to build up and keep biological structures. They can be involved in light harvesting processes, as it is the case for the C-phycocyanin, that we investigated. But all the time and through out all this different tasks the interactions between the protein and its surrounding environment, which is often an aqueous liquid, is of great importance.

Treating a biological subject with methods of a physicist always reveal besides technical problems and problems of data treatment and data analysis the problem to convince physicists of the interest of the biological problem and biologist of the interest using physical methods. Furthermore one has to take care of not neglecting neither the biological nor the physical aspect of the problem.
Trehalose is a disaccharide showing very interesting biological properties. It has been studied quite extensively. Most of these experiments investigated the biological properties of trehalose, for example its influence on the activity of enzymes. On the other hand there exist some work investigating the physical properties, especially its glass forming properties.
I tried during my work to find a way using both aspects, the physical and the biological. I used neutron scattering techniques, especially quasielastic neutron spectroscopy, always trying not to lose the biological aspect of our problem. I always tried to analyse and to interpret the obtained data in the sense of the biological

aspect of this work.

Neutron spectroscopy delivers information of the scattering behaviour of the sample. Most of the time models have to be used to interpret data. Here one has to be aware of not losing the physical and biological sense of the employed models. One also has always to consider the quality of the obtained data. It does not make very much sense trying to analyse data of medium quality with a very sophisticated model. I always tried to keep these points in mind when I analysed and discussed the obtained neutron scattering data.

In the first chapter of this work the investigated system is described. Both the trehalose and the C-phycocyanin are presented in detail. Sample preparation processes are reported.
In chapter two some theoretical aspects of the neutron scattering techniques time-of-flight, backscattering and spin-echo are given. The used spectrometer and methods of data analysis are briefly described.
To characterize dynamics of trehalose we performed neutron scattering experiments on aqueous trehalose solutions. Results are presented and discussed in the third chapter. These results will help in the discussion on data obtained on trehalose coated protein samples. The fourth chapter deals with these results.
Data obtained from the use of different spectrometers are shown and discussed in the context of the models proposed in literature. Results from divers instruments are combined to investigate dynamics on a time scale from few picoseconds to some nanoseconds.
Finally the given results are summarized and an outlook over possible further investigations is given.

1 The System Trehalose and C-Phycocyanin

In this chapter we will present some details on the systems we studied during our work: the trehalose and the C-phycocyanin. We will give information about the biological role of trehalose and try to motivate our approach in the investigation of this system. The C-phycocyanin is already quite intensively studied, especially in our group. Some details of this system will be given. We will also discuss the way, samples were prepared for the neutron scattering experiments; a protocol for the deuteration of trehalose is given.

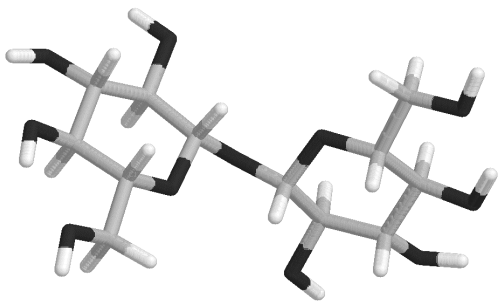

Figure 1.1: Sticks-model presentation of a molecule $\alpha - \alpha$-trehalose. Carbon atoms are represented in gray, oxygen in black and hydrogen in white.

1.1 Trehalose

Trehalose is the general name for the D-glucosyl-D-glucosides. Three isomers are known. The most common form is α-α-Trehalose that is widespread in nature. In figure 1.1 a model is shown. The chemical composition can be seen in figure 1.3. This sugar has been isolated from algae, bacteria, fungi, insects, invertebrates and yeasts as well as from lower vascular plants and a few flowering plants [24]. It has been found even in some mammalian systems. One of the most interesting facts of this non-reducing glucosides is that it has been found in large quantities in organisms that are able to survive extreme external stresses such as high or very low temperatures or periods of complete drought [2, 5, 25–27]. These organism pass in a state called *anhydrobiosis*, which is a state of suspended animation in which they may persist during several decades without suffering degradation. Once re-hydrated they resume their normal active metabolism, often within minutes [4].[1] In figure 1.2 an example of this mechanism can be seen.

Among all other known bioprotecting molecules trehalose seems to be the most effective concerning recovery of activity after re-hydration [3, 4, 29–39]. There exists a large series of *in vitro* experiments that try to explain the protective mechanism of α-α-trehalose especially investigating the stabilisation of membranes during freezing and/or dehydration [1, 3, 4, 19, 29, 30, 35, 37, 38, 40–68].
Investigations were performed using various techniques such as infrared or Raman spectroscopy, NMR-techniques, electron microscopy, neutron scattering spectroscopy or fluorescence spectroscopy.
Despite all these investigations neither the reason for the higher protective effect of trehalose nor an unique mechanism at microscopic length scale could be clearly explained .

In our work we did not investigate the difference between bioprotecting agents. We tried to examine the nature of interactions between trehalose and biomaterial.

[1] cryptobiosis or anhydrobiosis: "A state of apparent suspended animation entered by certain invertebrate animals in order to survive desiccation or other extreme stresses. It is best documented among the rotifers, nematodes, collembolans, tardigrades, and other minute inhabitants of mosses and lichens, where water film essential for active life is transient and sporadic. When the film dries out these animals appear to be dead for periods of days, weeks, or even years until moisture returns, when they 'come back to live' and resume their normal activities. Entering cryoptobiosis involves various processes. The animal typically retracts its legs and appendances, or curls up into a ball to minimize its surface area. Biochemical changes in the cuticle or the secretion of wax ensure that at least some water is retained, although this may be only 5% of the normal content, and the body becomes contracted and shrivelled. Sugars, such as trehalose, manufactured by the body cells protect the integrity of the cell membranes and also converts the cytoplasm to a glass like state. When reverting to its normal state the animal absorbs water, swells, and becomes active in a few hours." [28]

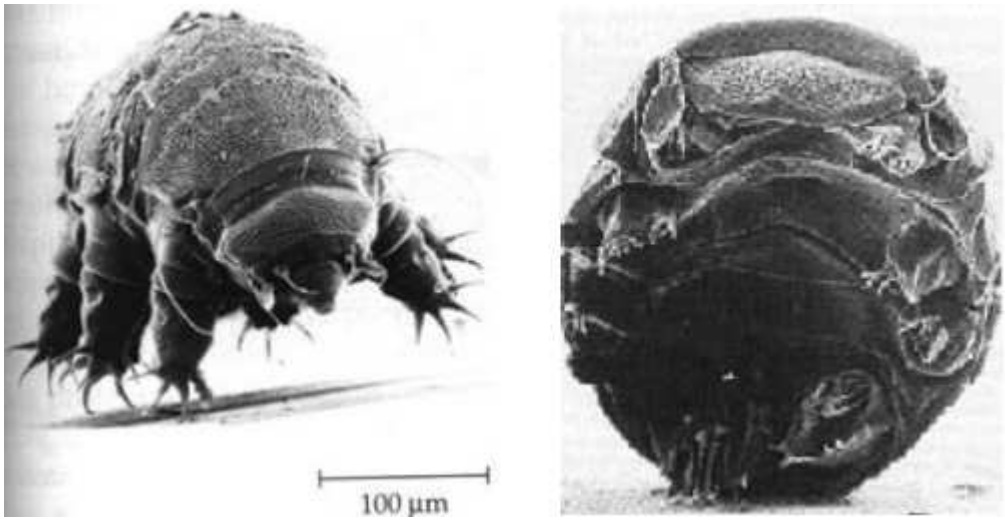

Figure 1.2: The mechanism of anhydrobiosis. left: a Tardigrade in its normal state; right: during drought, the animal passes in a state of suspended animation. It curls up to a ball to minimize its surface area. Pictures taken from `http://www.reed.edu/vvichit/tardigrade.htm`. Tardigrades have been found to be able to survive over 100 years in its dehyrated form. In addition one can froze the animal in this state to -270° C without killing it.

There exists in literature two main hypotheses to explain the protecting mechanism of trehalose. The first one, proposed by Green and Angell [8] is based on the very high glass transition temperature of trehalose solutions. Following this model the protected biomolecule is placed in a glassy trehalose structure and thus the formation of ice crystals would be hindered. The structure of the biomaterial would be conserved and life and decay processes would be suspended [69].
The other main hypothesis, the so-called 'water-replacement theory' was proposed by Crowe *et al.* [41]. It tries to find evidence for direct interactions between the protected biomaterial and the trehalose molecules. There are several examples where trehalose prevents lipid systems from fusion.
In fact, one has to distinguish between different types of protective effects. Trehalose protects biomaterial either against low temperatures where the danger arises mainly from the possible destruction of cellular material by formation of ice crystals, while at high temperatures damage occurs from the loss of cellular water. It is worth to note, that these two stress factors have some similarities, but finally they are quite different [32]. It is important to know, that during freezing a certain amount of water on the surface of biomolecules does not freeze while during dehydration the system looses all water contents what in principle leads to denaturation of proteins. It is evident, that in case of drying only direct interactions between the protected molecule and the protecting agent can assure the conservation of the molecular structure.

Molecules that protect against dehydration requires thus special properties, for example the ability to form hydrogen bridged bonds with the protected biomaterial. Only few molecules are known to be excellent protectors against dehydration while a large number of cryoprotectant substances is known.
Our investigations have to be placed closer to the type of cryoprotection. As we want to study dynamics we need in fact samples, where dynamics can be observed. In completely dehydrated samples every motion is slowed down beyond detectable time-scales [18, 70]. We studied both the dynamics of trehalose in aqueous solution as well as the dynamics of the CPC protein in the presence of trehalose in hydrated powder samples. In fact we want to get information, how the two molecules, the trehalose and the protein respectively, interact one with another. Protein dynamics are correlated to their function (see for example [71]). We investigate the dynamics of our system in order to probe, if and how the dynamics of the protein are modified by the presence of trehalose.

In the case of protection against freezing and/or freeze/drying there is no clear evidence whether direct interaction between sugar and the biomaterial is necessary. Crowe *et al.* reported in 1994 that the simple formation of a glassy state may not be sufficient to stabilize liposomes and proteins during freeze-drying [20] while other groups suggest the opposite fact [45, 50]. Nevertheless it seems clear from literature, that the protective mechanism could not be described by a simple model and depends strongly on the nature of the investigated sample as well as on the way of sample-preparation.

1.1.1 Deuteration of trehalose

For neutron scattering experiments deuterated samples can offer the possibility to vary the contrast and allow so, to separate different contributions in samples constituted of more than one type of molecule. Even for samples of only one type of molecule, partial deuteration can be very interesting [72]. In fact, protons and deuterons have very different scattering properties, as we will see in the naxt chapter. The so called incoherent and coherent scattering cross sections who describe the scattering at a sample allow to investigate different properties of the sample. For example structural information can be found in the coherent part of the scattered signal. In neutron spin-echo experiments one is interested to minimize incoherent contributions in the scattered signal. Completely deuterated samples would be ideal. Commercially deuterated trehalose is yet not available. In collaboration with Nadine Leygues from the the laboratory LADIR-CNRS at Thiais we modified an experimental procedure of Koch and Stuart for the catalytic deuteration of disaccharides [73, 74].
When one intends to deuterate a sample, two types of exchange has to be considered. Labile protons are protons of hydrophilic groups that exchange with the

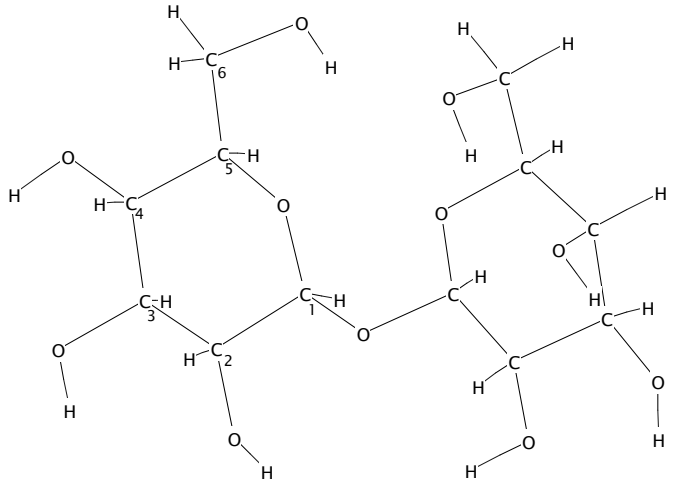

Figure 1.3: Representation of $\alpha - \alpha$-trehalose. The two rings of the molecule are spectroscopically equivalent.

solvent. They can be replaced by deuterons by putting the sample in an excess of heavy water. Hydrogen atoms that are bound covalently to the molecule can be replaced by deuterons only via chemical reactions. This can be done in some cases by catalytic reactions. The other way to obtain a deuterated product would consist in the complete synthesis starting from already deuterated products. The complete synthesis of trehalose is quite difficult, expensive and often not very effective. Industrially trehalose is prepared on a biochemical way [5]. The synthesis of deuterated trehalose should in principal be possible [75, 76], but would be very expensive and complicated.
This is why we tried the way of a catalytic exchange. The degree of deuteration can be easily monitored in ^{1}H- oder ^{13}C-NMR-spectra. NMR techniques probes the nuclear spin of the sample. Protons have a spin of $1/2$ while it is 1 for deuterons. In ^{1}H-NMR spectra, only protons are detectable. Proton decoupled ^{13}C-NMR-spectra show only signals for carbon atoms with a covalentely bound proton. By comparison of the spectra for deutarated and protonated sample one can thus determine, if a proton has been replaced by a deuteron.

Experimental details

We used a Raney nickel catalyst. When heating an alloy of nickel and aluminium in an aqueous sodium hydroxide solution, a highly porous form of nickel is formed.

This Raney nickel is useful for catalysing hydrogenation reactions.
Alcoholic protons of trehalose are previously exchanged against deuterons in an excess of heavy water.
1.44 g of Na is carefully dissolved in 20 ml D_2O. Once the reaction is finished and the solution is cooled to room temperature, 9.6 g Raney nickel is added slowly. One can observe a quite heavy reaction. The solution is diluted with D_2O to a total volume of about 90 ml. It is important to perform all these steps in a glove box in order to prevent undesired H-D exchanges.
6g of trehalose is added and the solution is heated under reflux to 115 °C during 48 hours. The solution is filtered. One has to take care, as dry Raney nickel is highly inflammable. The clear solution is evaporated. The dry residue is resolubilized with heavy water. The aluminium is purged from the solution with CO_2. The solution is filtered and passed on an ion exchange column to eliminate sodium ions. The solution is evaporated and one obtains the deuterated product. Alcoholic protons are again exchanged against deuterons by evaporating D_2O from it. If the product is yellow coloured, this might be due to degraded trehalose molecules. By heating with active carbon this can be eliminated and one obtains the deuterated product as a white powder.
The degree of deuteration can be determined from the ^{1}H-NMR and the ^{13}C-NMR spectra. In a ^{1}H-NMR spectra one investigates the modification of a magnetic field by the presence of the magnetic moment of a proton. The obtained information can give access to structural and dynamical properties of the sample. In our case, we use this technique to determine the number of protons bound to the trehalose molecule. Using the proton decoupled ^{13}C-NMR spectra and the 2D ^{1}H-NMR spectra we can attribute the obtained signals to each proton of the sugar molecule. After deuteration the signals for the exchaned protons will disapear and one can determine the level of deuteration.
In figure 1.4 the ^{1}H-NMR spectra of the protonated and the deuterated trehalose are shown. The attribution of the signals is listed in table 1.1. The signals can be attributed using the cosy 2D spectra shown in figure 1.5 in good agreement with literature [77]. The numeration of the atoms refers to figure 1.3.
One can see, that all protons have been exchanged against deuterons with the exception of the protons H_1 and H_5. These protons can not be exchanged by the reaction we used [73]. The ^{13}C spectra in figure 1.6 confirm these results. All signals but for C_1 and C_5 disappear in the NMR spectra after deuteration.
The protons bound to C_3 are not exchanged to 100%. This can be seen in the slightly perturbed signal, especially in the ^{1}H-NMR data. We estimate the level of exchange to about 80% with respect to all protons present on the molecule.

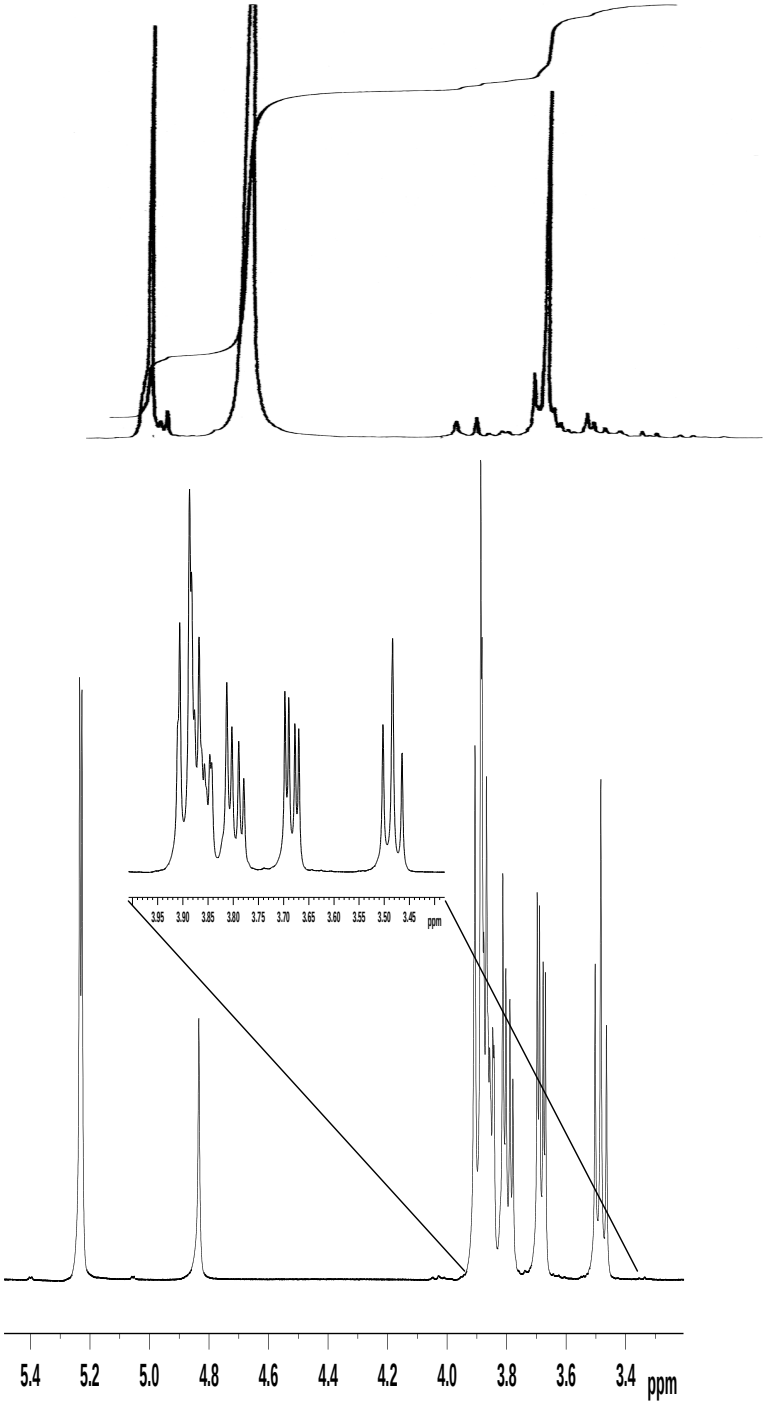

Figure 1.4: ^{1}H-NMR spectra of trehalose. Comparison between the protonated (down) and the deuterated (up) form. The protonated form shows a higher resolution as a 500 MHz spectrometer was used, while only a 200 MHz instrument was available for the deuterated form. The attribution of the signals is listed in table 1.1. One can see that in the spectrum of the deuterated molecule only two peaks, for the H1 and the H5 protons remains.

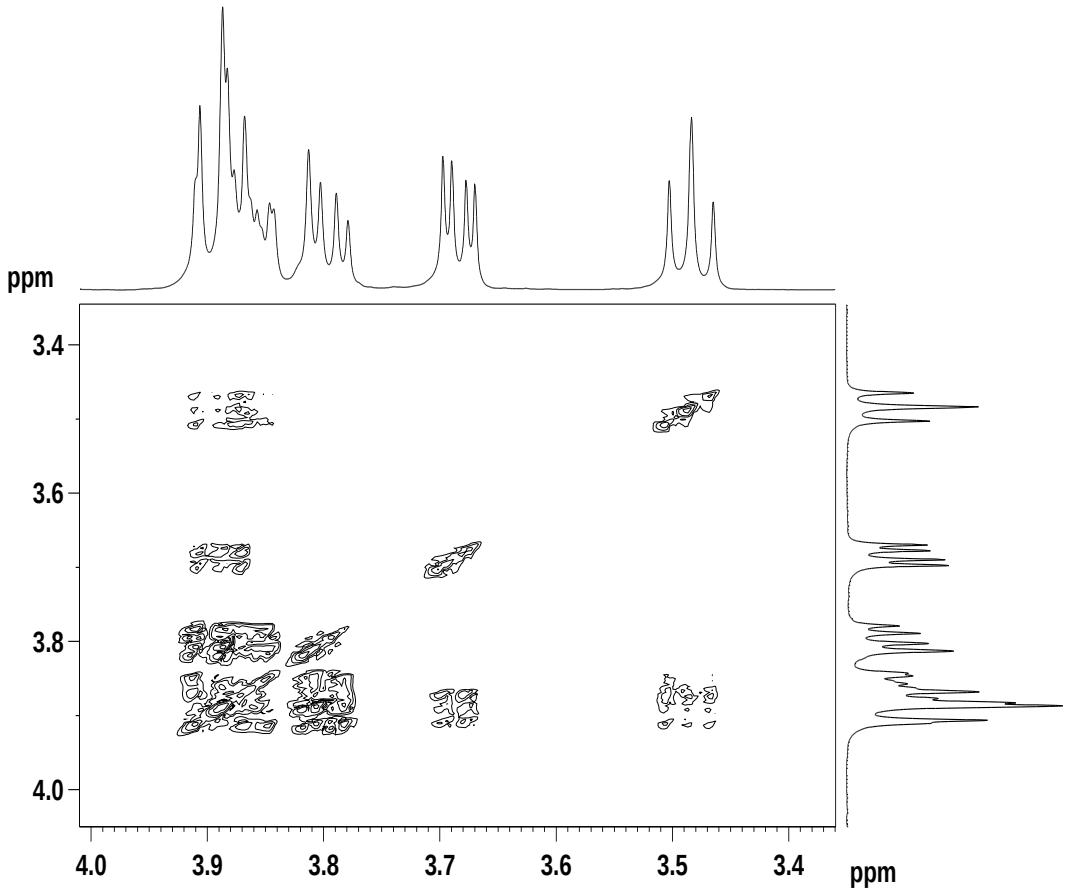

Figure 1.5: ^{1}H-COSY NMR spectra of protonated trehalose. Only the region between 3.4 and 4.0 ppm is shown. The spectra shows the coupling between The attribution of the signals is listed in table 1.1 in good agreement with literature [77].

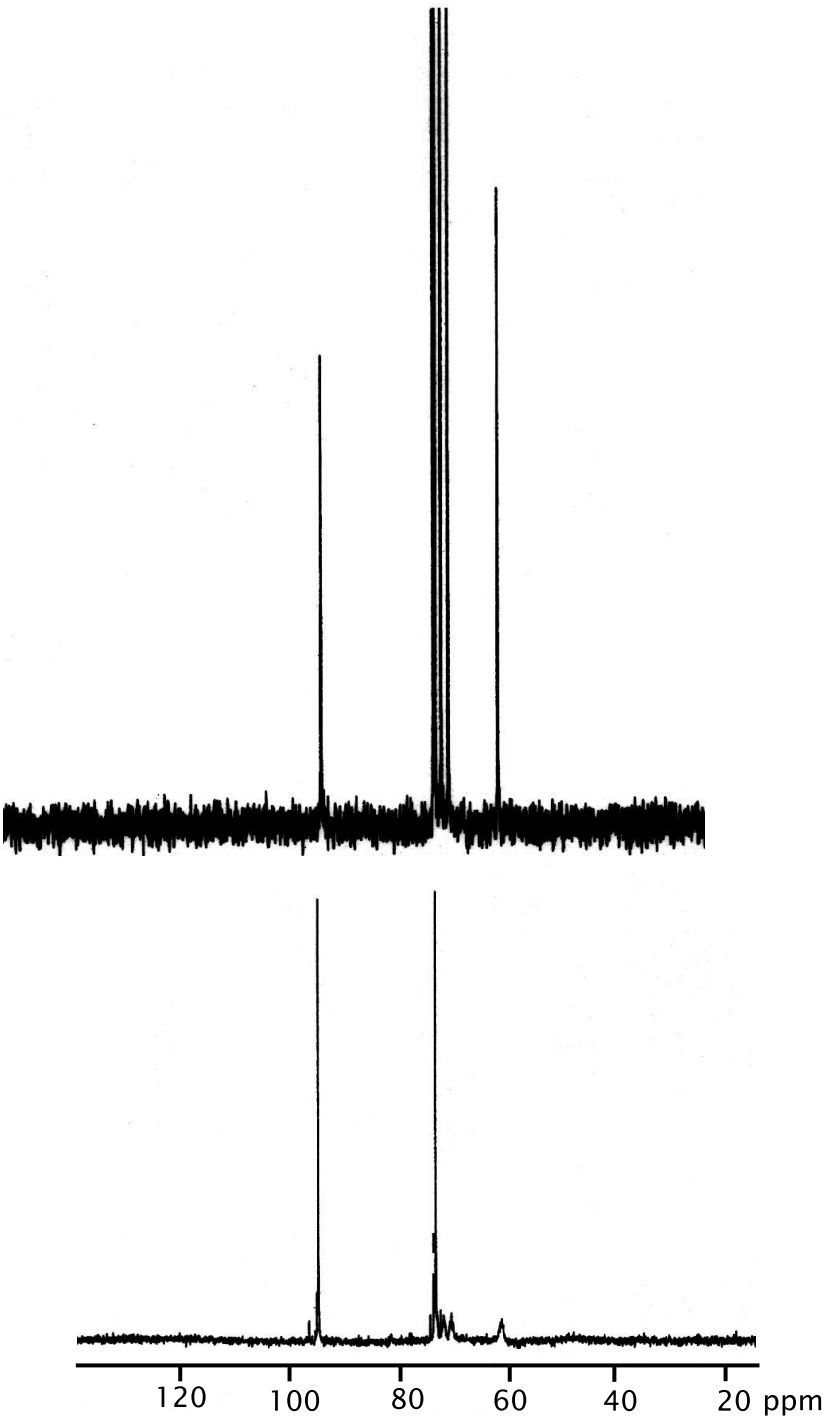

Figure 1.6: Proton decoupled ^{13}C-NMR spectra of non-deuterated (up) and deuterated (down) trehalose. The attribution of the signals is listed in table 1.1. One can see that after deuteration only two signals, for the C1 and the C5 carbon atoms remain. Protons on the other carbon atoms were replaced by deuterons.

		H-Trehalose		D-Trehalose	
		^{1}H	^{13}C	^{1}H	^{13}C
C_1	H_1	5.2 d	94.5	5.0 s	94.5
C_2	H_2	3.5 dd	73.8	-	-
C_3	H_3	3.9 *	72.3	-	-
C_4	H_4	3.5 t	70.9	-	-
C_5	H_5	3.9 *	73.4	3.5 s	73.5
C_6	$H_{6,6'}$	3.8 2xd	61.8	-	-

Table 1.1: Interpretation of the spectra in figure 1.4 and 1.6; d: doublet, t: triplet,dd: doublet of doublets, * the signal for H3 and H5 were not resolved in detail.

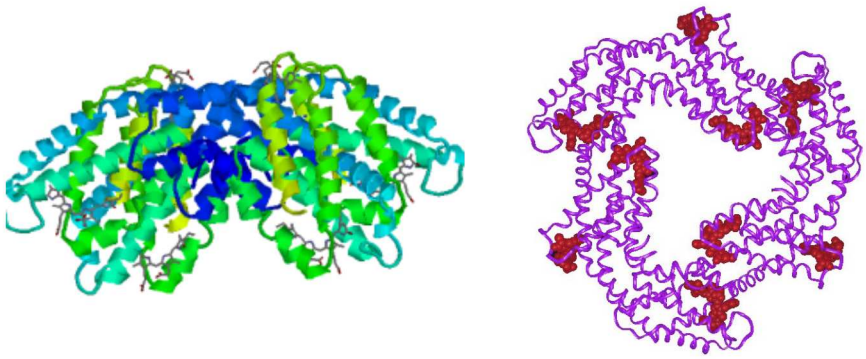

Figure 1.7: Schematic view of the monomeric and trimeric structure of the C-phycocyanin (PDB structure code 1cpc [79] and 1phn [80])

1.2 C-phycocyanin

The C-phycocyanin (CPC) is a protein, that plays an important role in the photosynthetic cycle of the cyanobacteria [78]. It can be found in the phycobilisomes of the bacteria, that represent the main complex in the light-harvesting process. The phycobilisomes are situated at the outer part of the thylakoid membrane in contact with the photosystem II. The CPC contains as all phycobiliproteins pigments that are responsable for the light-absorbing process. The so collected light-energy is transfered to the photosystem.
The structure of the protein is known at a resolution of 1.66 Å [79, 80]. The known structures from different types of cyanobacteria show quite important similarities from one to another one. Two polipeptidic chains α and β form a monomer that builds trimeric structures as can be seen in figure 1.7. We used the C-phycocyanin extracted from the cyanobacteria *synecchoccus lividus*. It was furnished by H.L. Crespi in form of a protonated and a completely deuterated form [9].
During the last years structural and dynamic properties of this protein [9, 81–84] as well as the dynamics of water at the protein surface [85, 86] have been studied. Recently S. Dellerue studied extensively the dynamics of the CPC protein by neutron scattering techniques and combined and explained the obtained results with data from molecular dynamics simulations [87, 88]. We will refer to his results in the following chapters. They will serve as a reference when we investigate the effect of trehalose on the CPC dynamics.

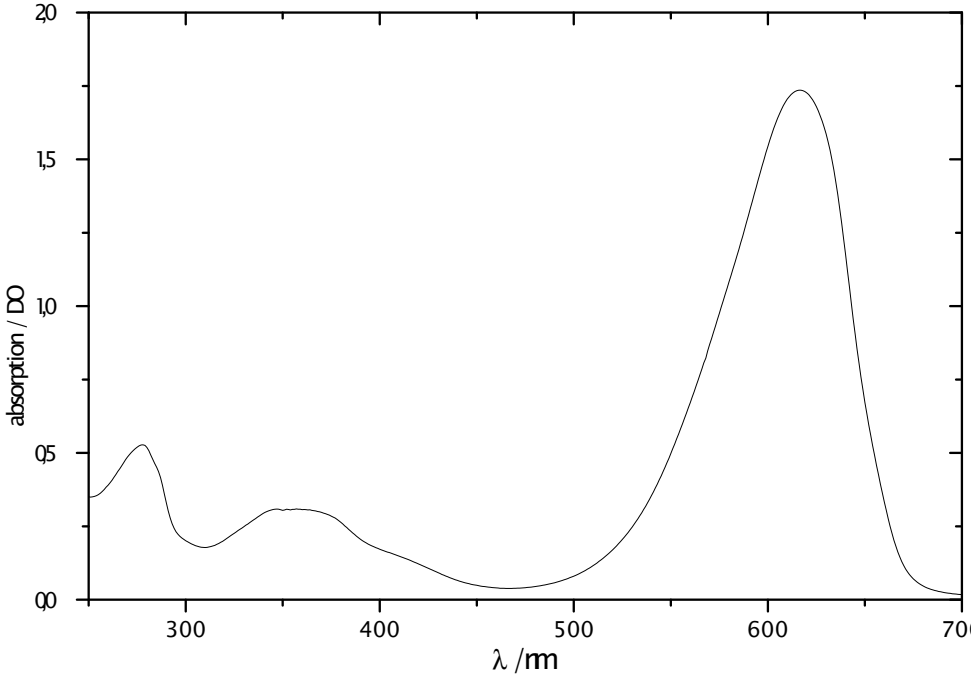

Figure 1.8: UV-vis spectrum of the CPC protein in aqueous solution. The purity is determined by the ratio between the peaks at 640 nm and 280 nm. It should be larger than 3.2 to ensure a clean product [89].

1.2.1 Sample treatment

The purity of the sample can be easily controlled by recording the UV-visible spectrum. The proportion between the peaks at 280 nm and 620 nm can give an information about the quality of the product.
We often worked on powder samples of the protein. The preparation way is as follows:
A solution of the protein, mostly in heavy water is lyophilized. During this procedure the solution is freezed in liquid nitrogen and exposed to vacuum to sublimate the water from the protein. To ensure absolutely dry powders, one can expose the lyophilized product to vacuum during some days. Dry powders are treated under controlled humidity in a glove box.
For mixed CPC/trehalose samples dry powders of protein and saccharide were mixed, solubilized in heavy water and than co-lyophilized. This treatment ensures a quite homogeneous distribution of trehalose molecules around these of the protein.

1.2.2 The primary structure in more detail

In table 1.2.2 the primary structure of the C-phycocyanin, taken from [79] is analysed in more details. One can see for example, that the amino acid alanine is the most frequent one. We will use the information about the number of exchangeable protons later on in the calculation of the scattering cross-sections of the molecule.

As we perform experiments on hydrated powder samples, we investigate internal dynamics of the protein at- short times and more precisely dynamics at the surface of the protein. Dellerue *et al.* showed by analysing molecular dynamics simulation that there exist a clear difference between side-chain motions and the motions of the backbone of the protein [11]. Furthermore they showed, that dynamics in the core of the protein are much hindered with respect to movements at the surface of the protein.

type of amino acid	occurrence	exchangeable H
alanine	111	1

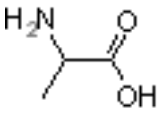

Ala - A

type of amino acid	occurrence	exchangeable H
arginine	32	5

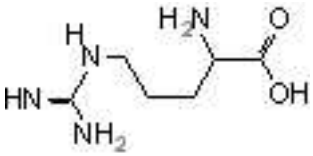

Arg - R

type of amino acid	occurrence	exchangeable H
asparagine	28	3

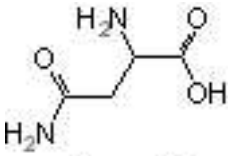

Asn - N

type of amino acid	occurrence	exchangeable H
aspartic acid	42	2

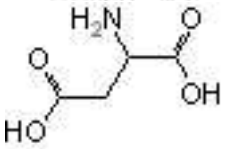

Asp - D

type of amino acid	occurrence	exchangeable H
cysteine	10	2

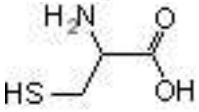

Cys - C

type of amino acid	occurrence	exchangeable H
glutamic acid	22	2

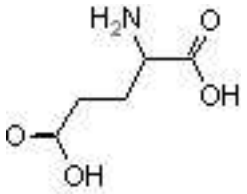

Glu - E

type of amino acid	occurrence	exchangeable H
glutamine	20	3

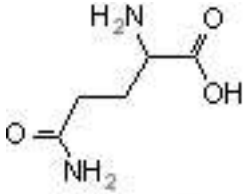

Gln - Q

type of amino acid	occurrence	exchangeable H
glycine	52	1

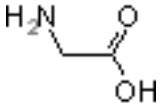

Gly - G

type of amino acid	occurrence	exchangeable H
histidine	2	2

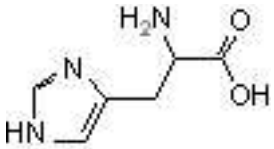

His - H

type of amino acid	occurrence	exchangeable H
Isoleucine	34	1

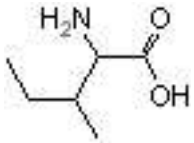

Ile - I

type of amino acid	occurrence	exchangeable H
leucine	56	1

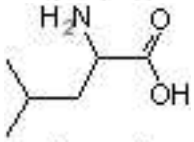

Leu - L

type of amino acid	occurrence	exchangeable H
lysine	28	3

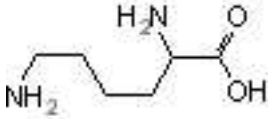

Lys - K

type of amino acid	occurrence	exchangeable H
methionine	16	1

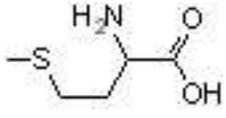

Met - M

type of amino acid	occurrence	exchangeable H
phenylalanine	20	1

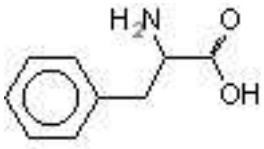

Phe - F

type of amino acid	occurrence	exchangeable H
proline	18	0

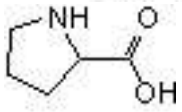

Pro - P

type of amino acid	occurrence	exchangeable H
serine	59	2

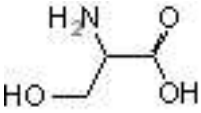

Ser - S

type of amino acid	occurrence	exchangeable H
threonine	40	2

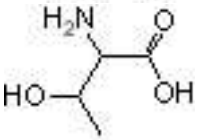

Thr - T

type of amino acid	occurrence	exchangeable H
tryptophan	2	2

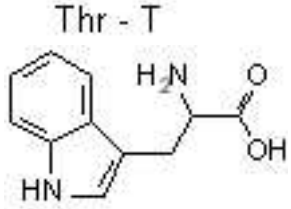

Trp - W

type of amino acid	occurrence	exchangeable H
tyrosine	40	2

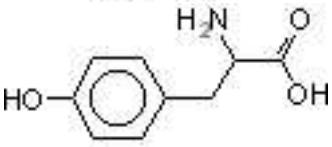

Tyr - Y

type of amino acid	occurrence	exchangeable H
valine	42	1

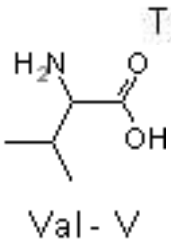

Val - V

Table 1.2: Analysis of the amino acid sequence of the C-phycocyanin (pdb-code 1CPC [79]). Listed are the occurrence of the individual amino acids and the number of labile protons per unit that can be exchanged against deuterons.

2 Neutron Scattering, Theoretical Background

Neutron spectroscopy is a powerful tool in the investigation of static and dynamic properties of soft and condensed matter physics. The energy of thermal neutrons is of the same order as molecular rotational level and its wavelengths corresponds to inter-atomic distances in condensed phases. Thus neutrons are well suited to probe rotational and translational motion. The incoherent and coherent scattering allows to separate individual dynamics of atoms from collective dynamics of the system.
In contrast to X-rays neutrons are sensible to hydrogen atoms. Further hydrogen can be substituted by the chemical equivalent isotope deuterium, thereby giving the possibility of labeling certain molecules or molecular units. Both characteristics make neutrons very useful in the investigation of biological systems.
This chapter will summarize some theoretical aspects of neutron spectroscopy and give the general formalisms, used in the data analysis. Furthermore the spectrometers used during this thesis will be presented.
A more complete information can be found for example in the books of Squires [90] or Bée [91].

Neutrons are produced in the core of a nuclear reactor. A neutron is a non charged particle with a mass $m_N = 1.66 \cdot 10^{-24}$g. It has a spin of $1/2$, which is used in the study of magnetic materials as well as for spin-echo techniques, as one can see later on.
In the frame of the particle-wave dualism a neutron can be considered as a particle, having a mass m, a velocity v with an energy $E = \frac{1}{2}mv^2$ or a plane wave of the wave-vector $k = mv/\hbar$ and the wavelength $\lambda = h/mv$; h is the Planck constant.

Due to the absence of a charge, neutrons can enter deeply into condensed matter. Interactions with any material occur between the incident neutron and the nucleus.

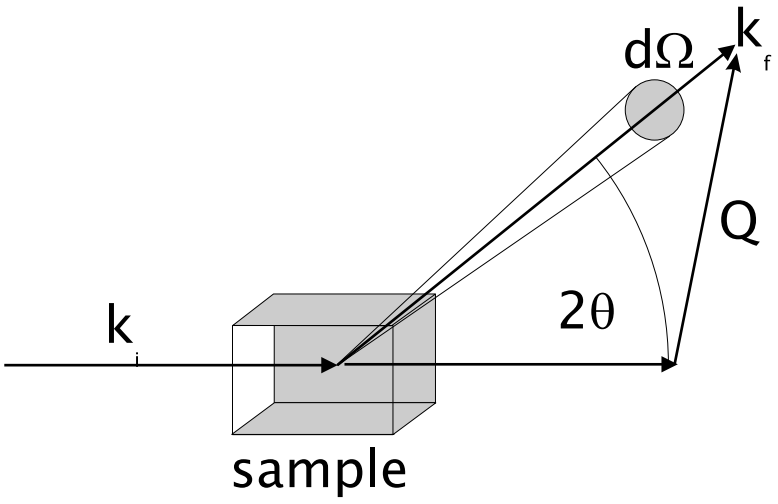

Figure 2.1: Schematic view of a scattering process

2.1 Neutron scattering

A typical neutron scattering experiment is schematically shown in figure 2.1. The incident neutron beam with the wave-vector $\vec{k_i}$ and the energy $E_i = \hbar\omega_i$ interacts with the sample under a potential V. The sample is a collection of atoms that we call *scattering system*. The scattered intensity can be expressed in terms of the quantity *cross section*. The total scattering cross section is proportional to the number of neutrons scattered per second in all directions. The differential cross section $d\sigma/d\Omega$ corresponds to the number of neutrons scattered per second into a solid angle $d\Omega$. A neutron interacts with a nucleus via nuclear forces that have a very short range compared to the thermal neutron wavelength and to the nuclear radius. Therefore, it can be shown that the neutron scatters isotropically at a single nucleus. Its strength or intensity can be characterised by a single parameter, the so called scattering length b. It depends thus on the type of nucleus and therefore on the type of isotope, as it can be seen from table 2.1. In an actual experiment, the sample is often composed of several given atomic species, each having a different scattering length. The average $<b_i>$ over all isotopes and spin-states is called the coherent scattering length. The incoherent scattering length is defined as the root mean square deviation of b_i from $< b_i >$. The difference between the coherent and the incoherent scattering length can be used to investigate only certain domains of a sample. Biological samples for example contain a large amount of protons. In experiments that investigate the incoherent scattering of a sample, for example standard time-of-flight or backscattering experiments, a deuteration of certain parts of the sample can hide this part from being detected. The obtained signal would mainly be due to the protonated part of the sample. In the same way the contribution from

a solution can be minimised when the investigated protonated solute is investigated in a deuterated solvent.

Isotope	b_{coh}/fm	b_{inc}/fm	σ_{coh} / barn	σ_{inc}/barn
^{1}H	-3.7409	25.217	1.7599	79.91
^{2}H	6.674	4.033	5.597	2.04
^{12}C	6.6535	0	5.563	0
^{14}N	9.37	1.98	11.03	0.49
^{16}O	5.805	0	4.235	0
^{32}S	2.804	0	0.9880	0

Table 2.1: Coherent and incoherent scattering lengths for some nuclei

During a scattering experiment, the incident neutron beam can exchange energy with the scattering system. The scattered beam will by characterised by the wave-vector $\vec{k_f}$ and the energy E_f. The exchanged energy between neutron and system is

$$E = \hbar\omega = E_f - E_i = \frac{\hbar^2}{2m_N} \tag{2.1}$$

During the interaction the neutron can gain or lose energy. We have adopted the definition of a positive exchange energy for a gain of energy of the neutron which corresponds to a loss of energy in the sample.
The partial differential cross section determines now the number of neutrons scattered in a solid angle $d\Omega$ and with the energy transfer $d\omega$. For a single fixed nucleus one finds:

$$\sigma_{tot} = \int\int \left(\frac{d^2\sigma}{d\Omega d\omega}\right) d\Omega d\omega = 4\pi b^2 \tag{2.2}$$

One can now determine the coherent and incoherent cross sections:

$$\sigma_{coh} = 4\pi b_{coh}^2$$
$$\sigma_{inc} = 4\pi b_{inc}^2$$

Thus the total scattering cross section can be written as the sum of coherent and incoherent terms:

$$\frac{d^2\sigma}{d\Omega d\omega} = \left(\frac{d^2\sigma}{d\Omega d\omega}\right)_{coh} + \left(\frac{d^2\sigma}{d\Omega d\omega}\right)_{inc} \tag{2.3}$$

According to the formalism of van Hove [92], the two terms on the right hand side of equation 2.3 can be expressed in terms of the correlation functions $G(r,t)$ and $G_s(r,t)$.

$$\left(\frac{d^2\sigma}{d\Omega d\omega}\right)_{coh} = \frac{1}{2\pi}\frac{k_f}{k_i}\frac{\sigma_{coh}}{4\pi}\int G(r,t)\exp(i(Qr-\omega t))drdt \quad (2.4)$$

$$\left(\frac{d^2\sigma}{d\Omega d\omega}\right)_{inc} = \frac{1}{2\pi}\frac{k_f}{k_i}\frac{\sigma_{inc}}{4\pi}\int G_s(r,t)\exp(i(Qr-\omega t))drdt \quad (2.5)$$

G_s is an autocorrelation function that gives the probability to detect a particle at the position r and at the time t, if the same particle was at the origin at t=0.

One can now introduce the following equations:

$$S(Q,\omega) = \frac{1}{2\pi}\int G(r,t)exp(i(QR-\omega t))drdt \quad (2.6)$$

$$I(Q,t) = \int S(Q,\omega)\exp(i\omega t)d\omega \quad (2.7)$$

S(Q,ω) is the dynamic structure factor and I(Q,t) is the intermediate scattering function.

It is worth noting, that at constant Q value

$$\int_{-\infty}^{\infty} S(Q,\omega)d\omega = S(Q) \quad (2.8)$$

and

$$\int_{-\infty}^{\infty} S_{inc}(Q,\omega)d\omega = 1 \quad (2.9)$$

This means, that the incoherent scattering is independent from the spatial direction, while the coherent scattering shows a Q-dependence. The coherent scattering contains structural informations on the scattering system.

The scattering vector $\vec{Q} = \vec{k_f} - \vec{k_i}$ and the energy $\hbar\omega$ are correlated via the equation:

$$\frac{Q^2}{k_i^2} = 2 + \frac{\omega}{\omega_i} - 2cos(2\theta)\sqrt{\frac{\omega}{\omega_i}+1} \quad (2.10)$$

In case of elastic scattering ($\hbar\omega = 0$) this is:

$$Q = Q_0 = \frac{4\pi}{\lambda}\sin\theta \quad (2.11)$$

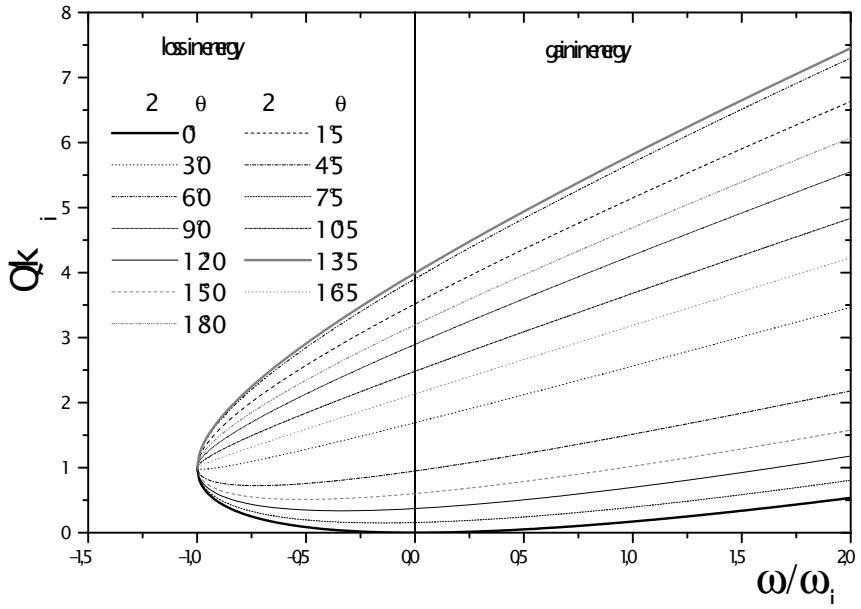

Figure 2.2: Visualisation of equation 2.10 for different scattering angles. The energy of the incident neutron beam was considered fixed.

In figure 2.2 we plot the dependence of the scattering vector from the energy for different solid angles according to equation 2.10. Inelastic scattering experiments are often performed at a constant scattering angle 2θ. To obtain informations at a constant Q-value, one has to interpolate data at different angles. In the figure, a constant Q-value would correspond in a horizontal line. We used the program package IDA to perform these transformations for data analysis (see footnote on page 75).

2.2 Neutron spectrometer

In this chapter we give a brief introduction about the neutron spectrometer used during the presented work. Most of these information and actualities of the neutron facilities of the Laboratoire Leon Brillouin and the Institute Laue-Langevin can be obtained on the internet under the following URLs:
`http://www-llb.cea.fr`
`http://www.ill.fr`

2.2.1 MIBEMOL, time-of-flight spectrometer

Neutron time-of-flight spectrometer provide information about the energy distribution of a neutron beam after interaction with a sample via measuring the time it takes the neutron to fly over a certain distance. The neutron beam is cut with a series of rotating discs, called choppers, into neutron pulses of a well defined wavelength. On the spectrometer MIBEMOL (a schematic view of the spectrometer can be seen in figure 2.3), situated in the guide hall of the reactor Orphée, six choppers are used. A chopper consists of a disk that is covered with neutron absorbing material. Neutrons can pass only through a small window in this disk. The choppers one and two of the spectrometer are counterrotating. Neutrons of the incoming white neutron beam can pass only when the windows in both choppers overlap. Thus one obtains short neutron pulses. The choppers five and six are also counterrotating. The phase between the first and the last pair of choppers is ϕ. Only neutrons with the velocity

$$V_0 = \frac{2\pi U d}{\phi + n\pi} \tag{2.12}$$

where d is the distance between the two sets of choppers, n an integers and U is the rotating frequency of the chopper.
To eliminate wavelength of higher order one uses the chopper three that rotates at the same velocity as the other ones but with the phase ϕ_3 with respect to the first set. Only neutrons with the velocity

$$V_0 = \frac{2\pi N d_3}{\phi_3} = \frac{2\pi U d}{\phi} \tag{2.13}$$

will pass all five choppers. The wavelength of the neutrons that arrive on the sample is $\lambda_0 = (\hbar\phi)/(m_N U d)$.
To obtain a better resolution one has to use a high rotation frequency of the choppers. It is now possible, that neutrons of different pulses begin to overlap, the fastest neutrons of the second pulse might arrive before the slowest neutrons of the first pulse. To avoid this, the chopper four is used. Its rotation velocity is chosen to

eliminate for example one pulse out of two.
The so produces neutron pulses are scattered by the sample. The scattered neutrons are detected by a set of detectors, their time of flight from the sample to the detector and so their energy is measured in channels of a given width.

For MIBEMOL the resolution in energy, which is given by folding the energy resolution of the primary and secondary spectrometer is well described by a Gaussian. The divergence or resolution in Q is essentially given by the incoming neutron guide. Depending on the energy or wavelength, different characteristics for the resolution have to be considered. Details are listed in table 2.2.
The choice of the wavelength and thus of the dynamic range end energy resolution depends on the nature of motions one expects to observe.

wavelength/Å	resolution/μeV	t_{max}/ps	Q_{min}/Å^{-1}	Q_{max}/Å^{-1}
4	446	3	0.693	2.929
6	96	14	0.462	1.953
9	28	47	0.308	1.302
11	16	82	0.149	1.073

Table 2.2: The effect of the instrumental resolution. Some experimental details related to the time-of-flight spectrometer MIBEMOL.

On a time-of-flight spectrometer one accesses the dynamic structure factor $S(Q,\omega)$. It is correlated to the incoming and outgoing neutron wavevector and to the scattering cross section:

$$S(Q,\omega) \sim \frac{k_i}{k_f}\frac{d^2\sigma}{d\Omega d\omega} \tag{2.14}$$

Experimental data are normalised to monitor count rates and transferred to absolute units by comparing with a well known standard vanadium scatterer. Contributions from the empty cell are subtracted beforehand without corrections for self absorption.
We analysed the data with the program IDA (ingenious data analysis) from Joachim Wuttke [1].

[1] The source code is available on the Internet under the address `http://www.e13.physik.tu-muenchen.de`

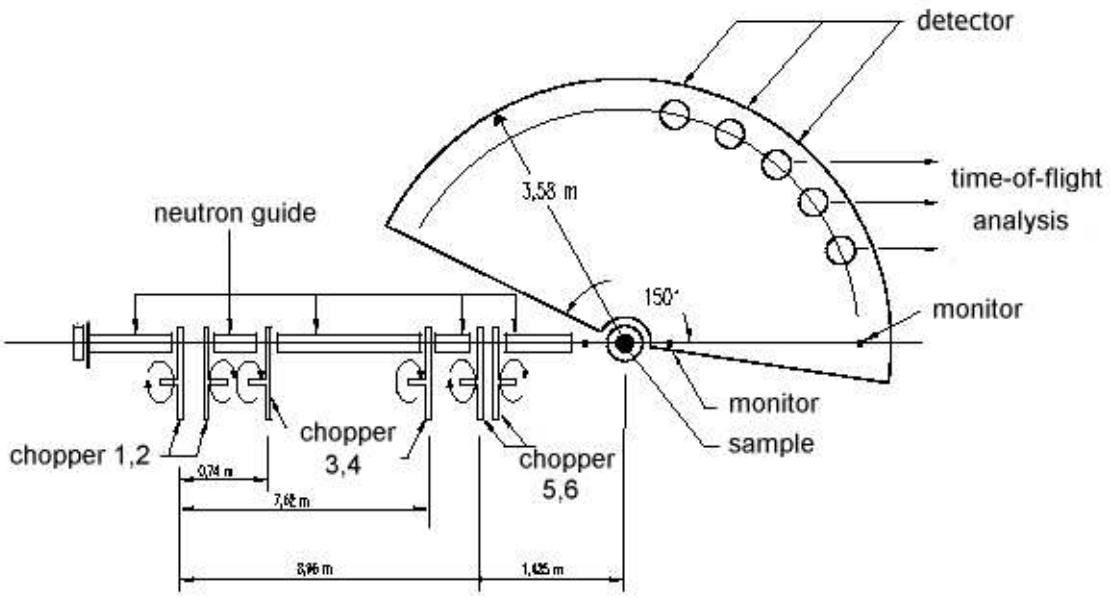

Figure 2.3: Schematic view of the time-of-flight spectrometer MIBEMOL. The incoming neutron beam is shown on the right of the figure. Its initial wavelength is adjusted by a set of choppers. After interaction with the sample the time to arrive on the detectors is measured. Thus one has access to the energy of the scattered neutrons.

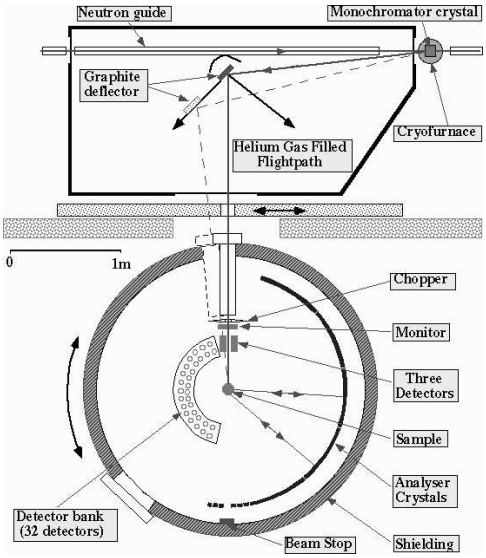

Figure 2.4: Schematic view of the backscattering spectrometer IN13. The neutrons enter in the upper left corner. The incident energy is chosen via a monochromator, a chopper creates pulses to be able to suppress those neutrons scattered directly into the detector without being analysed by backscattering at the analyser crystals. After interaction with the sample the scattered neutrons are reflected by the analysers on the detectors.

2.2.2 IN13, backscattering spectrometer

Backscattering spectrometers are another type of instrument to measure the dynamic structure factor $S(Q,\omega)$.
A schematic view of the spectrometer IN13 of the Institute Laue-Langevin(ILL) at Grenoble can be seen in figure 2.4. In this type of experiment, the energy transfer that occurs during a scattering process is analysed by varying the energy of the incident neutron beam k_i. On the spectrometer IN13 this energy is determined by using the Bragg diffraction of a monochromator crystal (CaF_2). Using the largest possible Bragg angle a high energy-resolution is obtained. One uses in fact the Bragg principle:

$$\frac{\Delta\lambda}{\lambda} = \frac{\Delta d}{d} + \Delta\Theta cot\Theta \tag{2.15}$$

Θ is the angle between the incident and reflected beam, d is the lattice parameter of the crystal. In backscattering geometry the resolution depends only on $\frac{\Delta d}{d}$ and thus on the quality of the crystal. The neutrons pass through a chopper to be able to suppress those neutrons scattered directly into the detector without being analysed by backscattering at the analyser crystals. The neutrons are scattered on

the sample towards the analyser crystals, a set of spherically curved CaF_2 crystals in (422) orientation. These crystals are chosen to reflect only neutrons with a given energy (λ=2.23Å) into the detectors. The analysers are kept at a fix temperature during the whole experiment. The incident energy is modified by changing the lattice parameters of the monochromator crystal by heating or cooling. The spectrometer works with a wavelength of 2.23 Å. Energy transfers can be detected from -100 μeV to 200 μeV with a resolution of 10 μeV (full width half maximum FWHM). This means that one can detect motions as slow as about 100 ps [93].
Using such a small wavelength as 2.23 Å rather high Q-values up to 5 $Å^{-1}$ are available. This is quite important in the study of motions in confined environment of low amplitude. The Q-dependence of the scattered signal can give information about the geometry of the dynamics. For the analysis of motions on a small length scale a large accessible Q-range is necessary.
Raw data have been treated using standard ILL software.

2.2.3 MUSES, resonance spin-echo spectrometer

The spectrometer MUSES of the Laboratoire Léon Brillouin(LLB) is a neutron resonance spin-echo spectrometer. We will give a short introduction to the theory of neutron spin-echo and show some details of the spectrometer.

The principle of neutron spin-echo was developed in 1972 by F. Mezei [94]. It uses the spin of a neutron to detect energy changes during a scattering process.We will first describe the basic principles of neutron spin-echo and present afterwards the modification invented by Gähler and Golub: the neutron resonance spin-echo [95,96].

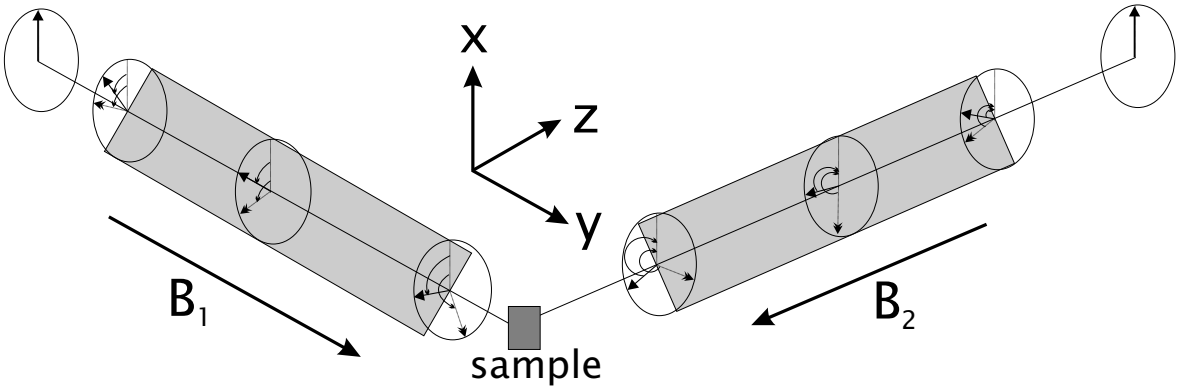

Figure 2.5: Schema of a neutron spin-echo experiment. The two arrows represent neutrons of a slightly different velocity. The polarisation vanishes while passing the first magnetic field B_1. After interactions with the sample the neutron beam enters the second magnetic field B_2 and the polarisation is rebuild.

For the description of the spin-echo principle consider figure 2.5. Polarised neutrons (with a polarisation in x-direction, while the flight direction is the y-axis) with a fairly wide distribution ($\Delta\lambda/\lambda \approx 0.15$) enter a magnetic field B_1 of the length L_1. They will precess around the field axis with the Lamor-frequency $\omega_1 = \gamma B_1$, γ is the gyro-magnetic ratio. The time t to travel through the field depends on its length L and on the velocity v_i of the neutron: $t = L/v_i$. The phase angle of the neutron at the end of the magnetic field is:

$$\varphi_1 = \frac{\omega_1 L}{v_i} \tag{2.16}$$

The polarisation in the x-direction is $P_x = cos\varphi_1$. Due to the initial broad distribution of the neutron beam, the polarisation seems to vanish after a short distance. After having passed the first magnetic field, the neutrons are scattered at the sample and enter into a second magnetic field, similar to the first one, but

having an opposite field direction. Thus the phase of the neutron is $\varphi_2 = -\omega_2 L_1/v_f$. For elastic scattering $v_i = v_f$, the sum of $\varphi_1 + \varphi_2$ will become equal to zero and the initial polarisation will be reconstituted at the spin-echo point. Changes in the length or the strength of one of the fields will cause oscillations in the detectable polarisation.
For quasielastic scattering the energy of the neutron and thus its velocity will change during the interaction with the sample. The mean velocity v_0 will nevertheless stay constant. The phase of the neutron polarisation at the spin-echo point can be described by:

$$\varphi = \omega L \left(\frac{1}{v_0 + \Delta v_i} - \frac{1}{v_0 + \Delta v_f} \right) = \frac{\omega L}{v_0^2} \Delta v \tag{2.17}$$

Here Δv is the change in velocity. The energy exchange during the scattering is $\hbar\omega = \Delta E_{kin} = m v_0 \Delta v$. Thus equation 2.17 leads to:

$$\varphi = \frac{\hbar \omega L}{m v_0^3} \omega \equiv \tau \omega \tag{2.18}$$

The spin-echo time τ depends on the mean velocity of the neutron and on the length and strength of the magnetic field. It varies typically from some pico to several nanoseconds. To determine the total polarisation one has to sum over all scatterer in the sample.

$$P_x = \int S(\omega) cos(\tau\omega) d\omega = S(\tau) \tag{2.19}$$

$S(\tau)$ is the intermediate scattering function.
Experimentally the function is determined by measuring the polarisation at the spin-echo point for different spin-echo times. These are determined by changing the magnetic field.
Data are normalised to the value at $\tau = 0$. Normalisation to a reference signal P_0 obtained from a well known scatterer (e.g. a quartz sample) is made by a simple division:

$$\frac{S(\tau)}{S(0)} = \frac{P(\tau)/P(0)}{P_0(\tau)/P_0(0)} \tag{2.20}$$

In 1988 Gähler and Golub [95–97] proposed a modification of the neutron spin-echo setup by replacing the magnetic field coils by sets of high-frequency resonance coils. These coils are placed in a non-magnetic environment. The shielding against the earth and other magnetic fields is made by a protection box of high permeable material. A neutron will travel through this box without precession.

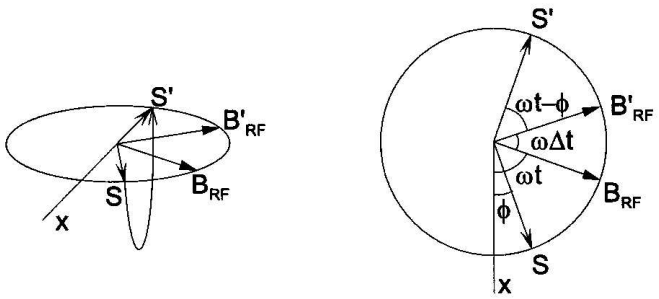

Figure 2.6: Movements of the spins in the magnetic field. a) The Spin S rotates around the field B_{RF}. The field is adjusted in a way, that the rotation ends in the same plane as is began. The magnetic field B_{RF} rotates in the same time around the z-axis. b) Determination of the phase-angle of the spin.

A resonance coil consists of two coils. One of both produces a homogeneous magnetic field B_z in z-direction, the other coil produces a field B_{RF}, that rotates in the xy plane with the frequency $\omega = \gamma B_z$. A neutron, polarised in the x-direction that enters the coil will precess around B_z with the same frequency as B_{RF}. Thus, the neutron will also precess around the field B_{RF}, the angle between the field and the neutron spin S will rest constant. The amplitude of the rotating field is adjusted to the neutron velocity in a way, that the neutron spin, when traveling through the coil of a distance l, will turn around B_{RF} with an angle $\pi = \gamma B_{RF} l/v$. So the polarisation of the neutron will be in the same plane xy at the beginning and at the end of the coil.
To determine the phase angle of the neutron spin S consider the scheme in figure 2.6. When the neutron enters the magnetic field the angle between the spin and the flight axis will be ϕ. The phase of the rotating field is ωt. The neutron will take the time Δt to cross the magnetic field. During this time the field will turn of about $\omega\Delta$t, the spin will rotate by an angle π around B_{RF}, the angle between S and B_{RF} will stay constant. Thus the angle of the spin at the end of the field is:

$$\phi' = \omega t + \omega\Delta t + \omega t - \phi = 2\omega t + \omega\Delta t - \phi \tag{2.21}$$

Equation 2.21 describes the phase angle of the neutron spin after the first resonance coil. The flight path between the first and the second coil is shielded from all magnetic field, so that the angle remains unchanged. A neutron, polarised in x-direction that enters the first coil at a time t_A will enter the second coil at a time t_B with an angle $\phi'_A = 2\omega t_A + \omega\Delta t$. The distance between the two coils is L so that $t_B = t_A + L/v$. At the end of the second coil the angle of the spin will be :

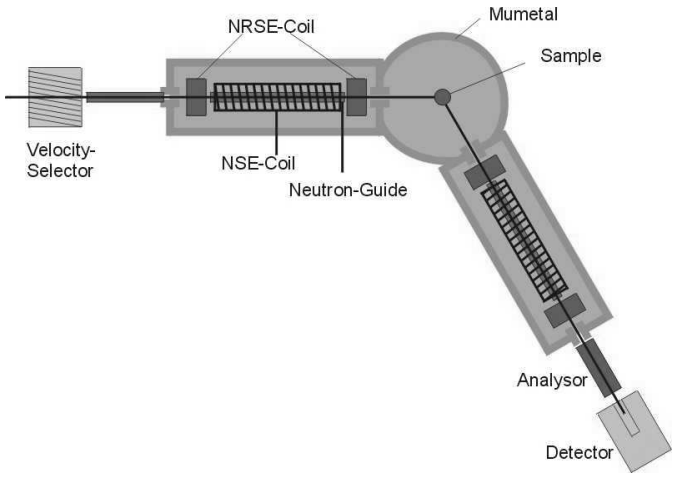

Figure 2.7: Schematic view of the neutron spin-echo spectrometer MUSES. The neutrons pass from the left to the right.

$$\phi'_B = 2\omega\left(t_A + \frac{L}{v}\right) + \omega\Delta t - \phi'_A \tag{2.22}$$
$$= 2\omega t_A + 2\omega\frac{L}{v} + \omega\Delta t - 2\omega t_A - \omega\Delta t \tag{2.23}$$
$$= 2\omega\frac{L}{v} \tag{2.24}$$

Comparison of equation 2.16 and 2.22 shows, that the combination of two resonance coils with a distance L can simulate a classical spin-echo coil of double length. Further development for the spin echo theory is equivalent for the resonance case. Measuring the spin-echo curve in the resonance case is not made by changing the magnetic fields but by varying the distance between the coils.
When replacing each resonance coil by a set of two coils with inverse static magnetic fields, the so called bootstrap principle, the spin-echo time can be multiplied by another factor two [98].

Figure 2.7 shows a scheme of the neutron resonance spin-echo spectrometer MUSES [99–101]. For small spin-echo times classical spin-echo coils as developed by F. Mezei are used. For higher spin-echo times the resonance principle is used. Both arms of the spectrometer as well as the sample region are protected against magnetic fields by a shielding of μ-metal. This allows measurements at high Q-values without use of guiding fields as they are used in classic spin-echo experiments.

wavelength/Å	t_{min}/ps	t_{max}/ps	E_{min}/μeV	E_{max}/μeV
6, option NSE	6	125	5	100
6, option NRSE	275	7000	0.1	2.4
10, option NSE	29	480	1.5	23
10, option NRSE	1280	16000	0.04	0.5

Table 2.3: Some experimental details for the neutron spin-echo spectrometer MUSES.

Data treatment

To obtain the intermediate scattering function using a spin-echo spectrometer, one measures the polarisation of the neutron beam after interaction with the sample. A detector able to measure directly the polarisation of the neutrons is yet not invented. Polarisation is measured by the supermirror polariser in front of the detector. The polarisation itself is tuned through the spin-echo point by varying the current in the second NSE coil or by changing the position of the fourth NRSE coil. A typical signal is shown in figure 2.8. The curve can be described by :

$$y = \frac{N}{2} \cdot (1 + P \cdot \cos\left(\frac{2 \cdot \pi \cdot x}{l} + \phi\right) \tag{2.25}$$

where N is the number of scattered neutrons, P the polarisation, l a geometrical factor and ϕ the phase angle of the echo.
As the polarisation of the neutron beam is polluted by field imperfections and even by the earth magnetic field, one has to take into account the instrumental resolution. When large Q-values are concerned we measure this resolution function with a quartz sample. This is a glass that scatters nearly fully coherent with high intensity between 1 and 2 Å^{-1} ($\sigma_{Si}^{coh} = 2.163, \sigma_{O}^{coh} = 4.235, \sigma_{Si}^{inc} = 0.019, \sigma_{O}^{inc} = 0.0$).
The measured function P(Q,τ) is normalised to unity for τ=0, which is in fact the static structure factor:

$$P(Q, \tau = 0) \approx \int_{-\infty}^{+\infty} S(Q, \omega) d\omega = S(Q) \tag{2.26}$$

A typical resolution function is shown in figure 2.9.
Experimental data are now normalised also to the value at $\tau = 0$ and divided by the resolution function such that:

$$P(Q, \tau) \sim I(Q, t) = \int_{-\infty}^{+\infty} S(Q, \omega) \exp(i\omega t) d\omega \tag{2.27}$$

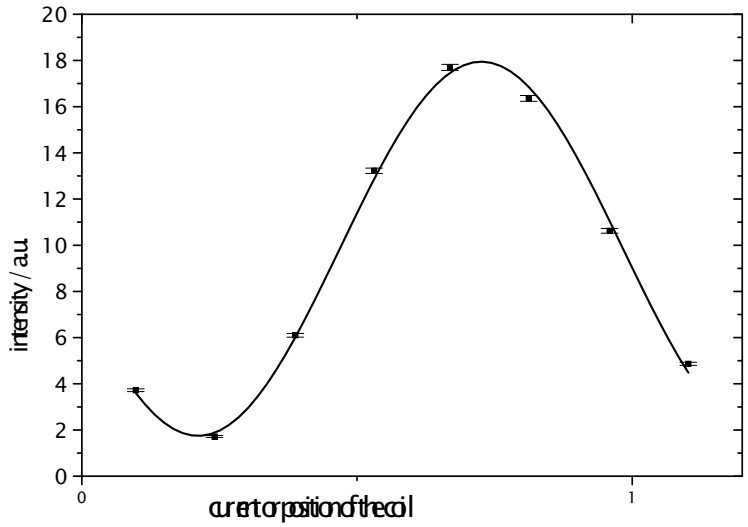

Figure 2.8: Determination of the polarisation of the neutron beam by changing field values or geometrical parameters. The solid line is a fit using equation 2.25

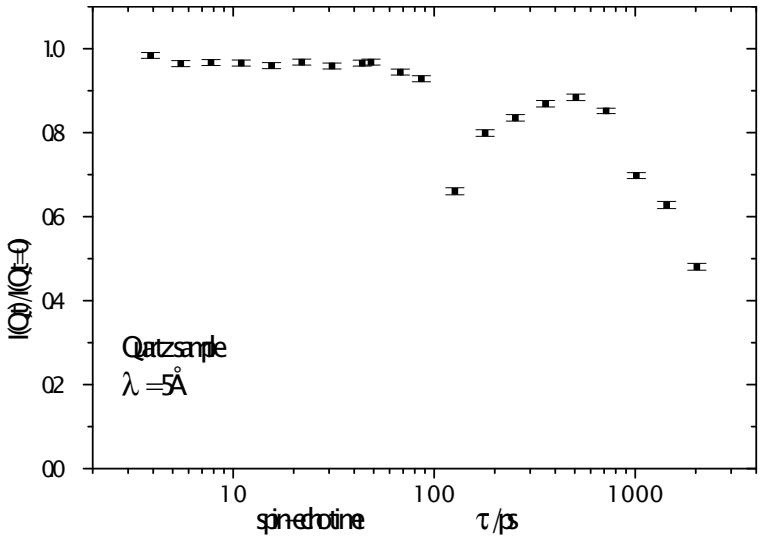

Figure 2.9: Resolution function of the spectrometer MUSES obtained with a quartz sample, using an incident wavelength of 5 Å. Data up to 100 ps are produces in the NSE mode of the spectrometer, data at longer times are available using the NRSE mode.

3 Trehalose in Aqueous Solution

To study the influence of trehalose on the dynamics of the CPC protein we characterise first the dynamics of the sugar in aqueous solution.

The system trehalose/water is already quite well investigated. One can find in literature several experimental as well as theoretical work to describe the behaviour of this system, often in comparison with other saccharide/water systems. In 1989 Green and Angell described the trehalose anomaly [8]. They found trehalose to have the highest glass transition temperature of all examined di-saccharides. Even with respect to quite similar molecules as for example maltose, the transition temperature is significantly higher. This is what they called trehalose anomaly. In fact it was their work, that serves as reference for the theory, explaining the high effectiveness of trehalose in conserving biological structure and function via forming glassy

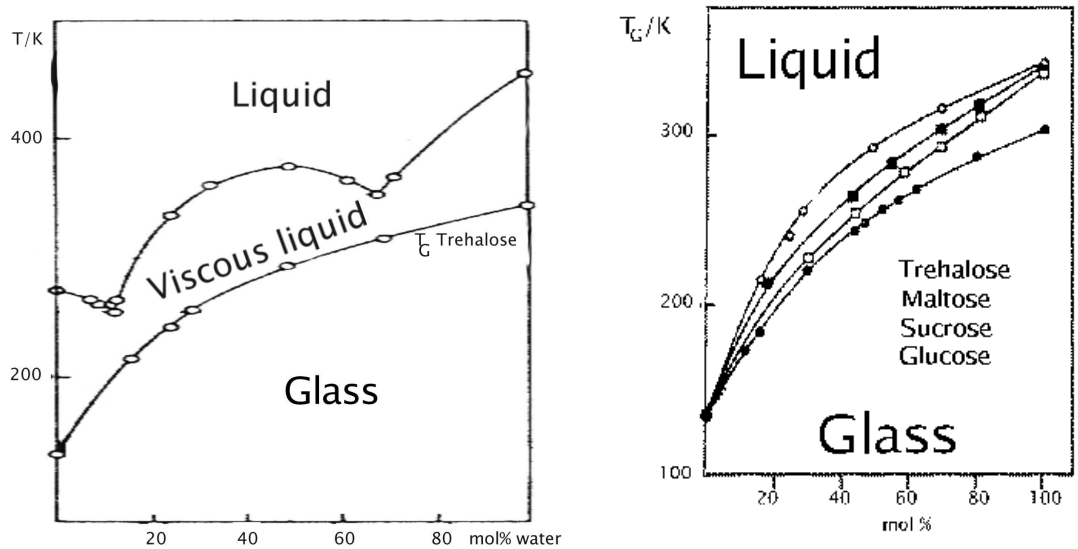

Figure 3.1: Phase diagram of the system trehalose/water and glass transition temperatures for different saccharides. The lower line in the left figure represents the glass transition for trehalose/water mixtures. Figures taken from [8]

structures. Wang and Haymet confirmed in 1998 these experiments by modulated differential scanning calorimetry. They found, that trehalose has the lowest heat of melting and heat of freezing among all other investigated saccharides [102]. They found evidence for strong intermolecular interactions between trehalose and water molecules.
Figure 3.1 depicts the phase diagram for the system trehalose/water. Also shown are the glass transition temperatures for trehalose, maltose, sucrose and glucose as a function of the water content in the sample.

Duda and Stevens found by chiroptical measurements, that the linkage geometry of trehalose in solution is relatively inflexible [103], a fact that has been confirmed by molecular dynamics simulations [104, 105].
Kawai *et al.* [106] and Magazu *et al.* [107] showed by NMR and ultrasonic measurements respectively, that trehalose has a very high ability to bind water. The hydration number varies as a function of temperature between 10 and 12 water molecules per trehalose molecule [107]. These authors found also that at high concentrations the two rings of the disaccharide should somehow overfold forming intermolecular hydrogen bridged bonds. A fact that was confirmed by Elias and Elias [108].
Akao *et al.* showed by infrared spectroscopic studies, that a cluster of a trehalose molecule and its bound water molecules behaves like a small water cluster. They called this effect "water-camouflage effect", explaining, that trehalose molecules could play the role of water on a membrane or protein surface. This corresponds to the so called 'water-replacement theory' from Crowe *et al.* [41].
Dynamics of trehalose in water have been studied by NMR-techniques [22, 109–112], photon correlation spectroscopy [113, 114] and neutron spectroscopy [23, 113].

Findings on the influence of trehalose on the dynamics and on the structure of water are quite controversial. It has been reported from molecular dynamics simulations, that trehalose affects the water structure either only slightly [115] or extensively [105, 116, 117]. Experimental details have been provided by quasielastic neutron scattering [23, 118], revealing only slight perturbations of the dynamical properties of water. Nevertheless the same authors report from another quasielastic neutron scattering experiment and from Raman spectroscopy analysis a significant influence of trehalose as well as that of maltose and sucrose on the dynamics of water [119, 120]. They attributed to trehalose the role of a "structure breaker" of the water network structure [121]. Furthermore it seems clear, that trehalose reduces the mobility of hydrogen-bonded water molecules [106] and reduces the amount of freezable water [121]. In comparison with maltose and sucrose Branca *et al.* reported from viscosity and compressibility measurements a higher interactions strength between trehalose and water [122].

We use incoherent and coherent quasielastic neutron scattering measurements to investigate dynamics of trehalose in aqueous solution. We do not investigate the

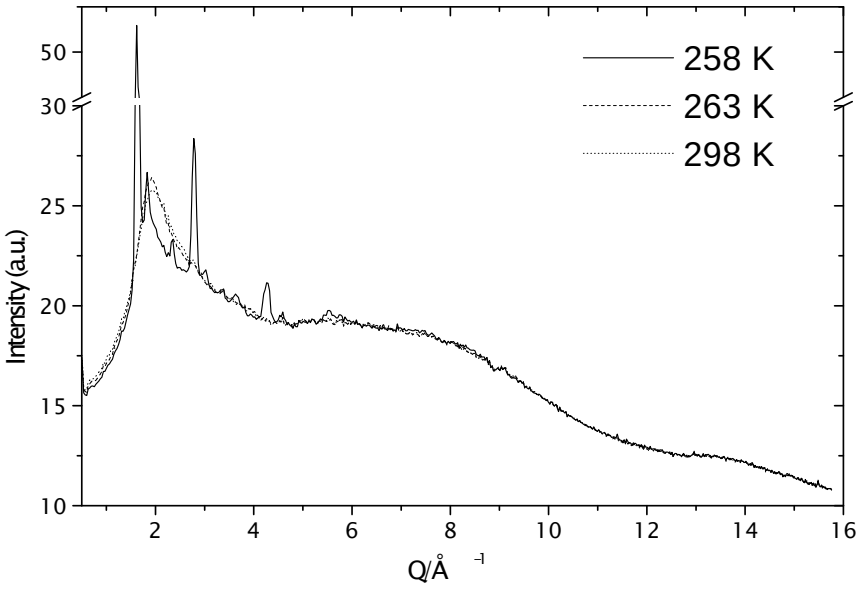

Figure 3.2: Structure factor for a 50 w % solution of trehalose in heavy water, measured at three different temperatures on the spectrometer 7C2. Bragg peaks at T=258 K show the structure of hexagonal ice crystals.

differences between trehalose and other disaccharides. Experiments were performed using neutron time-of flight and spin-echo techniques.

3.1 Structural investigation

First we present results of structural investigations of trehalose solutions. We performed an experiment on the spectrometer 7C2 of the Laboratoire Léon Brillouin. This instruments allows to measure the static structure factor over a very large Q-range [123]. We used a sample of 50 w % deuterated trehalose in D_2O (c=3.23 mol/l). The solution was placed in a cylindric vanadium cell with an inner diameter of 8 mm. Using a wavelength of 0.7 Å one can explore a Q-range from 0.5 to 16 $Å^{-1}$. Data are corrected for sample absorption, empty cell contribution and detector cell efficiency.
The obtained structure factor as a function of Q can be seen in figure 3.2.

One would expect for a typical structure factor oscillation at high Q arroud a value of 1. The decreasing signal that we observe is due to incoherent scattering contributions from the sample. The goal of this experiment was to get a global view of the structural properties of trehalose aqueous solution and not to perform a sophisticated analysis.

We performed a series of experiments by progressive cooling down the sample from room temperature down to 248 K. The results for temperatures between 298 K and 263 K are nearly the same. The curve corresponds to the typical signal of a liquid or an amorphous system. One can determine a maximum in the structure factor around 2.0 $Å^{-1}$. Between 263 K and 258 K the solution crystallises and one can observe Bragg peaks of D_2O crystals. These peaks are characteristic for ice that is crystallised in its hexagonal form [10, 124]. In our sample with a trehalose concentration of 3,2 M, the melting point of the solution is thus lowered from 277 K for pure heavy water by at least 14 K due to the presence of trehalose. Literature values for the glass transition temperature for a concentration of 50 w% are of about 190 K [22]. These results were obtained by differential scanning calorimetry on small samples. Due to the fact that our experiments that were performed on bulk solutions we could not reach this temperature. Crystallisation processes occurred before.

3.2 Trehalose dynamics

Dynamics of trehalose molecules in aqueous solutions were investigated using the neutron time-of-flight techniques with the spectrometer MIBEMOL. Neutron spin-echo experiments were performed on the spectrometer MUSES, both of the Laboratoire Léon Brillouin. Details of these spectrometers can be found in a preceding chapter.
We used samples of trehalose in water at rather high concentrations. Time-of-flight measurements were performed on the protonated form of the sugar, only labile protons were exchanged against deuterons. Spin-echo experiments were performed investigating both the coherent scattering using completely deuterated samples[1] as well as the incoherent scattering on completely protonated samples.

3.2.1 Time-of-flight experiments

We were able to investigate both the effect of the concentration as well as the temperature dependence of the dynamics of trehalose in aqueous solution.
Measurements were performed at a temperature of 298 K for a solution of 50 w% trehalose in heavy water and at temperatures between 270 K and 311 K for a solution containing 30 w% trehalose in D_2O. In time-of-flight experiments one investigates the incoherent scattering from a sample. We used samples of protonated trehalose in heavy water. Labile protons were exchanged against deuterons. The obtained signal is so mainly due to scattering from the non-exchanged protons of the trehalose molecules.
Experiments were performed at 6Å neutron wavelength, corresponding to an energy

[1] Completely deuterated means that we used the sugar with a level of deuteration of about 80% as described in the previous chapter.

resolution of 96 μeV (FWHM).
Two types of sample containers were used for the different experiments. A flat aluminium container of 1 mm thickness that was placed in the neutron beam with an angle of about 45 degree with respect to the incident beam. The second type was an aluminium hollow cylinder with a 21 mm outer diameter and a sample layer of about 0.5 mm thickness. Nominal transmissions are 87 % for the 50 w% sample and 89% for the 30 w% sample.
Data were collected for about 8 h, corrected for empty cell contributions and normalised to a standard vanadium scatterer. The obtained signal is mainly due to the incoherent scattering cross sections of the protons of the trehalose molecules. Nevertheless one has to take into account the contribution from the solution, in our case from heavy water.
To subtract this contribution we measured a sample of pure D_2O, using the same sample container as for the trehalose solution. The obtained signal can be described by a single Lorentzian line.
The dynamic structure factor of the trehalose solutions is now analysed using two Lorentzian lines, each of them folded by the measured resolution of the spectrometer and fixing the width of one of them to values obtained from the analysis of the pure water sample. Using this way of analysis we take into account the contributions from the buffer solution. The second Lorentzian line will describe the contributions due to the scattering of the trehalose molecules.
One could expect, that rotational motions of the trehalose molecules might contribute to the scattering signal. These motions would be neglected in our analysis. We consider rotational motions as to fast to be detected with the experimental resolution, they shold contribute to the background signal. This consideration is based on data published by Karger *et al* who found by NRM experiments rotational correllation times in the order of femtoseconds [22].

In figure 3.3 examples of the scattering function are given. The data can be described very well by the sum of the two Lorentzian functions. One can see, that the contribution from the heavy water to the scattering signal is very small. Nevertheless it is worth to say, that fit using only one Lorentzian line was not possible.

The temperature dependence of the diffusion coefficient as well as the effect of a change in concentration is shown in figure 3.4. The width Γ (FWHM) of the Lorentzian line that describes the trehalose dynamics as a function of the wavevector can be described by a DQ^2-law, where D is the diffusion coefficient. Deviation at small Q from this law might be due to multiple scattering effects.
Data obtained using 6 Å neutrons on a sample of 50 w% Trehalose in D_2O at 298 K are compared to those of a sample containing 30 w% trehalose at different temperatures. When varying the concentration the diffusion coefficient changes from $1.1 \cdot 10^{-6} cm^2 s^{-1}$ for the 50 w% sample to $2.2 \cdot 10^{-6} cm^2 s^{-1}$ for the 30 w% sample.

T/K	D(50 w%, 6 Å)	D(30 w%, 6Å)
270		$0.50 \cdot 10^{-6} cm^2 s^{-1}$
293		$1.75 \cdot 10^{-6} cm^2 s^{-1}$
298 / 300	$1.1 \cdot 10^{-6} cm^2 s^{-1}$	$2.20 \cdot 10^{-6} cm^2 s^{-1}$
311		$2.80 \cdot 10^{-6} cm^2 s^{-1}$

Table 3.1: Diffusion coefficients for aqueous solutions of trehalose obtained by neutron time-of-flight experiments.

Numerical values are listed in table 3.1. For comparison, for the diffusive motions in bulk water one finds a diffusion coefficient of about $2.3 \cdot 10^{-5} \mathrm{cm}^2\mathrm{s}^{-1}$.[2] The effect of the temperature is an increase by a factor of about 5 when the temperature is raised from 270 K to 311K. This corresponds to an increase in the viscosity as reported by Magazu *et al* [110]. They found that for concentrated trehalose solutions the viscosity increases by a factor of 7 when the temperature is lowered from 360 K to 250 K. The viscosity of the solution should be directly correlated to the velocity of a diffusing particle.

[2] as measured by a time-of-flight experiment on the spectrometer mibemol in similar conditions as for the experiments with aqueous trehalose solution.

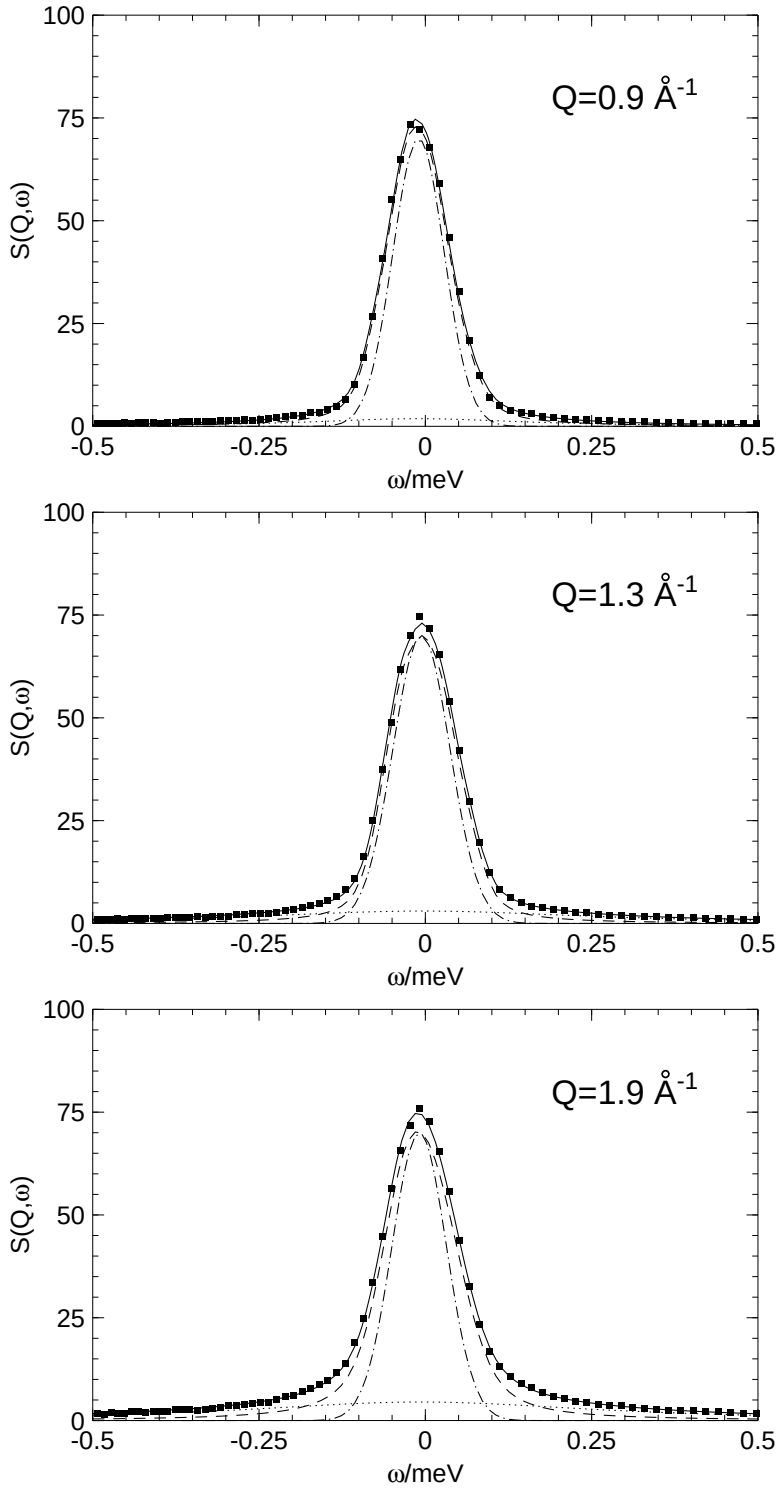

Figure 3.3: Quasielastic scattering for a 50 w% trehalose/D_2O mixture at 298 K at different Q-values. Solid lines represent best results using two Lorentzian lines. The dashed line shows the trehalose contribution, the dotted lines shows the contribution from the buffer. Also included is the experimental resolution function.

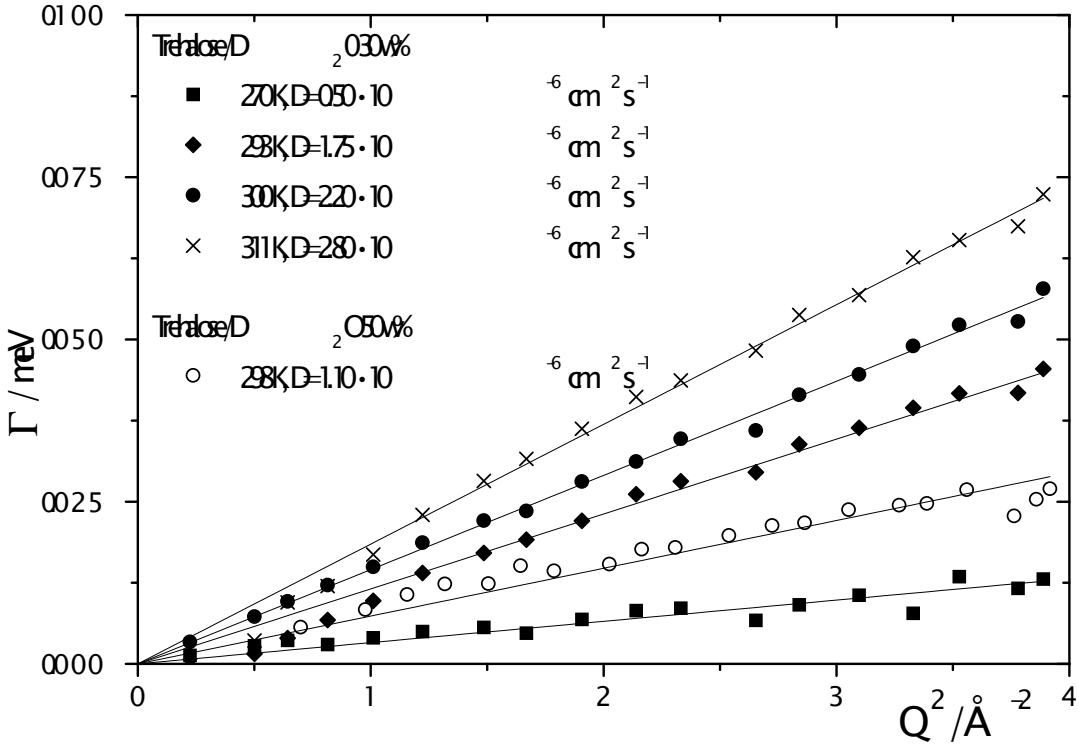

Figure 3.4: Width of the Lorentzian lines describing the dynamics of trehalose as a function of Q^2: influence of the temperature, experiments performed at 6Å. Solid lines represent fits according to a DQ^2-law, numerical values for the diffusion coefficients are shown in the figures.

3.2.2 Neutron spin-echo experiments, coherent scattering

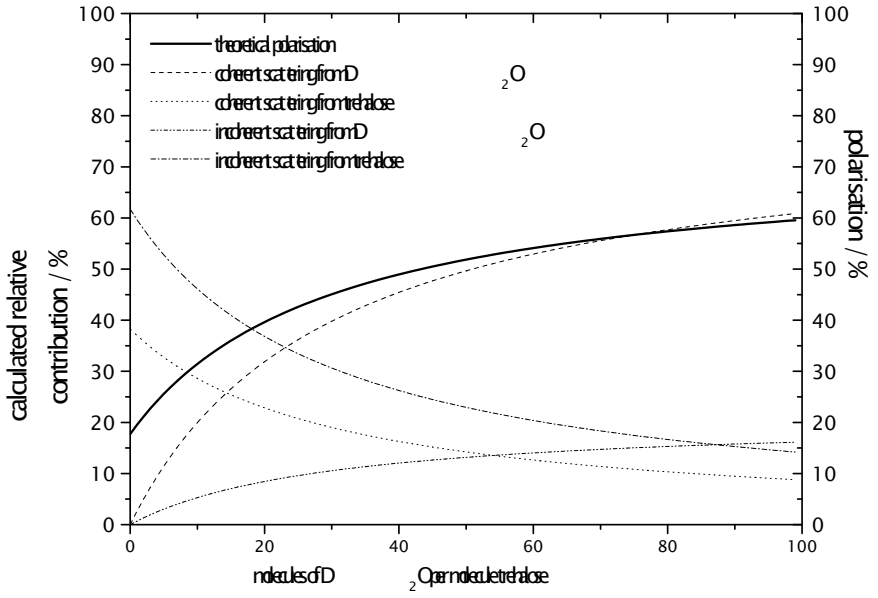

Figure 3.5: Analysis of the coherent and incoherent scattering contribution as a function of the sample concentration of deuterated trehalose in heavy water. The theoretical polarisation is calculated according to equation 3.2

All the spin-echo experiments we present were performed on the resonance spin-echo spectrometer MUSES. We performed experiments investigating the coherent scattering of a sample containing 50 w% deuterated trehalose in heavy water.
The solution was placed in a flat aluminium cell of 1 mm thickness that was closed by an indium seal. The cell was oriented with an angle of 45 degrees with respect to the incident beam. We used wavelengths of 4 and 4.8 Å. The resolution function of the instrument was measured using a quartz crystal.
We performed experiments at different temperatures and different Q-values around the maximum in the structure factor of about Q=1.9 $Å^{-1}$ (see figure 3.2). Data were collected for about 10 hours per temperature. Each data point is the result of the fit of an echo-point, determined by eight points. Even with a highly deuterated sample, the polarisation obtained from a refinement of the the raw data was limited to about 40%. This could explain the quite poor statistics of the data. In figure 3.5 some analysis of the incoherent and coherent contribution to the scattering signal as a function of the sample composition is shown. The theoretical polarisation is, at least for $\tau = 0$, proportional to:

$$P \sim \frac{I^{coh} - \frac{1}{3} I^{inc}}{I^{tot}} \tag{3.1}$$

Here $I^{coh}, I^{inc}, I^{tot}$ are respectively the coherent, the incoherent and the total scattering intensities. They are proportional to the equivalent scattering cross sections, thus:

$$P \sim \frac{\sigma^{coh} - \frac{1}{3}\sigma^{inc}}{\sigma^{tot}} \tag{3.2}$$

The chosen concentration of 50 w% corresponds to a molecular concentration of 20 molecules D_2O per molecule trehalose. According to equation 3.2 a polarisation of P=40% is calculated for this concentration. This value coincides perfectly with the experimental data.

In figure 3.6 one can see the obtained intermediate scattering function at two Q-values: Q=1.94 $Å^{-1}$, that corresponds to the maximum in the structure factor, and Q=1.7 Å. Experiments were performed in a temperature range between 250 K and 300 K. The data at Q=1.7Å and T=290 K have been extended to short times by adding data from time-of-flight experiments. The intermediate scattering function can be obtained by a Fourier transformation of the dynamic structure factor, obtained in the time-of-flight analysis, according to equation 2.7. [3]
For 250 K and 256 K the sample was probably already crystallized, as shown from experiments on the spectrometer 7C2. In effect Bragg peaks have been observed at these temperatures (see figure 3.2). We suppose, that also the fluctuations in the spin-echo signal at T=261 K could be attributed to an at least partially crystallized sample.

All the experimental curves can be described using a stretched exponential function of the Kohlrausch-Williams-Watt type:

$$I(Q,t) = A \cdot \exp\left(-\frac{t}{\tau(Q)}\right)^{\beta(Q)} \tag{3.3}$$

This type of analysis, often used in the description of glass forming liquids corresponds to a distribution of relaxation times, present in the system. β describes the width of this distribution. We do not find any temperature dependence for β; $\beta = 0.38$ at Q=1.7$Å^{-1}$ and $\beta = 0.35$ at Q=1.94$Å^{-1}$. The obtained relaxation times are shown in table 3.2.

[3] We show here in fact results obtained from different scattering processes. In the time-of-flight experiment we probe the incoherent scattering mainly from the trehalose molecules, while the spin-echo data describe the coherent scattering from the trehalose molecules and the water. Nevertheless, the observed dynamics should be similar as it can be seen by the good overlap of the two curves. Nevertheless we do not fit the combined data. The shown curve results by fitting only the spin-echo data.

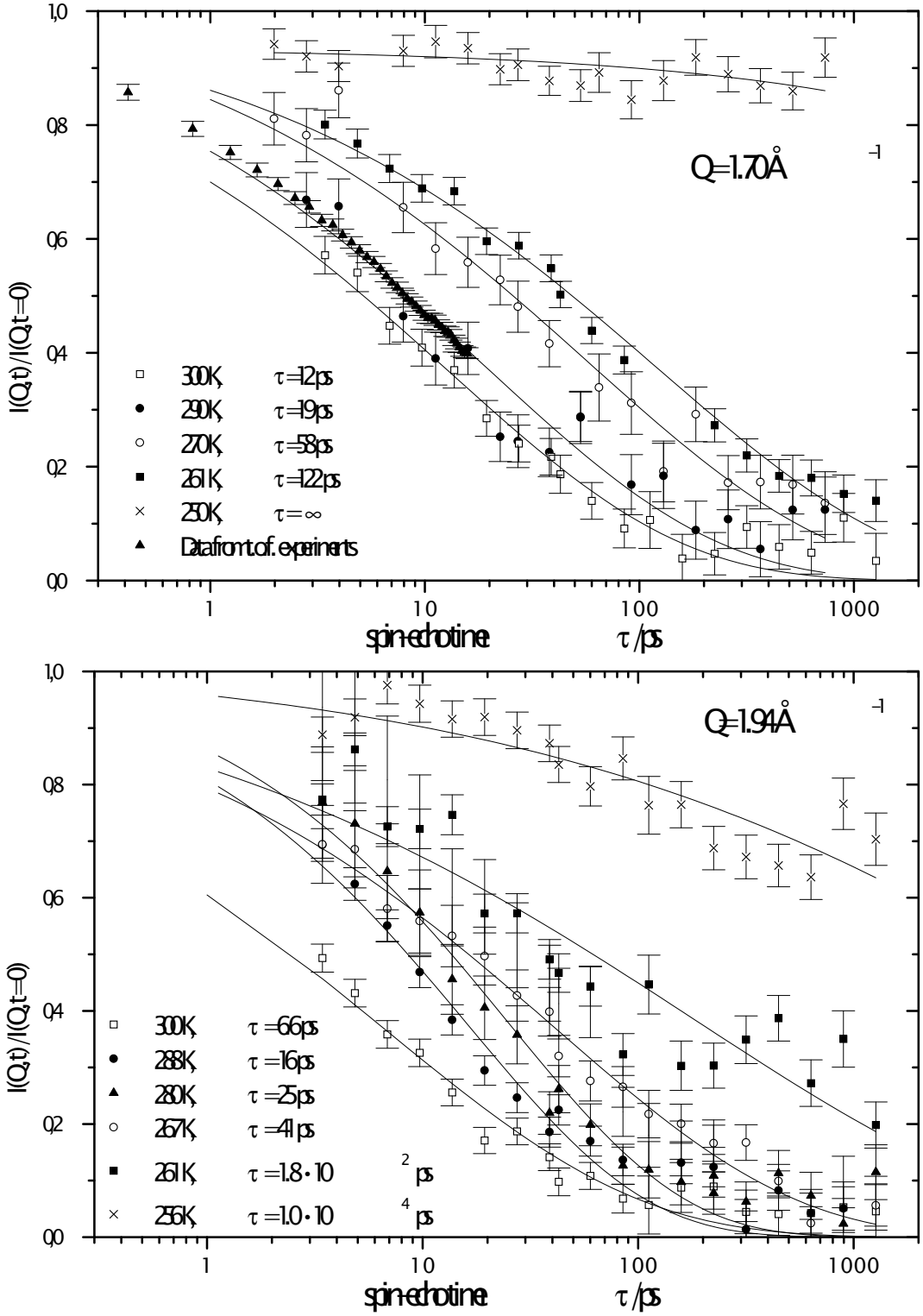

Figure 3.6: Intermediate scattering functions for a sample containing 50 w% trehalose in D_2O at different temperatures and at two Q-values. Solid lines represent refinements according to equation 3.3.

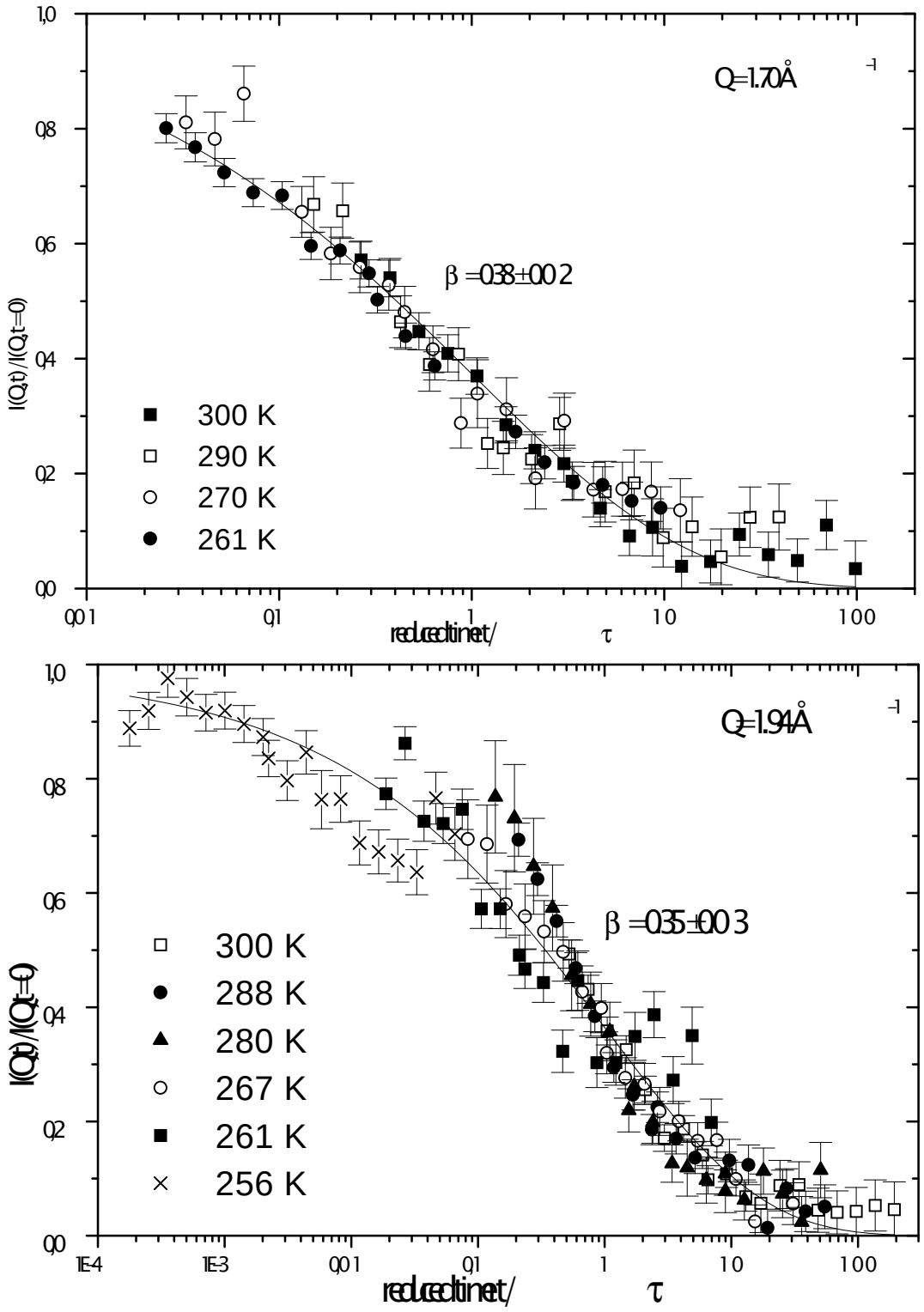

Figure 3.7: Master curve representation of the data shown in figure 3.6. On a reduced time scale experimental data for temperatures >261 K can be described by a single stretched exponential function.

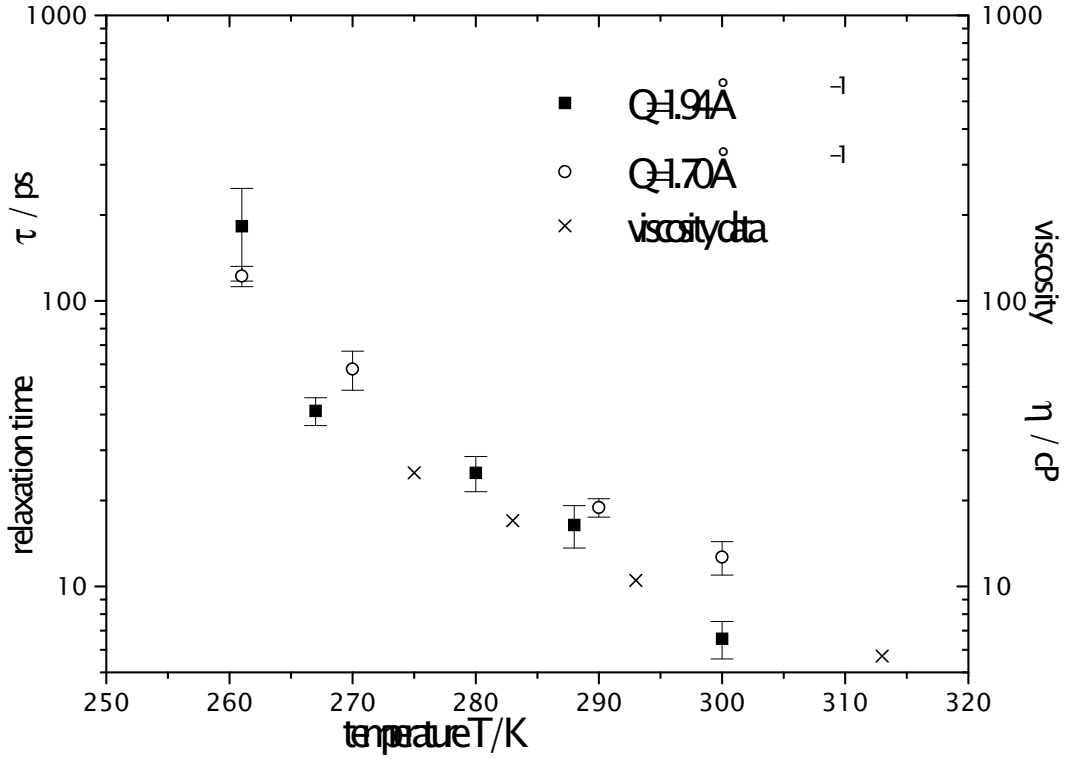

Figure 3.8: Relaxation times τ of the refinements shown in figure 3.6. We included viscosity data from [121] obtained for a sample containing 0.487 w% trehalose in H_2O.

Q/Å^{-1}	T/K	τ/ps	β
1.7	300	12 ± 1.7	0.38 ± 0.03
1.94	300	6.6 ± 1.0	0.35 ± 0.03
1.7	290	19 ± 1.4	0.38 ± 0.02
1.94	288	16 ± 2.8	0.35 ± 0.03
1.94	280	25 ± 3.5	0.35 ± 0.05
1.7	270	58 ± 9.0	0.38 ± 0.02
1.94	267	41 ± 4.6	0.35 ± 0.02
1.7	261	122 ± 10	0.38 ± 0.04
1.94	261	180 ± 65	0.35 ± 0.04
1.94	256	$2{\cdot}10^4 \pm 1 \cdot 10^4$	0.35± 0.03
1.7	250	∞	-

Table 3.2: Parameters of the curves shown in figure 3.6. The relaxations times are shown as a function of temperature in figure 3.8.

Data for all temperatures can be plotted on a master-curve where the spin-echo time is divided by the obtained relaxation time. In figure 3.7 one can see that all the data points can be described by a common master curve according to equation 3.3 obtaining a value for β of about 0.35 for Q=1.94 Å^{-1} and 0.38 for Q=1.7 Å^{-1}. Data for Q=1.94 Å^{-1} and 256 K were included in the graph. For Q=1.7 Å^{-1} and T=250K it was impossible to determine a reasonable relaxation time [4]

In figure 3.8 the evolution of the relaxation time τ as a function of temperature can be seen. It increases nearly exponentially when decreasing the temperature. One has to consider, that data obtained at Q=1.94 Å and T=256 K hardly can be described by equation 3.3. The relaxational process is slowed down to time scales that are no longer covered by the experimental conditions. The relaxational process is shifted from a ns-time scale to longer times. The experimental data obtained in the time-window of the spectrometer do not give enough information to be properly fitted by equation 3.3.

We obtain an increase in the relaxation times by an order of magnitude when decreasing the temperature from 300 K to 260 K. This is in quite good agreement with findings from viscosity measurements [121,125]. They showed that the viscosity of aqueous trehalose solutions increases by about a factor of 7, when the temperature is reduced from T=330 K to T=250 K. As one can see from figure 3.8 the viscosity for a similar sample shows the same temperature dependence as our relaxation times. When we suppose, that the protein motions are correlated to the viscosity of its hydration shell, an increase in the viscosity should lead to a slowing down of the protein dynamics. In fact, viscosity measurements describe a macroscopic phenomenon while our experiments access microscopic properties. Nevertheless, both techniques are complementary. The viscosity is proportional to the relaxation time.

[4] In fact we performed an iterative fitting procedure. The data for the different temperature were first fitted individually. With the obtained relaxation times we obtain a master curve. Here we get the parameter β that can now be reintroduced to re-fit the relaxation times.

3.2.3 Neutron spin-echo experiments, incoherent scattering

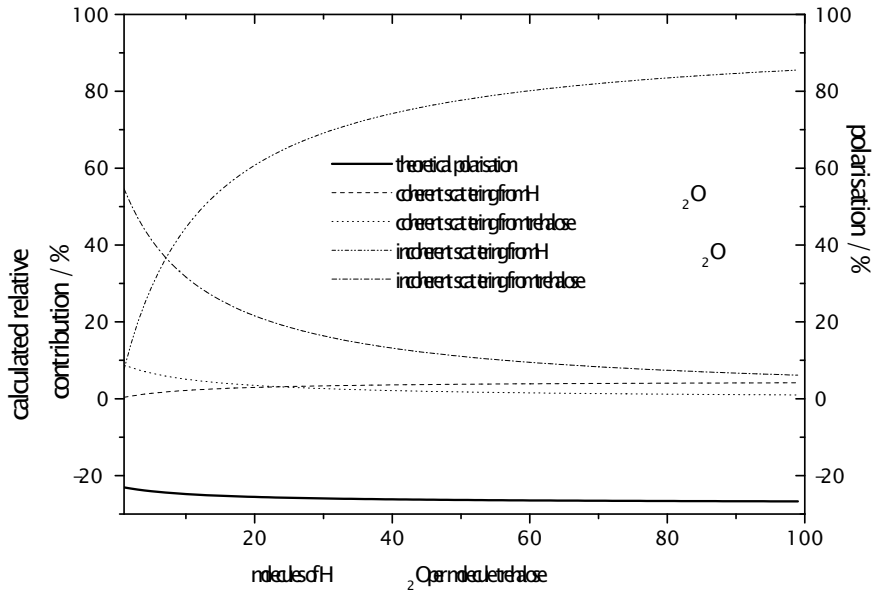

Figure 3.9: Analysis of the coherent and incoherent scattering contribution as a function of the sample concentration of trehalose in H_2O. The theoretical polarisation is calculated according to equation 3.1

We performed also an spin-echo experiment using of the incoherent scattering of a completely protonated sample, $C_{12}H_{22}O_{11}$ in H_2O. The investigation of an incoherent scattering signal using the spin-echo technique is quite disadvantaged. Protons have a spin of 1/2. When a neutron, also with spin 1/2 interacts with a proton, the neutron spin can be flipped with a probability of 50 %. As the polarisation is directly correlated to the orientation of the neutron spin, the polarisation of a completely polarised neutron beam decreases to 1/3. This is the explanation for the subtraction of $1/3 \cdot I^{inc}$ in equation 3.1. The polarisation might also be lowered by the instrumental imperfections, the coherent contribution from the sample and multiple scattering effects. A theoretical analysis according to equation 3.1 of the polarisation and of the coherent and incoherent scattering contributions are shown in figure 3.9. One can see, that the polarisation one could obtain is of about -20 %, and this nearly independent from the sample composition.

We prepared a sample containing 50 w% trehalose in H_2O. The solution was placed in a hollow cylinder with 0.2 mm space between the inner and the outer cylinder. Data were collected at different Q-values between 0.2 and 1.7 $Å^{-1}$ and at temperatures between 263 K and 295 K. Data collection time per Q/temperature

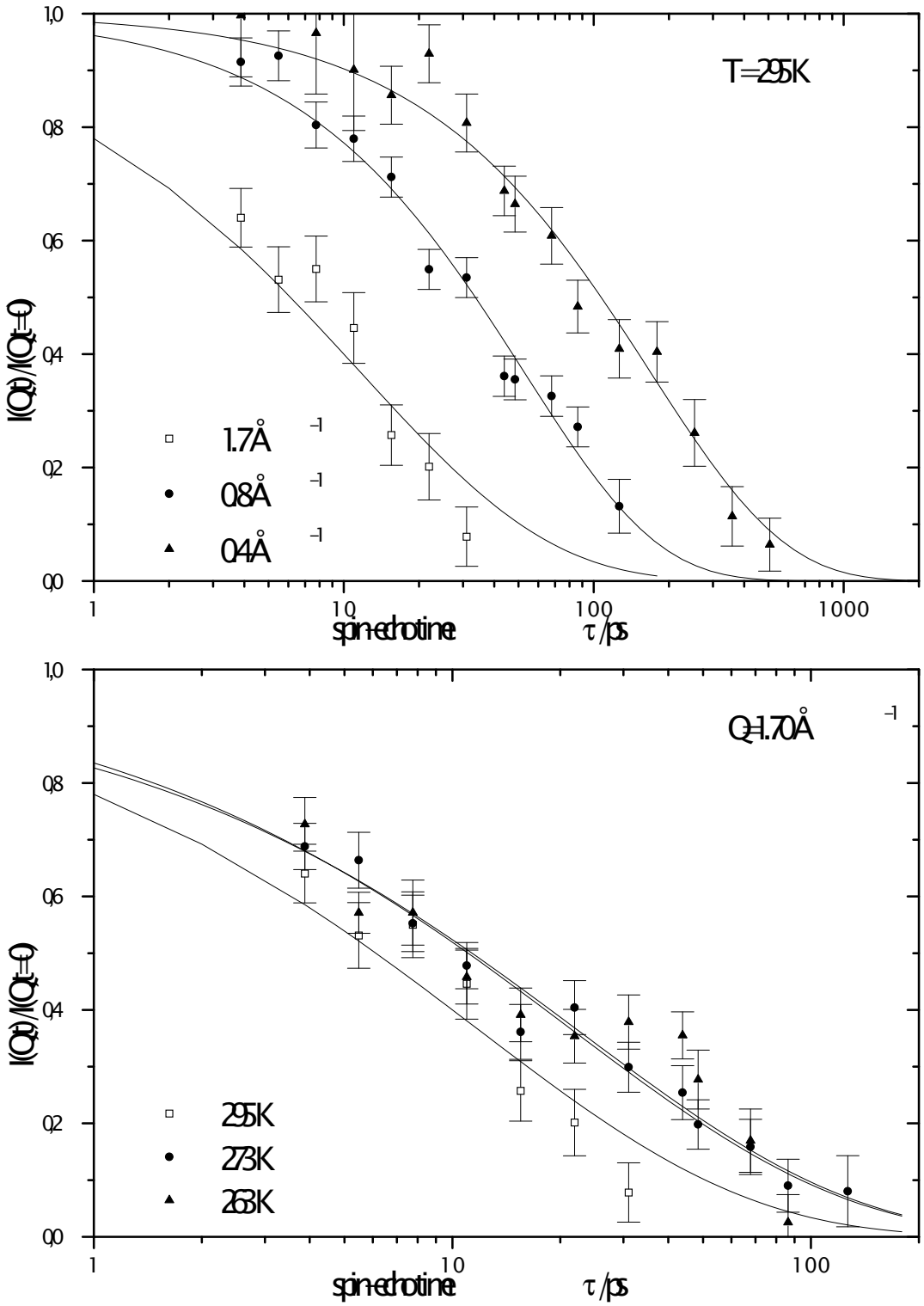

Figure 3.10: Intermediate scattering functions for a sample of 50 w% trehalose in H_2O. Solid lines represent fits using equation 3.3.

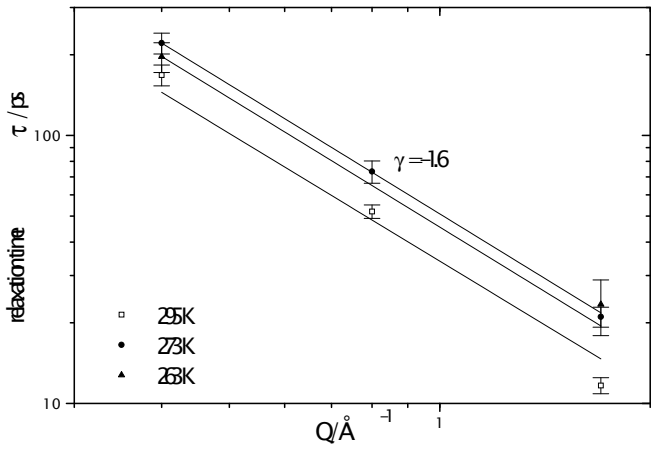

Figure 3.11: Relaxation time from data shown in figure 3.10 as a function of the scattering wavevector. The solid lines represent an adjustment using a power law.

pair was of about 12 hours. As one expects for an incoherent scattering signal, there was no structure in the polarisation or the intensity as a function of the wavevector. The obtained polarisation was of about 15 % over the whole Q-range.

In figure 3.10 are shown the obtained intermediate scattering functions. We present both the dependence on Q at a fixed temperature as well as a slight temperature dependence at one scattering angle. The curves can be described quite well using a stretched exponential function according to equation 3.3. The stretching parameter β decreases for higher Q-values. The observed relaxational process fits perfectly the instrumental time window. The obtained relaxation times vary between 10 and 200 ps. Their evolution as a function of Q is shown in figure 3.11. The slope can be described at all three temperatures by a power law:

$$\tau(Q) = A \cdot Q^{\gamma} \tag{3.4}$$

finding a unique value of the exponent γ=-1.6. For a free diffusion one would expect a value for γ=2. This shows that, probably due due the relatively high concentration, the diffusion of the trehalose molecules as well as the diffusion of the water molecules in the solution are hindered. A fact that has also been shown by Molecular Dynamics simulations of aqueous trehalose solutions [105, 115, 116]. Indeed the role of a structure-braker of the water structure has been attributed to trehalose [104, 126].
In figure 3.12 the intermediate scattering functions are presented on a reduced time scale using the same principle as described for the coherent scattering experiments. As in the coherent scattering experiments all data follow a master curve.

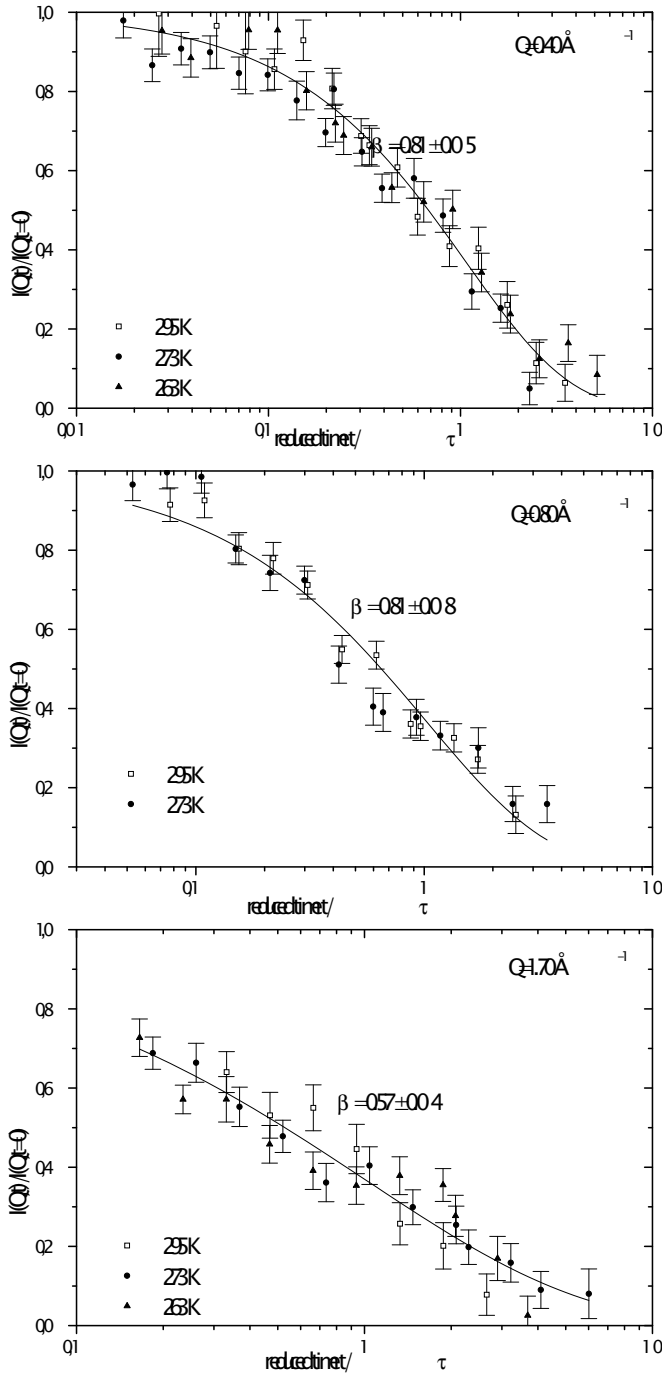

Figure 3.12: Master curve representation of the data obtained on a sample containing 50 w% trehalose in H_2O. The superposed curves can be described by a stretched exponential function.

3.3 Summary

In this chapter we presented results obtained on aqueous solutions of trehalose. The structural aspects were investigated showing a structure factor with a maximum at Q=2 $Å^{-1}$. Dynamics were investigated using neutron time-of-flight and neutron spin-echo spectroscopy. Time-of-flight experiments on samples of protonated trehalose in heavy water ($C_{12}H_{14}D_8O_{11}/D_2O$) gave access to the diffusion of trehalose molecules in solution. With neutron spin-echo experiments we performed both coherent scattering experiments on completely deuterated samples ($C_{12}H_4D_{18}O_{11}/D_2O$) and the incoherent scattering on completely protonated sample ($C_{12}H_{22}O_{11}/H_2O$). We investigate here the collective dynamics from both the trehalose as well as from the water molecules.
Dynamics up to 10 ps could be described using a simple diffusion model; the time-of-flight data could be analysed on an energy scale using a single Lorentzian line. When using neutron spin-echo techniques one investigates dynamics on a larger dynamical scale. Slower motions might now contribute to the scattering signal. Thus dynamics become more complicated and have to be described by a distribution of relaxation times, using a stretched exponential function.
Incoherent spin-echo measurements showed, that the stretched exponential behavior increases when increasing the scattering vector Q. For Q=0.4 $Å^{-1}$ a stretch exponent $\beta = 0.8$ was found, while β was equal to 0.57 for Q=1.7 $Å^{-1}$.
For the incoherent as well as for the coherent scattering results, the temperature superposition has been applicated. Data on a reduced time scale could be described using a single expression with a unique stretching exponent β.

Figure 3.13 shows experimental data obtained on a sample containing 50 w% deuterated trehalose in heavy water($C_{12}H_4D_{18}O_{11}/D_2O$). Spin-echo data at 290 K can be extended to shorter times by adding data from time-of-flight experiments. The refinement shown in the figure is a refinement of the spin-echo data and not on the combined data. The time-of-flight data overlap nevertheless quite well with the theoretical curve. They can be described by a single exponential decay. In fact our analysis on the energy scale using a Lorentzian function to describe the trehalose dynamics corresponds to such an analysis. The transformation of the corresponding width of Γ=0.013 meV (see figure 3.4) corresponds to a relaxation time of τ=20 ps. On a larger dynamical scale a single exponential decay is no longer valid. One has to introduce a stretched exponential behaviour, corresponding to a distribution of relaxation times. Nevertheless the obtained mean relaxation time of τ=19 ps corresponds perfectly to the time-of-flight data. The stretched exponential behaviour is due to other contributions that contribute to the scattering signal, as for example molecular rotations, that are not or only less visible at short times. In the spin-echo experiments one has also to consider contributions from the water molecules. In fact we measured in our neutron spin-echo experiments the collective motions in the

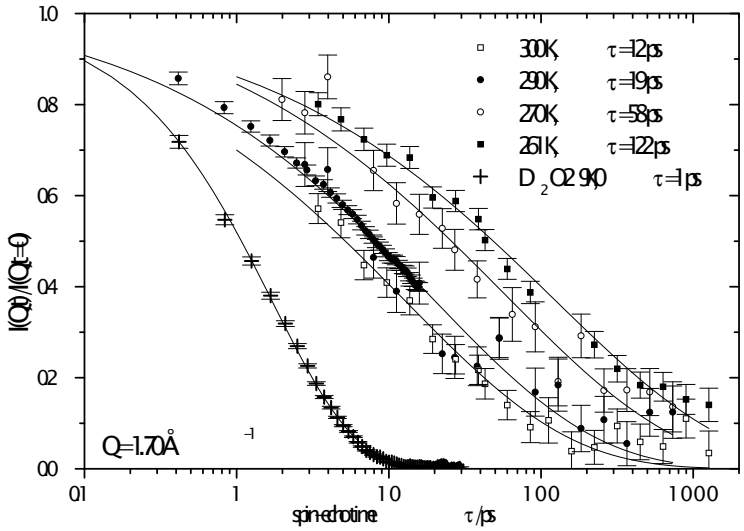

Figure 3.13: Intermediate scattering functions at Q=1.7 Å for samples containing 50 w% deuterated trehalose in heavy water, compared to results obtained on a sample of pure heavy water. Solid lines are adjustments using stretched exponential functions for the trehalose data and a single exponential decay for the water sample.

sample. An quantitative analysis of the scattering contributions shows, that for a sample containing 50 w% trehalose (equivalent to 20 molecules water per trehalose molecule) the coherent scattering from the water is slightly more important than the coherent scattering from the trehalose molecules (see figure 3.5).
The scattering data from a time-of-flight experiment on a sample of pure D_2O are included in figure 3.13. The decay can be described by a single exponential function with a relaxation time of τ =1 ps.
These results will help to discuss and to understand the different contributions when investigating samples, that contain the C-phycocyanin protein in the presence of trehalose and water in hydrated powder forms as described in the next chapter.

4 Protein Dynamics in the Presence of Trehalose

In this chapter we will present results of experiments using samples that contain C-phycocyanin protein and trehalose. We investigate the influence of the presence of the sugar on the protein dynamics. Experiments were performed on different instruments with different spatial and time resolutions: the time-of-flight spectrometer MIBEMOL, the backscattering spectrometer IN13 and the spin-echo spectrometer MUSES. Details of these instruments can be found in chapter 2. Using these spectrometers we cover a time range from less than 1 picosecond up to several nanoseconds.
We can compare our results with data from S. Dellerue, who investigated the dynamics of the C-phycocyanin both by neutron spectroscopy as well as by Molecular Dynamics simulation [87, 88].
We performed experiments on hydrated powder samples. Details of sample preparation and treatment can be found in chapter 1. The use of hydrated powders has the advantage that the scattering signal is mainly due to internal motions of the protein. Contributions from diffusive movements of the whole protein can be neglected. The price for this choice is a high elastic signal with small quasielastic contributions. Observable motions of such a system have rather small amplitudes in space and can be best investigated at high Q-values.
We investigate both the dynamics of the side chain motions as well as the geometry of motions. To interpret the quasi-elastic signal a model of a diffusion in a sphere is used and discussed. Data from the backscattering spectrometer IN13, that give access to quite high Q-values are especially useful.
Spin-echo measurements were performed on the spectrometer MUSES which gives also access to rather high Q-values and offers a rather high experimental resolution.

Recently Palazzo *et al.* studied the effect of trehalose on the electron transfer kinetics in a reaction center of *rhodobacter sphaeroides* [127]. They found, that the presence of trehalose inhibits thermal fluctuations among conformational substates. They reported also a large hindering of the internal dynamics of trehalose coated reaction center. Trehalose plays furthermore an important role in preserving the integrity of the biomaterial.

A quite extensive study has been performed using different techniques describing the influence of trehalose on the dynamics of myoglobin and hemoglobin. Hagen *et al.* [53, 54] investigated by flash photolysis experiments kinetics of ligand rebinding in trehalose coated myoglobin samples. By comparing their results with those of Austin [128] and Ansari [129, 130] on myoglobin samples without trehalose, they found an increase in the recombination reaction that they attributed to a more confined structure of the protein in the presence of trehalose. The trehalose hinders relaxational modes so that ligand molecules cannot escape from the binding site, as it was seen at lower temperatures. Here Ansari attributed this behavior to an increase in the viscosity of the solvent rather than to a change in internal energy barriers [129, 130]. Gottfried *et al.* found a similar behavior for hemoglobin in the presence of trehalose. They concluded both from fluorescence and from time-resolved Raman that trehalose reduces many dynamical processes in the protein, and prevents furthermore conformational changes.
Sastry and Agmon proposed a quantitative model to describe these experimental findings. To their eyes viscosity effects are the main reason for the observed phenomena [56].
Librizzi *et al.* studied the dehydration process of trehalose and sucrose coated myoglobin using FTIR techniques [64, 131]. They found that during the dehydration of a sample of carbonmonoxy-myoglobin micro-crystallisation process takes place. Furthermore embedding a protein in a glassy saccharide structure seems to conserve the three-dimensional structure of the protein. Denaturation effects are hindered. It seems that traces of water incorporated in these glasses would have a stabilizing effect. Trehalose glasses seem to be able to incorporate more water molecules than sucrose glasses.
In 1999 Cordone *et al.* published an experiment using neutron scattering techniques [18]. They measured the atomic mean-square displacement of a sample containing trehalose coated dry myoglobin as a function of temperature . Doster found in 1989, that for a sample containing hydrated myoglobin powder, the mean-square displacement as a function of temperature shows two different domains [132]. At low temperatures protein motions can be described by an harmonic model, while at about 220 K a transition versus a non-harmonic regime can be observed. In the meantime, this transition has been found for many other proteins. Recently Zaccai attributed these two domains to differences in the flexibility of the protein, expressed in terms of different force constants [133]. Cordone *et al.* now found for a sample of dry trehalose coated myoglobin, that this dynamical transition no longer exists in the observed temperature range. The experimental data can be described by an harmonic model, even at relatively high temperatures (up to 300K).
Cottone *et al.* tried to describe a similar system of myoglobin, embedded in a trehalose-water matrix, using a molecular dynamics simulation approach [134]. Their system contained one molecule of myoglobin, 231 trehalose molecules and 538 water molecules. As in the experimental work they found, that the amplitude of the non-

harmonic internal motions of the protein are reduced with respect to a hydrated protein without trehalose.

Our approach is somehow different to these latter works, as we use powder samples with a high level of hydration. In fact we are interested in observing the dynamics of the protein under the influence of trehalose. This is why our samples contained less trehalose and more water than the systems used in the previously described work. From Rupley and Careri it is clear, that to ensure protein dynamics, a certain amount of hydration water is essential [16], varying for different proteins between 0.1 and 0.4 gram water per gram protein.

4.1 Diffusive motions confined inside a spherical geometry

We used hydrated powder samples of CPC protein in oder to avoid contribution from long range diffusive motion of the whole protein. We observe only dynamics on a small amplitude. To describe these motions we use a model proposed by Volino and Dianoux in 1980 [13]. They developed a formalism describing the diffusive motion of a particle confined inside a spheric environment.
In time-of-flight and backscattering experiments one measures the dynamical structure factor S(Q,ω). In our case it can be described using the sum of an elastic and a broadening term according to:

$$S(Q,\omega) = DW \cdot [A_0(Q) \cdot \delta(\omega) + (1 - A_0(Q)) \cdot L(Q,\omega)] \tag{4.1}$$

Here $DW \sim exp(-Q^2 < u >^2)$ is the Debeye Waller factor and $L(Q,\omega) = \frac{1}{\pi} \cdot \frac{\Gamma(Q)}{\Gamma(Q)^2+\omega^2}$ a Lorentzian line of the width (FWHM) Γ.

The length scale of the observed motions is inverse proportional to Q. At small Q values a system as described above would show a behavior independent of Q up to a value Q_0, that corresponds to the size of the sphere. For larger Q one should observe classic diffusion according to a DQ^2 law, with D being the diffusion coefficient. In figure 4.1 the theoretical behavior of the half width at half maximum Γ of a Lorentzian curve describing the diffusive motion is shown as a function of Q^2. The signal obtained from such a system should have, at least at small Q, a large elastic contribution. One can introduce the elastic scattering factor, which is the contribution of the elastic scattering to the total scattering. In the case of incoherent scattering it is called elastic incoherent structure factor (EISF). Volino and Dianoux described its behavior as a function of Q for a particle diffusing inside a sphere. One would expect a behavior for the EISF according to

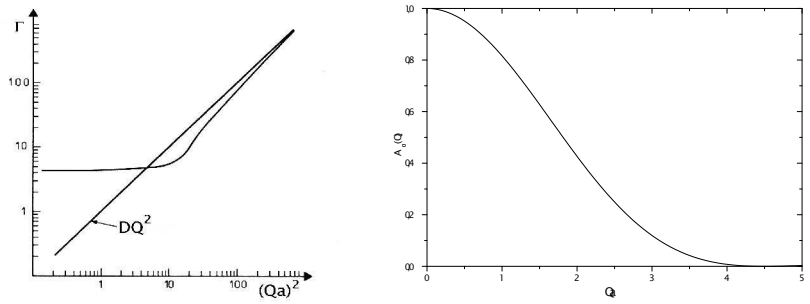

Figure 4.1: left: Theoretical behavior of a Γ vs. Q^2 plot for a diffusion of a particle, confined inside a sphere (taken from [13]); right: Evolution of the elastic incoherent structure factor for such a particle according to equation 4.2

$$A_0(Q) = \left(\frac{3j_1(Qa)}{Qa}\right)^2, \tag{4.2}$$

with $j_1(x) = (sin(x) - x \cdot cos(x))/x^2$, a Bessel function of the first order and a the radius of the sphere. The function is plotted in figure 4.1.

Experimental data always depend on instrumental resolution. It limits the time window in which motion can be detected. Dynamics that are to fast for the dynamical scale will contribute to the background signal, slower motions to the elastic scattering signal. In this case the EISF function does not achieve zero values in the experimental range. To take into account this effect we introduce a fraction p, that corresponds to those motion, that are to slow to be detected and that are thus invisible to the experimental conditions.

$$EISF = p + (1 - p) \cdot A_0(Q) \tag{4.3}$$

4.2 Dynamics at low resolution

We performed a series of experiments using the time-of-flight spectrometer MIBEMOL. We investigated the incoherent scattering signal using samples containing 0.3 g of deuterated trehalose per g protein. With a sample containing deuterated trehalose, heavy water and protonated protein we mask the contributions from the sugar and the hydration water. The obtained signal is thus mainly due to incoherent scattering from the protons of the protein. Motions that we observe correspond thus to movements of the protein.

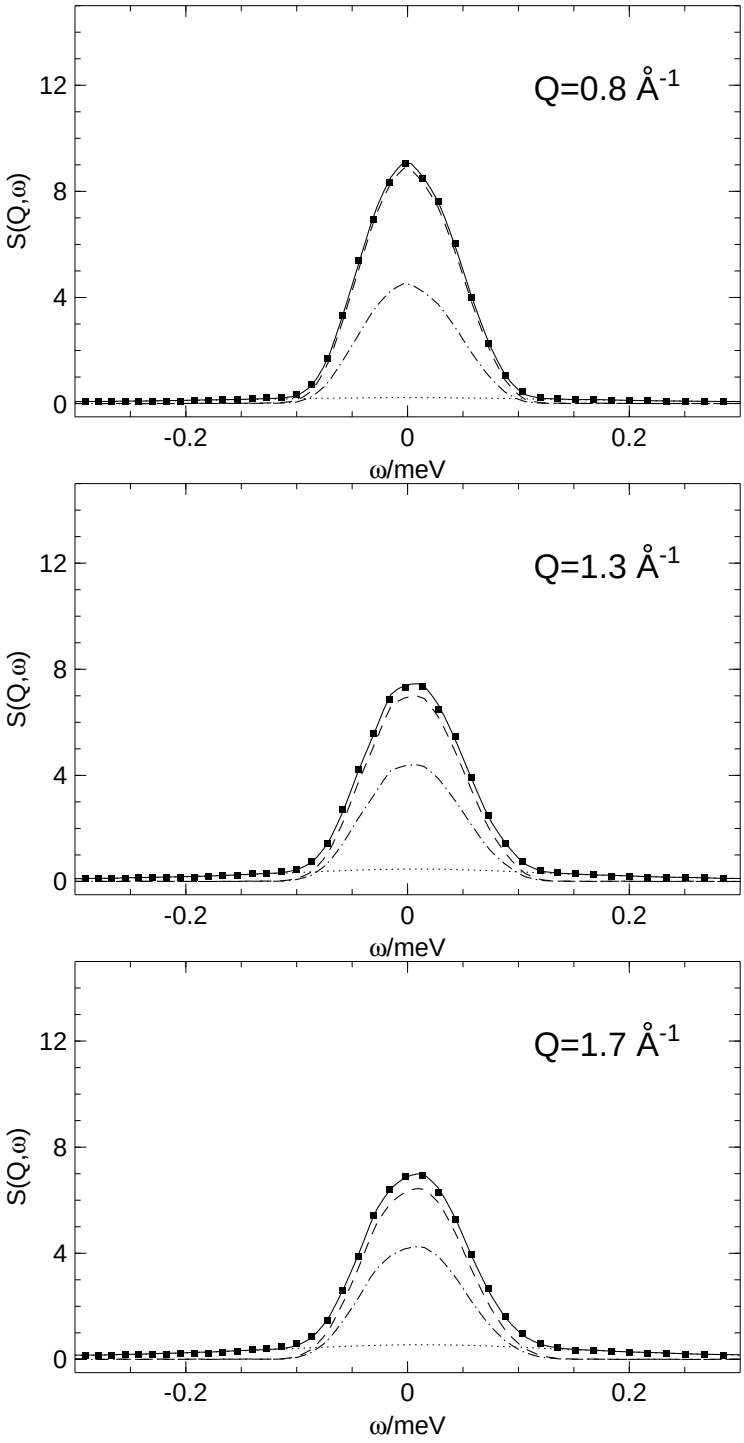

Figure 4.2: Analysis of the dynamic structure factor according to equation 4.1 obtained on a sample containing 0.3 g trehalose and 1.0 g D_2O per gram CPC protein. The lines show the fit result (solid), the elastic (dashed) and the quasielastic (dotted) contribution. Measurements performed at T=311K on the time-of-flight spectrometer MIBEMOL using an incident wavelength of 6Å and a resolution of FWHM=96 μeV. The experimental resolution function is shown as a dotted-dashed line.

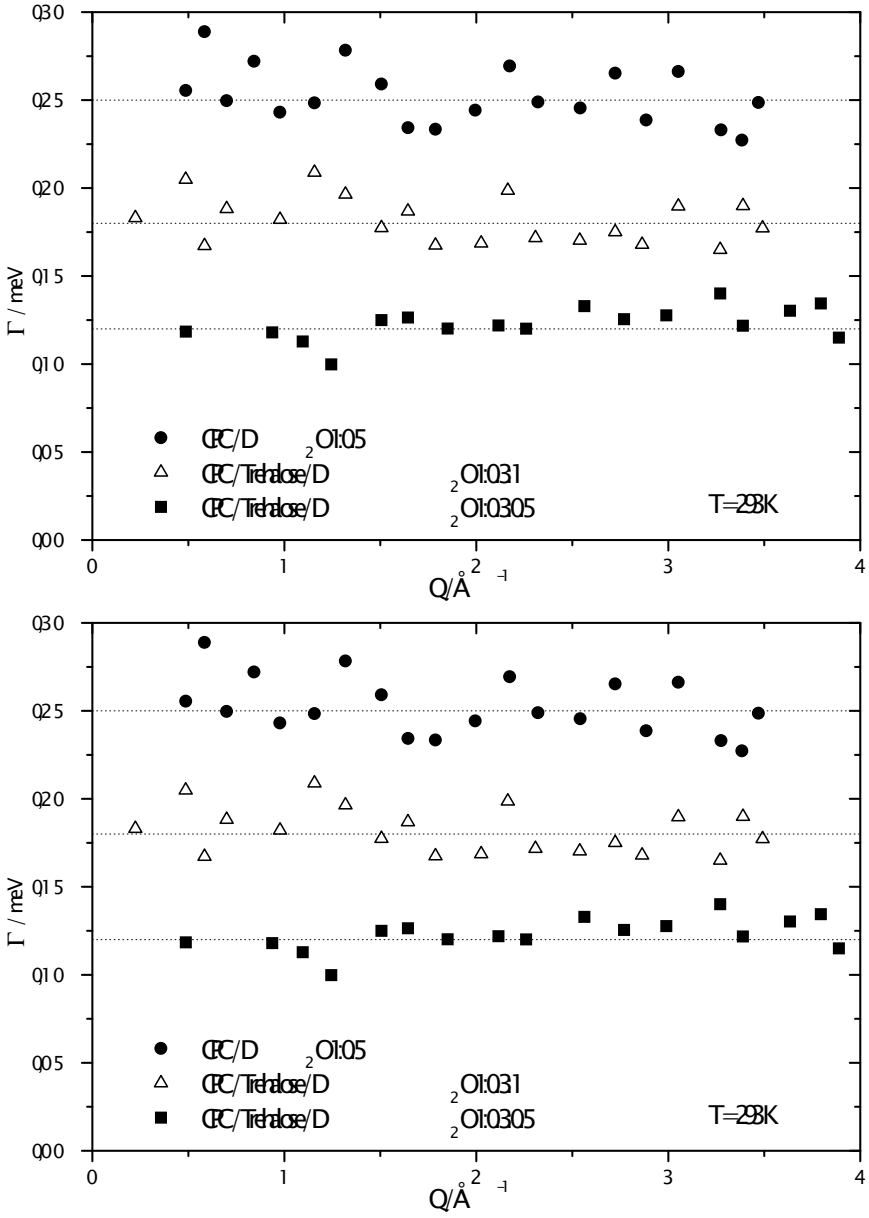

Figure 4.3: Half width at half maximum Γ of the Lorentzian line describing the broadening of the scattered signal, as a function of the momentum transfer vector. Dashed lines are guides to the eyes. Due to the limited Q-range of the spectrometer we can not observe the increasing part of the curve as predicted by the model of Dianoux and Volino. Experiments were performed on the time-of-flight spectrometer MIBEMOL using an experimental resolution of 96 μeV (FWHM).

The co-lyophilized powders were placed in flat rectangular aluminium cells and hydrated under a heavy water atmosphere to hydration levels of 0.5 g and 1 g D_2O per g protein. To determine the effect of the trehalose we compare our results with data from an experiment on hydrated CPC protein (h=0.5g D_2O/g protein) [10].

The dynamic structure factor can be described using equation 4.1. An example of this analysis for the sample with a hydration level of h=1.0 can be seen in figure 4.2. One can see, that especially for small Q values the signal has a high elastic contribution.

In figure 4.3 we show the half width at half maximum obtained using the analysis described above for different sample compositions and at temeratures of T=293 K and T=311 K. One observes a constant value over the whole Q-range. The predicted increase of the signal is not detected due to the limited accessible Q-range of the spectrometer.
The amplitude of the plateau is proportional to the diffusion coefficient. We observe a clear slowing down of the protein dynamics when trehalose is added to the sample.

The elastic incoherent structure factor $EISF = A_0(Q)$ can be directly determinated.
Using this analysis we describe the dynamics in the sample by one single process. This approximation is valid only at a quite low resolution where only some dynamical processes contribute to the scattering process. It has to be changed when higher resolutions are used as we will see in the next paragraphs.
In the time-of-flight experiments as presented below we used an incident wavelength of 6 Å which corresponds to an instrumental resolution of about 96 μeV (FWHM). We investigate the influence of the level of hydration on the protein dynamics as well as its temperature dependence.

4.2.1 Influence of the temperature and hydration

We performed experiments at 293 K , 311 K and 323 K on trehalose coated samples to study the influence of the temperature and the level of hydration on the protein motion. Raw data are corrected for empty cell contributions and normalised to a standard vanadium scatterer.
The dynamic structure factor for all samples has been analysed according to equation 4.1.

In figure 4.4 the elastic incoherent structure factors for two samples containing CPC protein powder, coated with 0.3 g trehalose hydrated with 0.5 g or 1 g D_2O per gram of dry protein are plotted. The Q-dependence can be described using the model introduced in chapter 4.1. Results of the fit using equation 4.2 are listed in table 4.1.

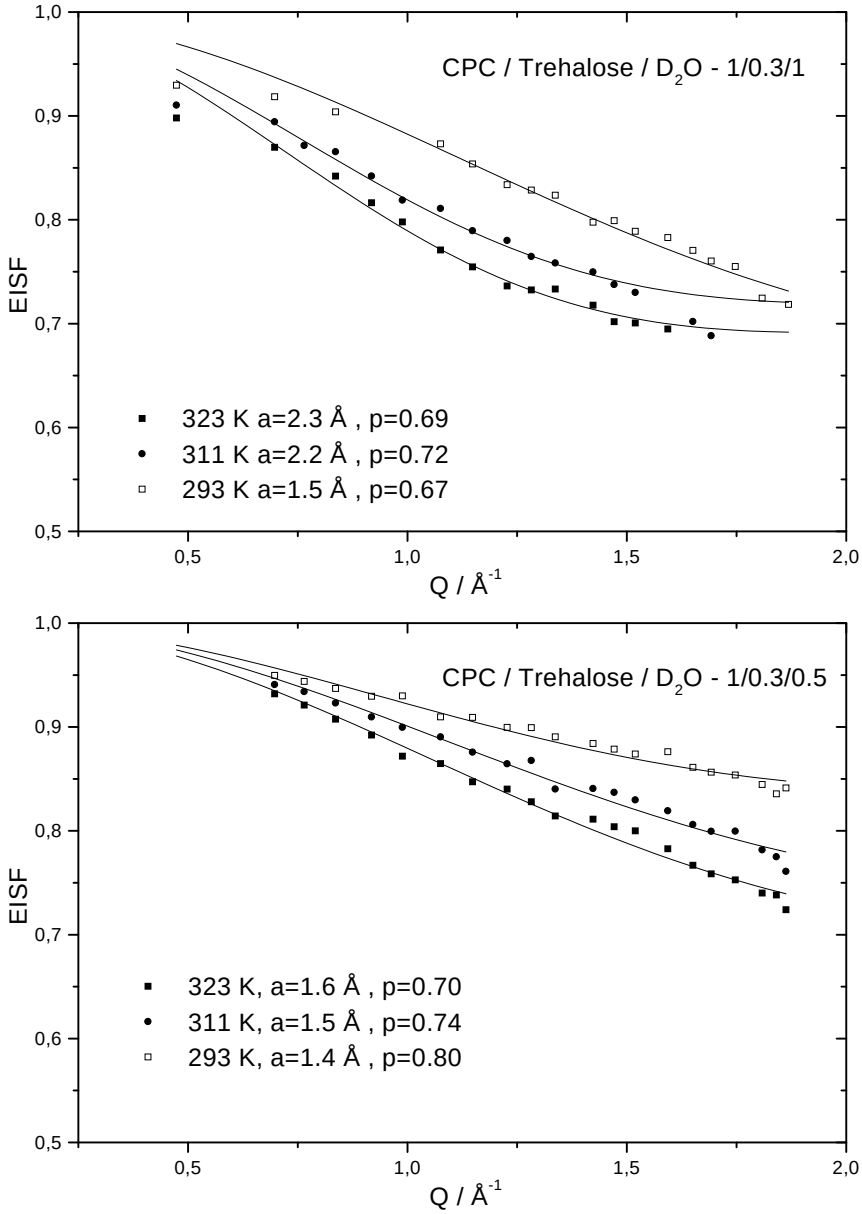

Figure 4.4: Elastic incoherent structure factors for two samples of hydrated CPC/trehalose powders with a different amount of hydration water, both at three different temperatures. Solid lines are fits according to equation 4.3. The obtained parameters are given in the figure. Note that the origin of the y-axis is set to 0.5 for better visibility. Experiments were performed on the time-of-flight spectrometer MIBEMOL using an experimental resolution of 96 μeV (FWHM).

T	p		*a*	
	h = 0.5	h = 1.0	h = 0.5	h = 1.0
293 K	0.84	0.67	1.4 Å	1.5 Å
311 K	0.74	0.72	1.5 Å	2.2 Å
323 K	0.70	0.69	1.6 Å	2.3 Å

Table 4.1: Parameters p and a from the adjustment of the elastic incoherent scattering factors in figure 4.4 as a function of different level of hydration h. Samples contained hydrated, trehalose coated CPC powders (0.3g trehalose per g protein). h corresponds to the amount of water per gram protein.

The spectrometer MIBEMOL is limited at the used resolution of FWHM=96 μeV to a Q-range up to 1.8 $Å^{-1}$. In this range the EISF function has not achieved its plateau value. Nevertheless one can observe a clear temperature dependence of the signal, at least for the value p. The given values are results of a fit according equation 4.3. The radius of the sphere exhibits small variations as a function of the temperature. Only the value for T=293 K and a hydration level of h=1 shows significant difference to values at higher temperatures at the same level of hydration. From figure 4.4 one can see, that the experimental points can be described rather poorly by the refinement. Especially at low Q-values the deviation from experimental results from the theoretical curve are quite important.

Different level of hydration show a strong effect; when comparing results for the radius a at similar temperatures one observes a reduction of the radius of about 30 % (see table 4.1). This is consistent with the fact, that water is essential to allow protein motions as described for example in [135]. In other words, when more water is present, the environment of the protein becomes softer and more liquid-like so that larger movements become possible. At the same time the values for p are only slightly infected by a change in the level of hydration. The number of 'visible' protons at the same temperature remains more or less the same. Here again, only the values for the measurement at T=293 K and h=1.0 differ from this trend.

4.2.2 Influence of trehalose

In figure 4.5 we compare samples with the same level of hydration h=0.5, but one sample contained only hydrated CPC powder while in the other sample the protein was trehalose coated. Results are presented for two temperatures 293 K and 311 K. The results for the protein without trehalose are reanalysed data from S. Dellerue [10]. A summary of the obtained parameters can be found in table 4.2.

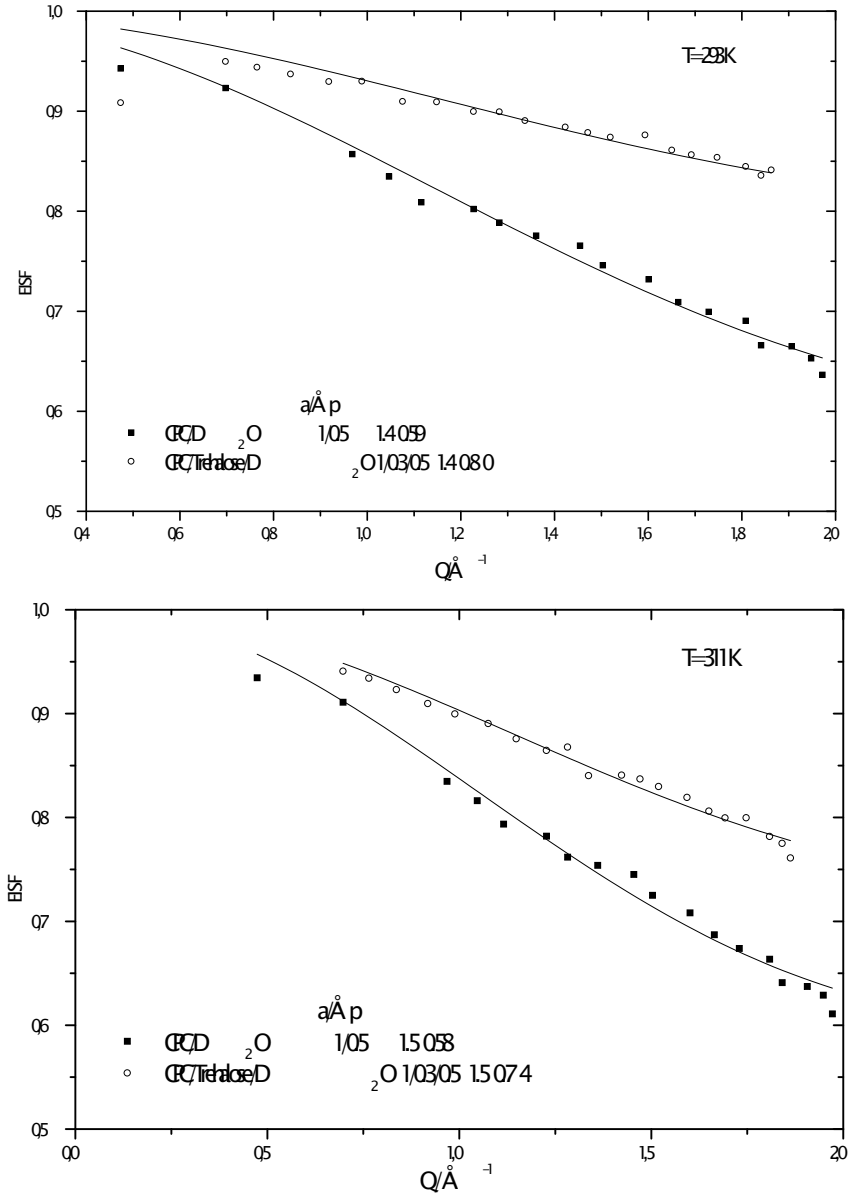

Figure 4.5: Elastic incoherent structure factors at two temperatures, T=293 K and T=311 K, for samples of hydrated CPC/trehalose powder and hydrated CPC powder. Solid lines are fits according to equation 4.3. The obtained parameters are given in the figure. Note that the origin of the y-axis is set to 0.5 for better visibility. Experiments performed on the MIBEMOL spectrometer using a resolution of FWHM=96 μeV.

The experimental data can be described over a Q-range up to 2 $Å^{-1}$ using the model of a confined diffusion inside a sphere using equation 4.3 and 4.2. Results for the trehalose coated sample were already presented above.

T	p		*a*	
	with	without	with	without
293 K	0.80	0.59	1.4 Å	1.4 Å
311 K	0.74	0.58	1.5 Å	1.5 Å

Table 4.2: Parameters p and a from the adjustment of the elastic incoherent scattering factors in figure 4.5. Samples contained hydrated CPC powder (h=0.5). One sample was coated with trehalose.

The main influence of the trehalose coating is a strong increase in the elastic scattering contribution. This is seen by an increase in the value for the plateau parameter p at high Q-values when trehalose is added to the sample.
The value for a, which corresponds to the size of the sphere is not affected by the presence of the sugar.
Thus one observes, that a quite important fraction of protons of the proteins are slowed down in a way that their motions are no longer observable in the given time window (up to about 10 ps). They contribute now to the elastic part of the scattering signal. The movements of the remaining protons can be described using the same model as for the sample in the absence of trehalose. This might indicate, that the type of movement is not affected by the presence of the saccharide. It might by only slowed down.

4.3 Dynamics at higher resolution

The backscattering spectrometer IN13 of the ILL, Grenoble has the advantage to give access to a large Q-range up to values of about 5 $Å^{-1}$. We used this instrument to measure the incoherent scattering function. As in the time-of-flight experiments we used hydrated powder samples of protonated CPC protein, coated with deuterated trehalose and hydrated with heavy water. Thus we investigate mainly motions of the protein. With an incident wavelength of 2.3 Å one obtains a resolution of 10 μeV (FWHM), which corresponds to a times as long as 100 ps.
We performed two types of experiments. In the elastic scan mode one investigates the scattering without energy transfer. Thus one has access to the Debeye Waller factor. When analysing the data as a function of the scattering vector Q, one obtains the mean square displacement of the scattering particles.
In the quasielastic mode one measures the dynamic structure factor S(Q,ω).

4.3.1 Elastic scattering

We performed experiments on different samples containing trehalose coated CPC protein in different ratios and with different levels of hydration. Cordone *et al.* performed a quite similar experiment on trehalose coated dry myoglobin [60]. They found that a dynamical transition present in hydrated myoglobin [132] cannot be detected in dry trehalose coated protein. We can confirm these results for the CPC protein. But we also investigated the effect of trehalose coating in hydrated powder samples.

We performed elastic neutron scattering scans in a temperature range from 40 K up to 330 K, counting 90 minutes per temperature. Data were corrected for empty cell contributions and normalised to a standard vanadium scatterer using standard programs of the ILL. The intensity of the scattered signal is proportional to:

$$S(Q,\omega=0) \propto exp\left(-\frac{Q^2 \cdot \langle u^2 \rangle}{3}\right) \tag{4.4}$$

For each temperature we can analyse the data over a Q-range up to Q=4 $Å^{-1}$ using equation 4.4. Some examples are shown in figure 4.6. The slope of the solid lines corresponds to the mean square displacements.
The mean square displacement for different samples as a function of temperature is shown in figure 4.7. To normalise the data from different experiments to a common scale, the harmonic region at low temperature was assumed to be linear. Data were extrapolated and normalised to be 0 at T=0K.
Figure 4.7 shows the mean square displacements for the following samples: a dry sample of trehalose coated CPC (1 g trehalose per g CPC), a sample containing hydrated CPC protein (0.5 g D_2O per gram protein) and two samples of hydrated

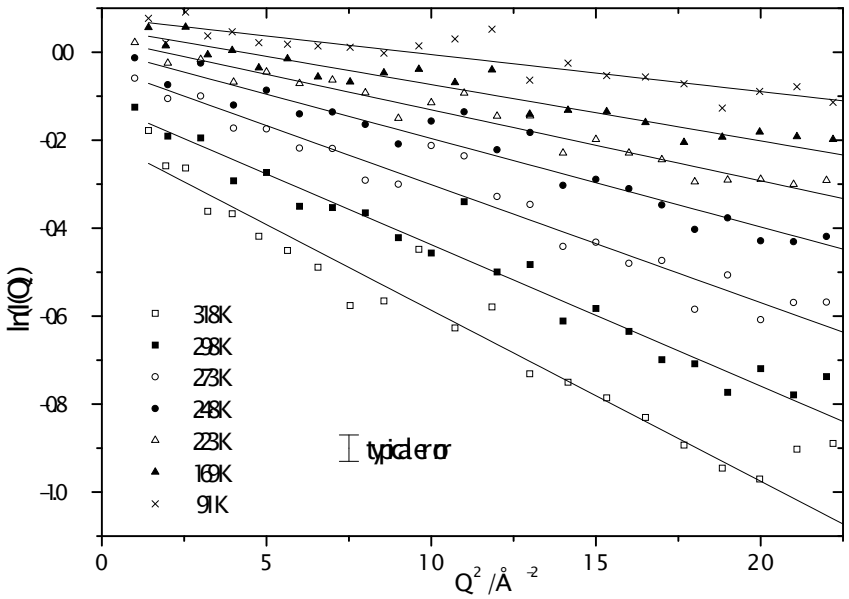

Figure 4.6: Analysis of the elastic scattering data at several temperatures for a sample containing 0.75 g trehalose and 0.75 g D_20 per gram protein. The scattering intensity is plotted versus the scattering wavevector. Using a linear model and according to equation 4.4, the slope of the straight lines corresponds to the mean square displacements. The curves have been spread out for better visualisation. Experiments performed on the spectrometer IN13 using an experimental resolution of FWHM=10 μeV.

trehalose coated CPC with 0.75 g trehalose and 0.75 g D_2O and 0.3 g trehalose and 0.7 g D_2O per gram protein respectively.
At low temperature up to about 200 K all samples show a classical harmonic behavior. For the dry sample this behavior continues even at highest temperatures, a fact that is consistent with findings from Cordone *et al.* on trehalose coated myoglobin. When hydrating the samples a dynamical transition can be observed at temperatures higher than 200 K. The mean square displacements are only slightly influenced by the sample composition. In the presence of trehalose one can see a tendency, that the amplitudes are reduced. The values for the trehalose free sample seem to be a little bit higher than that of the trehalose coated ones. Furthermore the values for the samples containing less trehalose (0.3 g trehalose and 0.7 g D_2O per g protein) are slightly higher than for the sample containing a large amount of trehalose and a similar degree of hydration (0.75 g trehalose and 0.75 g D_2O per g protein), especially at highest temperatures.

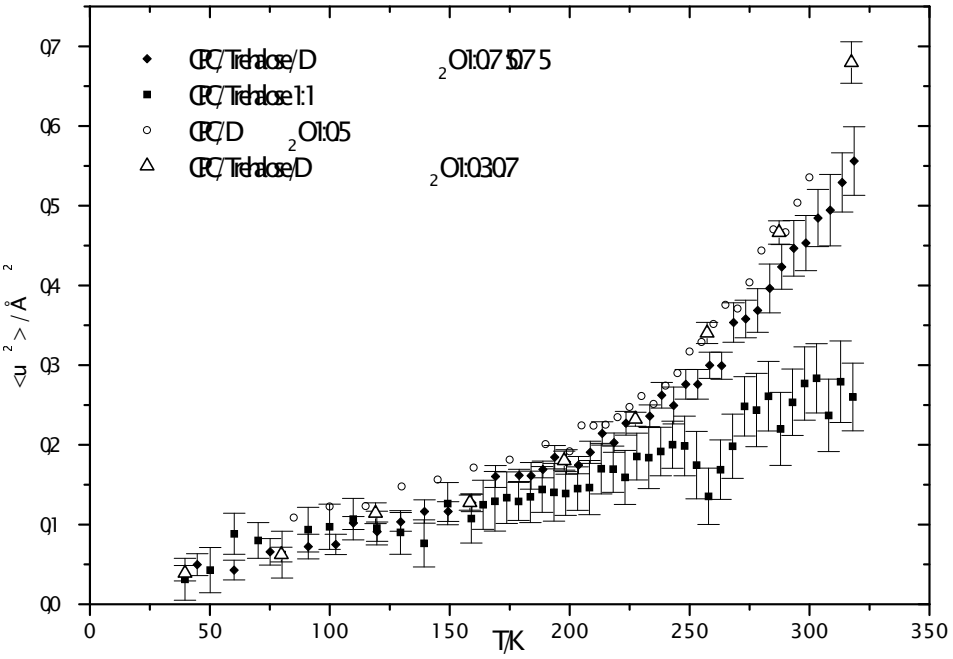

Figure 4.7: Mean square displacements $<u^2>$ as a function of temperature for samples of different composition of CPC protein, trehalose and heavy water. Experiments performed on the IN13 spectrometer using an experimental resolution of FWHM=10 μeV.

4.3.2 Quasielastic scattering

The analysis of the quasielastic scattering is quite difficult. As the neutron flux on the instrument is not very high and as one single scan over an energy range from -110 to 100 μeV takes 10 hours, data collection times were of about three days per sample to obtain sufficient statistics. Even after this time the quality of the spectra is not very satisfying, partially due to the highly elastic signal with only little quasielastic contributions. In figure 4.8 the dynamic structure factors at three different Q-values are shown for a sample containing 0.75 g deuterated trehalose and 0.75 g heavy water per gram protonated CPC protein.
We performed experiments at different sample composition and at different temperatures. To be able to compare our results to previous results of a sample containing hydrated CPC powders [10], one of the chosen temperatures was 280 K, where the signal of our trehalose coated samples showed only a small broadening of the scattered signal.
The scattered signal can be described using the sum of an elastic and a quasielastic term, as shown in equation 4.1. We analyse the results in the same way as described for the time-of-flight data.

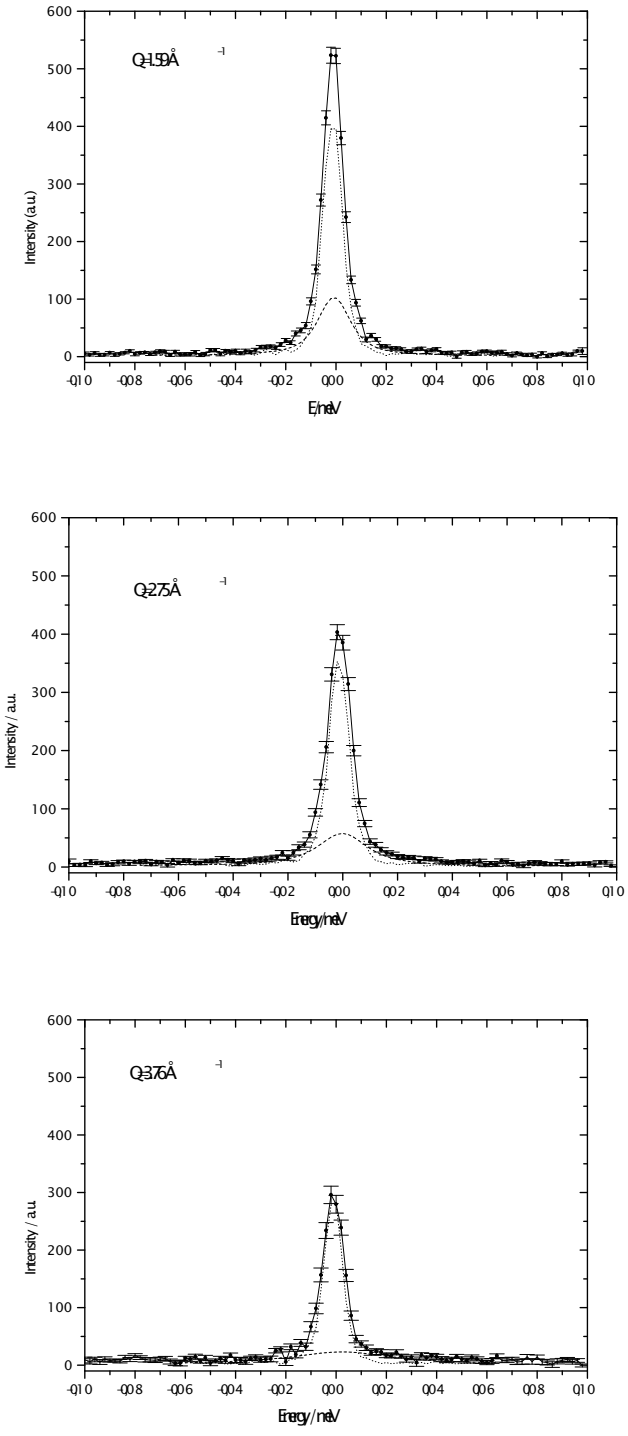

Figure 4.8: Dynamic structure factors for a sample containing 0.75 g deuterated trehalose and 0.75 g heavy water per gram protonated CPC protein measured at 280 K. The solid line describes the fit according to equation 4.1. The dotted lines shows the elastic contribution, the dashed one the quasielastic contribution. Experiments performed on the IN13 spectrometer with a resolution of 10 μeV.

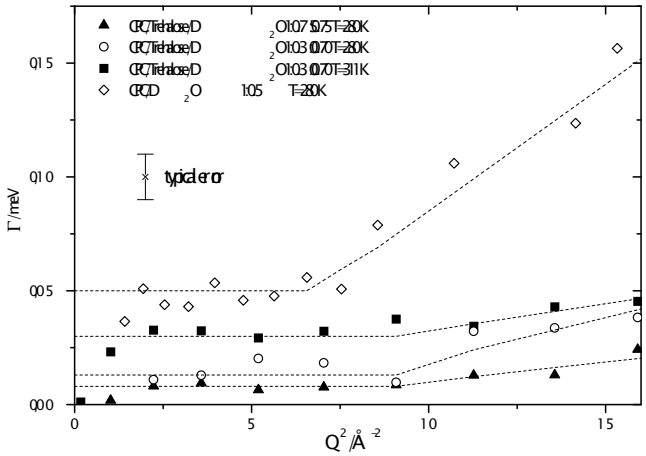

Figure 4.9: Half width at half maximum Γ of the Lorentzian line describing the broadening of the scattered signal, as a function of the momentum transfer vector. Dashed lines are guides to the eyes to demonstrate the two different regions according to the model of Dianoux and Volino [13]. Experiments performed on the spectrometer IN13 with a resolution of 10 μeV (FWHM).

Figure 4.9 shows the half width at half maximum Γ of the Lorentzian term in equation 4.1. One can see the typical behavior of a confined diffusion as mentioned in the model described in chapter 4.1. A first region with a constant value for Γ is followed by a region with a linear dependence of Γ as a function of the momentum transfer. The value of the plateau at small Q depends on the diffusion coefficient. The Q-value, that marks the point, where the behavior changes, is inversely proportional to the radius of the sphere. Due to the large errors we only present a qualitative analysis of these parameters.
In figure 4.10 the elastic incoherent structure factors for different sample compositions are shown. The curves can be described using equation 4.2 and 4.3.

We will discuss two effects. The influence of trehalose on the dynamics of the system as well as its temperature dependence. From figure 4.9 one can see a clear slowing down of the protein motions due to the addition of trehalose. The difference in the plateau value, directly proportional to the diffusion coefficient is of about one order of magnitude when comparing a sample containing hydrated CPC protein (h=0.5) with a sample containing trehalose coated hydrated CPC protein (0.75 g trehalose per g protein, h=0.75). The difference between the samples with different contents of trehalose, 0.75 and 0.3 g trehalose per gram protein, is less pronounced. The effect of a change in temperature is evident and quite straightforward. We performed the quasielastic measurement on a sample containing 0.3 g trehalose per gram protein, hydrated to 0.7 g heavy water per gram protein at 280 K and 311K.

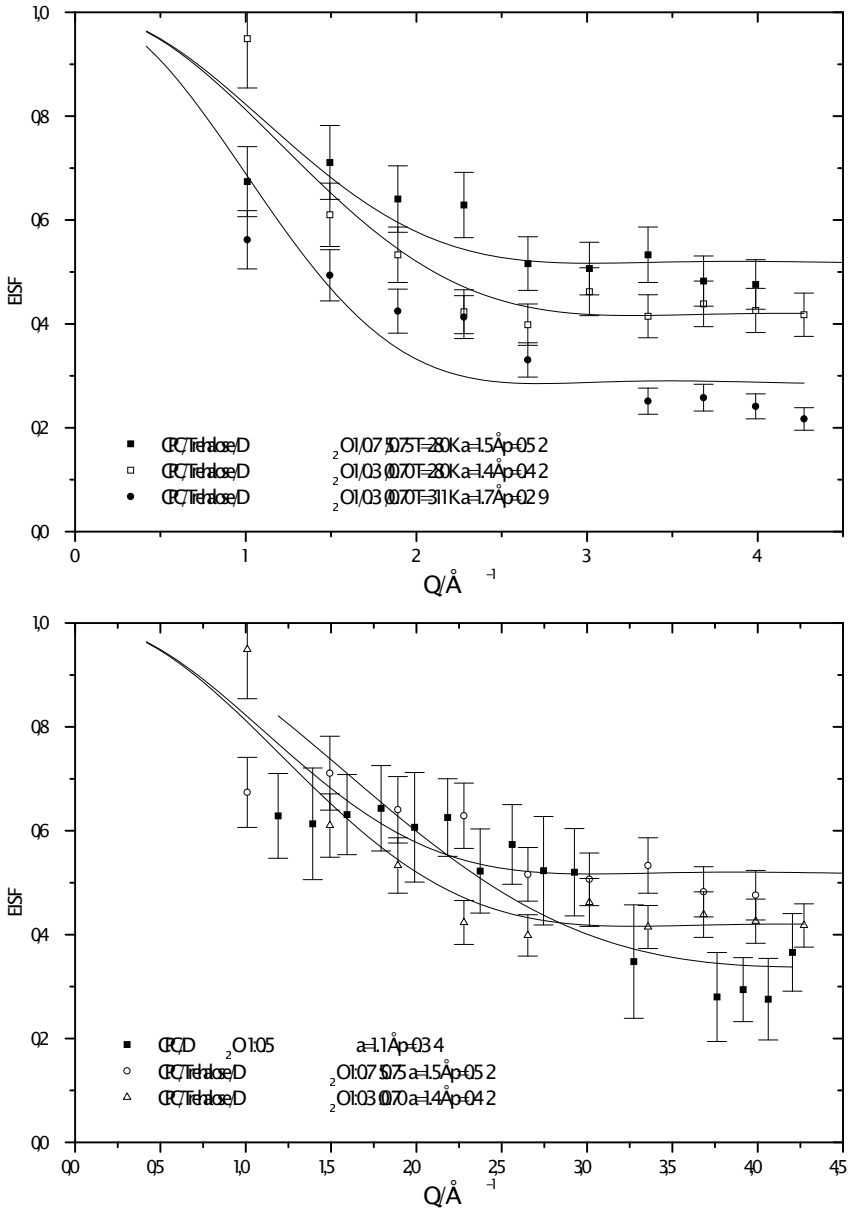

Figure 4.10: Elastic incoherent structure factors for samples containing trehalose coated, hydrated CPC powders. up: influence of the temperature, down: influence of the sample composition. Solid lines represent adjustments according to the model of a particle diffusing inside a sphere. Experiments performed on the spectrometer IN13 with a resolution of 10 μeV (FWHM).

As one could expect, the diffusive motion at the higher temperature is faster by a factor of about 5. We do not try to determine a value for a from the Γ vs. Q plots for reason of to high incertitudes in the experimental data.

The same effect can be seen in the elastic incoherent structure factors in figure 4.10. The parameter p is correlated to the number of protons, contributing to the signal. The higher p, the more elastic is the signal, the less mobile protons are visible to the instrumental resolution. For the sample containing the highest amount of trehalose (0.75 g per gram protein) only 50 % of all protons contribute to the signal, while in the sample without trehalose only about 35 % of the protons contribute to the elastic scattering signal. For the sample containing 0.3 g trehalose the proportion is still about 42 %. One has to keep in mind, that the samples containing trehalose are hydrated to a higher level of hydration than the sample without trehalose. The pure protein sample was hydrated to h=0.5 while we used hydration levels of h=0.75 and h=0.7 for the trehalose coated samples. The signal of the trehalose coated samples would become even more elastic at a lower level of hydration, as seen in chapter 4.2. When rising the temperature from 280 K to 311 K the amount of non-detectable proton motions decreases from 42 % to 29 %, as one would expect. We obtain here values different to those obtained in the time-of-flight experiments due to the fact, that the dynamic range in both experiment is different. Thus we do not probe the same motions.
The determination of the radius a of the sphere is quite uncertain due to the considerable statistical error of the data. The following trends can be observed: the fit for the sample without trehalose gives the smallest value for a, followed by the samples containing trehalose at 280 K. The highest value for a is obtained for the experiment at 311 K.

4.4 Dynamics at high resolution

The neutron spin-echo technique has the advantage to provide a very high energy resolution. The experimental time-range covers easily three orders of magnitude. This makes this technique a powerful tool in the investigation of protein dynamics. The disadvantage is, that one should ideally perform experiments on fully deuterated samples, as hydrogen atoms with a spin of $\frac{1}{2}$ would cause spin flipping and thus lower the polarisation of the neutron beam. Incoherent measurements are also possible, but here the polarisation is limited to a maximum value of 1/3.
We had the advantage to posses a fully deuterated form of the CPC protein. Experiments were performed on hydrated trehalose coated powder samples. We used the deuterated form of trehalose. But even for this highly deuterated samples and probably due to some hydrogen atoms still present in the sugar, the obtained maximal polarisation was of about 40 %, probably due to the non-exchanged protons on the trehalose molecules.
In a spin-echo experiments one measures, via the polarisation of the neutron beam, the intermediate scattering function. This function is nothing else but the Fourier transform of the dynamic structure factor obtained in time-of-flight or backscattering experiments.
As the intermediate scattering function is a function of time, the analysis can be done in terms of correlation times. An analysis equivalent to that of the previously described experiments using the sum of an elastic and a Lorentzian term would correspond to an interpretation using a single exponential decay, followed by a constant background term. As we will see, and as it is well known from several other systems, for example polymers or glass forming liquids, the relaxational process over such a large time-scale often cannot be described by a single process, but by a distribution of them. A typical function to describe such processes is the Kohlrausch-Williams-Watt law (KWW):

$$I(Q,t) = A(Q) \cdot exp - \left(\frac{t}{\tau(Q)}\right)^{\beta(Q)} + E. \tag{4.5}$$

Here β is a parameter that describes the width of the distribution of relaxation times τ. The term E had to be added to describe an elastic contribution that could not be resolved by the instrumental resolution.

4.4.1 Incoherent scattering

We performed experiments on a sample containing CPC protein in its protonated form, coated with 0.3 g trehalose and hydrated with 1 g H_2O per gram protein. Using this composition the obtained signal is dominated by the incoherent contributions from the protein (∼30 %) and from the hydration water (∼50%). Due to the

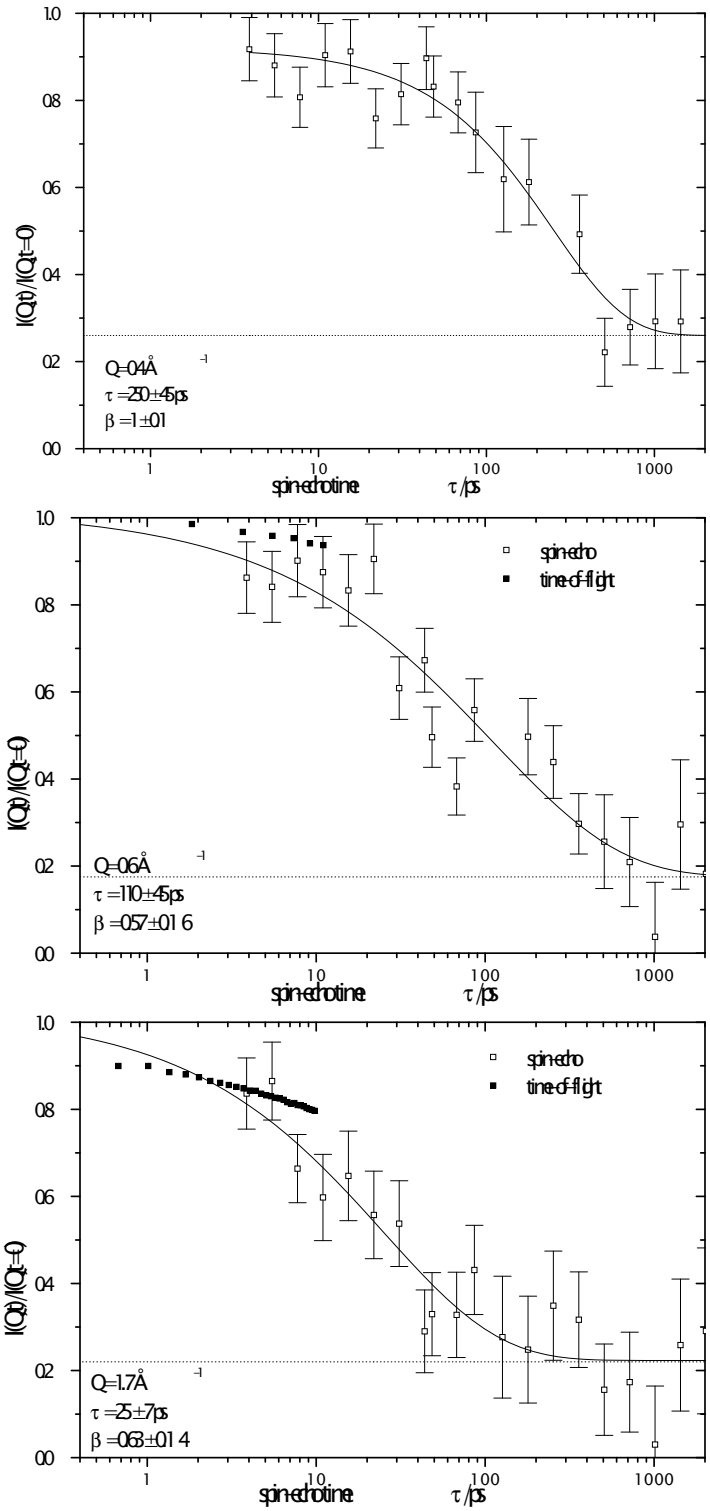

Figure 4.11: Intermediate scattering functions for a sample containing 0.3 g trehalose per g CPC, hydrated with 1 g H_2O per gram protein. As all components are in their protonated form , the observed signal is due to the incoherent scattering. Solid lines represent fits according to equation 4.5. The dotted lines show the plateau value at long times. For Q=0.6 Å and Q=1.7 Å data from time-of-flight experiments are included in the figure.

coherent scattering from oxygen, carbon and nitrogen atoms present in the sample, the polarisation is reduced by at least 25 % with respect to a pure incoherent scatterer. Experiments were performed at room temperature and for different Q-values between 0.4 and 1.7 $Å^{-1}$. The raw data were scaled to 1 for τ=0 and deconvoluted by the scattering signal from a quartz crystal. The intermediate scattering functions for Q-values 0.4, 0.6 and 1.7 $Å^{-1}$ are shown in figure 4.11. They can be analysed according to equation 4.5. The data show an exponential decay, that ends for long times in a plateau. We attribute this plateau to an elastic contribution in the scattering signal that corresponds to slow motions of the protein which are not resolved by the instrumental resolution.

Q / $Å^{-1}$	τ/ ps	β
0.4	250 ± 45	1 ± 0.1
0.6	110 ± 45	0.57 ± 0.16
1.7	25 ± 7	0.63 ± 0.14

Table 4.3: Fitting parameters obtained by adjusting intermediate scattering functions of a sample CPC/trehalose/H_2O 1:0.3:1 at 298 K as shown in figure 4.11.

In table 4.3 the obtained parameters are listed. One can see, that at the smallest Q-value, the relaxational process can be described by a single relaxational decay, while a stretched behavior has to be considered for higher Q-values. The obtained relaxation time τ decreases with increased Q-value.
For Q=0.6 Å and 1.7 Å we can extend the time-scale to shorter times by combining results from the spin-echo experiments with data obtained by time-of-flight measurements on similar samples. Data from both experiments will overlap up to 10 ps; the first spin-echo point that we measured was at 3.5 ps. Time-of-flight experiments performed at an incident wavelength of λ=6 Å as described above, can provide data starting from 0.1 ps depending on the scattering angle.
Time-of-flight data were measured as described in Chapter 4.2 on a sample containing 0.3 g deuterated trehalose and 1 g D_2O per gram protein. Thus the scattering contributions from the different components trehalose, protein and hydration water are different to those of the purely protonated sample used in the spin-echo experiments. Furthermore time-of-flight data are measured on an energy scale, while the intermediate scattering function observed by spin-echo spectroscopy is a function of time. To combine the two techniques we transform the time-of-flight data by an interpolation to constant Q and a Fourier transformation according to equation 2.7. These operations were performed using the program IDA from J.Wuttke (see footnote on page 75).
The transformed data are normalised to unity for τ=0 and deconvoluted with the

resolution function, measured on a standard vanadium scatterer.
The overlap between the two curves is not very satisfying. One has to take into account, that in the different experiments the signal is the result of different contributions from the sample. In the time-of-flight experiments the sample consisted of protonated CPC protein, coated with deuterated trehalose and hydrated with heavy water. The obtained signal is mainly due to the incoherent scattering from the protein. In the spin-echo experiments all components of the sample were protonated. The obtained intermediate scattering function represents a mean value of contributions from the protein, the sugar and the hydration water, weighted by their individual scattering contributions.
Especially the decay in the picosecond region is due to dynamics of the hydration water [11]. The relaxation time for bulk water is of about one picosecond. The decay at short time, faster for the spin-echo curve with respect to the time-of-flight data could be explained by a more important contribution from the hydration water as well as from the trehalose molecules.

4.4.2 Coherent scattering

Coherent scattering experiments were performed on samples containing deuterated CPC protein, coated with deuterated trehalose and hydrated with heavy water.
When calculating the incoherent and coherent scattering sections one can determine the contributions from each species (protein, trehalose, water) in the sample to the total scattering signal. For a sample containing 0.5 g trehalose and 1 g D_2O per gram protein, the coherent scattering signal is mainly due to contributions from the protein (41%) and the hydration water (42%).
The obtained polarisation as well as the scattering intensities were very low, so that only measurements around the maximum of the structure factor were possible.
In figure 4.12 we show the intermediate scattering functions obtained at Q=1.6 $Å^{-1}$ and Q=1.7$Å^{-1}$. Measurements were performed at T=298 K. The incident wavelength was λ=5Å to maximise the neutron flux on the sample.
The experimental data could be described using a stretched exponential decay including a constant term to take into account of the plateau already observed in the incoherent scattering experiments.

In figure 4.13 the experimental data for Q=1.7 $Å^{-1}$ are compared to data obtained on a sample containing hydrated CPC protein without trehalose and to the results obtained from Molecular Dynamics simulation of that system [10, 11]. Data from simulation and experiment for the sample without trehalose show a fast decay in the picosecond regime followed by a plateau up to at least 3 ns. It can be fitted using a stretched exponential function with a relaxation time of one ps and a stretching parameter β=0.27. The system containing trehalose shows a much slower decrease with a relaxation time of τ=111 ps. One has to take into account, that the sample of Dellerue *et al.* contained CPC protein that was hydrated up to 1.5 D_2O

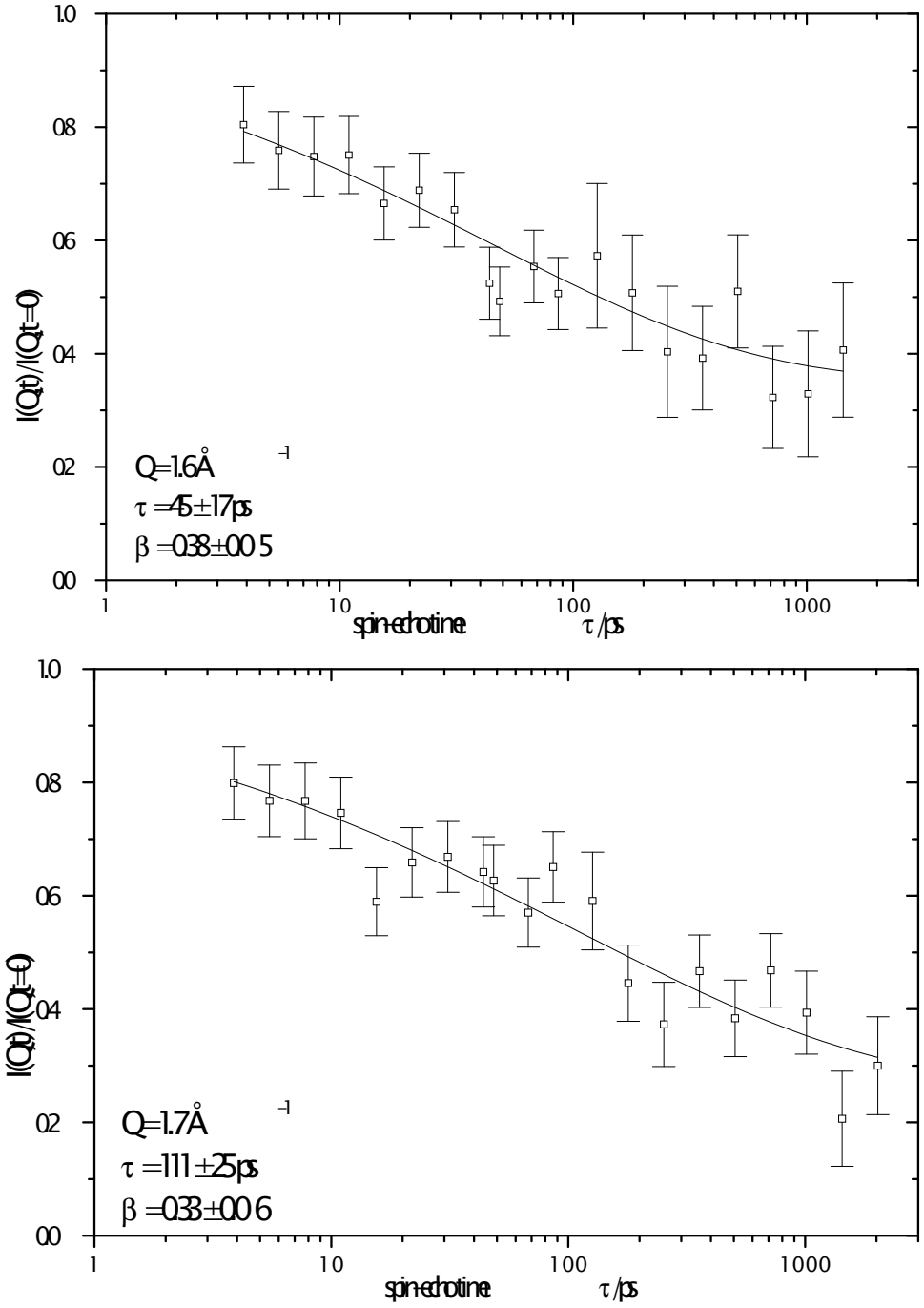

Figure 4.12: Intermediate scattering functions for a sample containing 0.5 g trehalose and 1 g water per gram protein. All products were completely deuterated. Solid lines represent fits using a stretched exponential decay. The obtained numerical values of the relaxation times τ and the stretching parameters β are shown in the legend. A constant term was added to describe the long-time behaviour. Experiments were performed at T=298 K on the MUSES Spin-echo spectrometer using an incident wavelength of 4.8 Å.

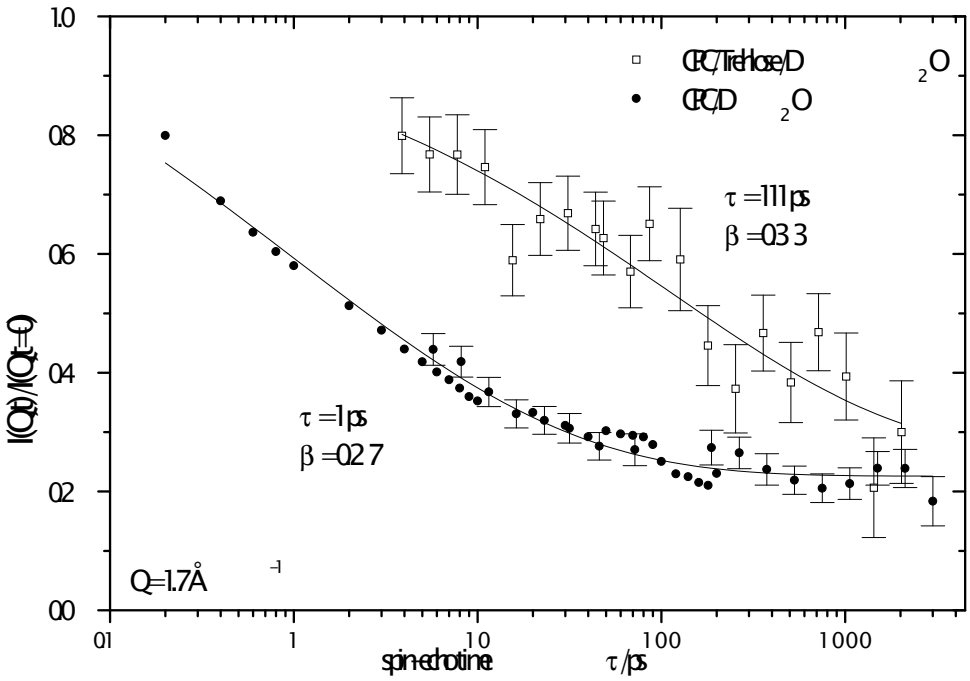

Figure 4.13: Intermediate scattering functions of trehalose coated CPC protein at T=298 K. Comparison with data of hydrated protein in combination with results from Molecular Dynamics simulations [10]. Solid lines represent fits by a stretched exponential according to equation 4.5. The values of the fitting parameters τ and β are given in the figure.

per gram protein so that the contribution of the hydration water to the scattering signal is more important than in the sample containing trehalose. Thus the first decay should be mainly due to water dynamics, while at least at longer times protein motions contribute the most to the scattering signal. Dellerue *et al.* decomposed the combined intermediate scattering function from MD simulation and spin-echo experiments in contributions from bulk water, from hydration water and from the protein. For times greater than 10 ps the contributions from the protein dominate the scattering signal. So one can attribute at least the differences at longer times in the curves in figure 4.13 as an influence of trehalose on the protein dynamics.

4.5 Putting things together

The use of neutron scattering instruments with different energy (or time) resolutions, gave us the possibility to study the dynamics of a complex system such as the trehalose coated CPC protein over a wide time scale. Short time dynamics up to 10 ps were visible in the time-of-flight experiments. Backscattering techniques covered a time range up to about 100 ps. Finally using neutron spin-echo techniques we studied dynamics from 3 ps to 4 ns. With all the instruments we investigated local movements at rather high Q-values. This choice results from the nature of the samples chosen. As we used hydrated powder samples, long range translational motions can be neglected and one can observe, at least, at a ps-ns time scale, mainly motions of side chains and internal backbone movements.
Dellerue *et al.* analysed a MD trajectory of hydrated CPC protein [11]. They found that relaxational processes in the backbone in a Q-range up to 2Å^{-1} take place mainly in a time window between 10 and 100 ps. Side-chain dynamics is mainly situated between 20 and 500 ps. One has to notice, that these relaxation times are mean values over the concerned part of the protein. They result from an analysis based on a stretched exponential behaviour with a stretching parameter β varying between 0.3 and 0.4. In figure 4.14 we show the obtained relaxation times as well as the stretching parameters as a function of Q. In the same work, the behaviour of individual residues at the backbone and side chains have been reported.

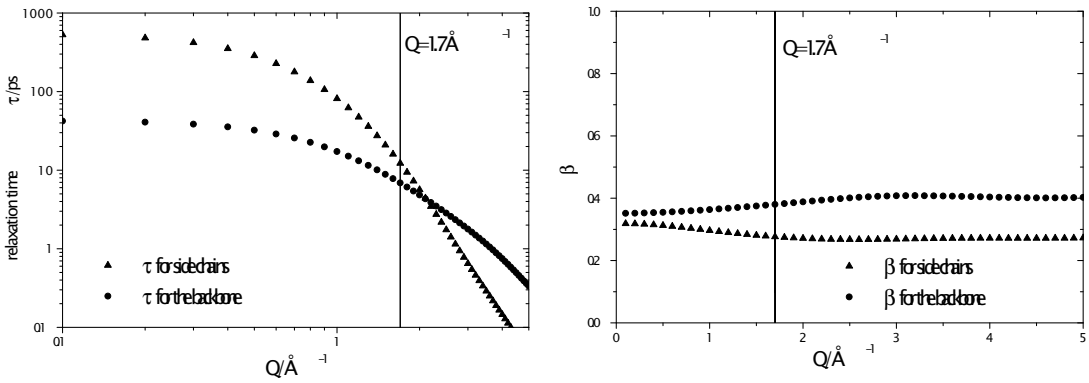

Figure 4.14: Analysis of a MD simulation of hydrated CPC protein powder. Separation of side-chain and backbone motions. The relaxational motions were described by a stretched exponential decay with a stretching parameter β and a relaxation time τ. Figures taken from [11].

The different types of experiments give access to different parts of the scattering functions. In a time-of-flight experiment as well as in a backscattering measurement one obtains the dynamic structure factor $S(Q,\omega)$. Neutron spin-echo experiments

give access to the intermediate scattering function $I(Q,t)$. These two expressions are correlated via a Fourier transform.

$$I(Q,t) = \int S(Q,\omega) \cdot exp(i\omega t) d\omega \tag{4.6}$$

To combine data from the different experiments we transformed the time-of-flight data and compared them with spin-echo data on a common time-scale. To study the influence of trehalose on the CPC dynamics we compare our combined results with data from S. Dellerue obtained by neutron spin-echo and MD-simulation on hydrated CPC protein. When combining time-of-flight and spin-echo data one has to consider that the obtained signal can contain different contributions according to the used technique. In time-of-flight experiments the measured signal is due to the incoherent scattering cross sections of all atoms present in the sample. With a sample composed of protonated protein, deuterated trehalose and heavy water, the main contributions to the signal come from the protons of the protein due to the dominating incoherent scattering cross section of protons (see table 2.1). In the spin-echo measurements, we used either completely deuterated or completely protonated samples. We measured thus a signal, that is due to all different molecule types present in the sample proportional to their concentration.
In table 4.4 we present calculated relative coherent and incoherent scattering cross sections for sample compositions we used in different experiments. We separate contributions from the protein, the trehalose and the hydration water. Depending on the sample composition, different contributions dominate the scattering signal.

In figure 4.15 we present a summary of data obtained at Q=1.7 $Å^{-1}$ and T=298 K.

Data for the hydrated CPC protein powder sample can be described by a stretched exponential decay with a mean relaxation time of 1 ps and a stretching parameter β=0.27. This quite fast relaxation time is due to a high contribution of water to the scattering signal. Non-resolved protein dynamics contributes to a plateau at longer times with an amplitude of 0.21.
The experiments with the trehalose coated samples were performed using sample compositions of 0.3 g trehalose and 1g D_2O per gram protein in the time-of-flight experiments and 0.5 g trehalose and 1 g D_2O in spin-echo experiments. Thus different contributions compose the signal. The time-of-flight data show a higher contribution of scattering from the protein than the spin-echo data.
The spin-echo data can be described by a stretched exponential decay with a relaxation time τ=110 ps and a stretching parameter β=0.3. Data from the time-of-flight experiment extend this decay to shorter times with a good overlap. One should remark, that a fit of the combined time-of-flight/spin-echo data does not change the fitting parameters obtained from the spin-echo curve alone. The essential decay of the curve takes place between 50 ps and 500 ps. In this time window the decay is described only by spin-echo data.

	h-CPC	d-CPC	h-trehalose	d-trehalose	H_2O	D_2O
time-of-flight, backscattering experiments						
ratio / g	1			0.3		1
molecular ratio	1			30		1800
relative σ_{coh}	0.10			0.03		0.12
relative σ_{inc}	0.67			0.05		0.03
spin-echo experiments, incoherent scattering						
ratio / g	1		0.3		1	
molecular ratio	1		32		1970	
relative σ_{coh}	0.03		0.01		0.03	
relative σ_{inc}	0.32		0.09		0.52	
spin-echo experiments, coherent scattering						
ratio / g		1		0.5		1
molecular ratio		1		53		1900
relative σ_{coh}		0.28		0.11		0.29
relative σ_{inc}		0.05		0.18		0.08

Table 4.4: Calculated relative scattering contributions for some samples used in different experiments. The numerical values show the contributions of the protein (protonated or deuterated), the trehalose (protonated or deuterated) and the hydration water (H_2O or D_2O) to the total scattering.

One can also see from the curve, that the decay leads at longer times to a plateau as it has been observed for the sample without trehalose. An amplitude of 0.29 has been found. This value is the result of the best fit. We admit, that the statistic error is quite important. Furthermore the amplitude of the plateau and the correlation time are correlated. A lower plateau value results in a higher relaxation time.
The difference in the amplitudes for the samples with and without trehalose, indicates a more important elastic contribution has to be concidered for the trehalose coated protein. A higher fraction of the dynamics of the system could not be resolved, when the protein is coated with the sugar.
We include in figure 4.15 also data obtained on aqueous trehalose solution with a concentration of 50 w%. The shown curve is composed both of data from time-of-flight and from spin-echo experiments as described in chapter 3.2.2. One observes for the intermediate scattering functions an exponential decay with a relaxation time of τ= 19 ps and a stretching parameter β=0.38. At longer times the curve decays to 0 within the observable time-range.
Also included in figure 4.15 is the intermediate scattering function obtained on a sample containing bulk water by time-of-flight experiments. It shows a fast single exponential decay with a relaxation time of τ=1 ps. The function decays to 0 al-

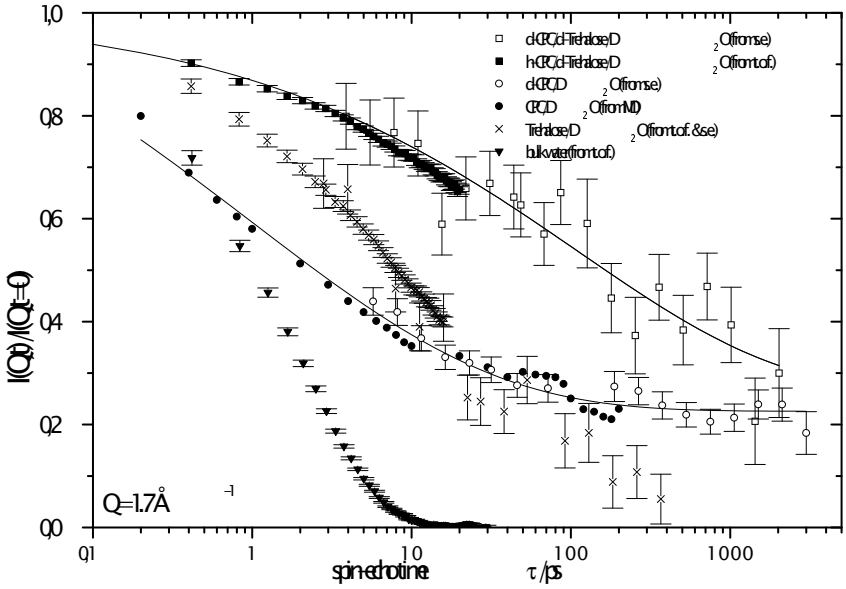

Figure 4.15: Intermediate scattering function for different samples obtained by different techniques: Neutron time-of-flight (t.o.f.) and spin-echo (s.e.) experiments as well as by Molecular Dynamics simulation (MD). Comparison between hydrated protein powder samples with (□) and without (∘) trehalose. For comparison data of bulk water (+) and aqueous trehalose solutions (x) are included.

ready at 10 ps. No dynamics is detected at longer times.

Comparison of the data of the different samples presented in figure 4.15 leads us to the following conclusions:
The dynamics of the protein is slowed down, when it is coated with trehalose. It is difficult to quantify exactly the effect, as the scattering function is due to different contributions from the protein, the trehalose and from the hydration water. These contributions are proportional to the individual scattering cross sections and the individual concentration, therefore quantitative predictions from these values remain difficult and uncertain. One can get an idea on the individual contributions by performing experiments with a systematic variation of the respective concentrations of protein, trehalose and hydration water. For the sample without trehalose the contribution of the hydration water is rather important. This can be seen in a relaxation time in the same order of magnitude as it has been found for bulk water. Nevertheless the relaxational behaviour is stretched and at least at longer times the scattering function corresponds to motions of the protein.
Let us now consider the contributions from the trehalose molecules. We have information of the diffusion behavior of trehalose in aqueous solution from the experiments presented in the previous chapter. Let us assume that we have a protein in

an aqueous trehalose solution instead of hydrated trehalose coated powder. Thus comparison with the scattering function from the trehalose/water solution is interesting. In the case of trehalose/water solutions, one gets a faster relaxation with respect to that of the protein solution for similar trehalose/water ratios. This is due to the contributions of the slower protein dynamics. The increase in the relaxation time of the protein with respect to the sample without trehalose is of two orders of magnitude. In addition the plateau value at longest times, that corresponds to an elastic contribution and thus to non resolved motions, seems to increase, when trehalose is added to the protein. Thus, some motions would be slowed down in such a way, that they can no more be resolved by the instrumental resolution.

We find it interesting to mention, that the stretching parameter β is nearly the same, both for the sample with and without trehalose. A stretched exponential decay can be interpreted in terms of a distribution of relaxation times around a mean relaxation time τ. In this description to the width is given by the parameter β. Thus this width is not infuenced by the presence of trehalose.

The analysis of the elastic incoherent structure factor (EISF) using the model of Dianoux and Volino gives information about the geometry of the observed motions. The model describes the diffusive motion of a particle confined inside a spherical environment. When we investigate the internal dynamics of a protein by quasielastic neutron scattering, we obtain mean values of the motions of all atoms of the sample. One can imagine, that the complex trajectory of each atom could be described by an envelope of spherical geometry. A similar approach has been used in the study of the dynamics of the paravalbumin [14]. Carpentier *et al.* validated this model for the dynamics of alkyl chains [15]. They found by using partially deuterated aliphatic chains a dependence of the observed radius in the EISF on the level of deuteration. The more protons were present on the chains, the bigger was the radius, that could be observed.
Our results show, that the size of the sphere describing the geometry of motion depends strongly on the level of hydration of the sample. This indicates, that protein motions are possible, only in presence of at least a small amount of hydration water. This confirms the work of Rupley and Careri [16] and is in agreement with results reported by Rector *et al.* They found a strong correlation between the viscosity of the hydration shell and the rate of fluctuations on the surface of myoglobin [17]. In the absence of any hydration shell, motions are completely stopped, at least in the time domain we investigated. This fact has been already reported by Cordone *et al.* on dry trehalose myoglobin samples by elastic neutron scattering experiments [18]. Our results about the atomic mean square displacements in a dry trehalose coated sample showed also a completely harmonic behaviour.
When trehalose is added to a hydrated protein sample, the elastic part of the scattering contribution increases, because a part of the motions, observed on a sample

without trehalose gets slowed down. They are then no longer detectable within the experimental time-window. In the EISF the plateau value at the high Q end increases. Nevertheless the geometry of the dynamics both in the sample without as with trehalose can be described using the same model. Even the obtained sizes of the spheres are the same in both cases. The mean square displacements in figure 4.7 show for samples with different amounts of trehalose and hydration water very similar results. From the curves one could detect a tendency, that the signal decreases with increasing trehalose content. One finds, that, within small variations, trehalose influences the protein motions by reduction of the amplitudes of the fluctuations or by slowing down.

Based on the experimental results presented above we suggest the following picture of the interactions between trehalose and the CPC-protein:
The quasielastic scattering experiments reveals clearly, that the internal dynamics of the protein, that is to say motions of the side chains and of the backbone of the protein, are strongly slowed down. At the same time the geometry of these motions remains nearly unchanged.
From our point of view these facts are in agreement with the model proposed by Green and Angell [8]. According to their model the trehalose molecules change the viscosity of the hydration shell around the protein molecules. As a consequence in this more viscous liquid, the dynamics of the protein is slowed down.
Another model proposed by Crowe *et al.* [1] suggests some mechanism in terms of direct interactions between trehalose and the biomolecules. We think that in this case the protein motions and so their geometry would be affected. A polipeptidic chain bound to water molecules would have to move differently when bound to heavier and less flexible trehalose molecules. We did not detect any change in the geometry of motions which leads us to exclude this later model.

5 Summary & Outlook

Dynamical processes in biological systems cover wide domains in space and in time. There exists no method to cover the whole dynamics in one single experiment. Neutron scattering experiments using thermal neutrons can provide information on dynamics on a ps- to ns-time-scale. By performing experiments at a Q-range up to 5 $Å^{-1}$ one accesses to motions on an atomic length scale.
We used elastic and quasielastic neutron scattering experiments to investigate the influence of trehalose on the internal dynamics of the CPC protein. Trehalose is a disaccharide with the chemical composition $C_{12}H_{22}O_{11}$. It is known to be a very effective bioprotectant against external stresses such as drought or extreme temperatures. Two main hypotheses have been proposed to explain the protective mechanism of trehalose at a molecular level. Crowe *et al.* proposed a mechanism via direct interactions between the sugar and the biomolecule [4]. Green and Angell explained the protective effect by the formation of a glassy state of trehalose which would protect the embedded biomaterial [8].
We investigated these two hypotheses on a model system. The C-phycocyanin is a globular protein that contributes to the photosynthetic cycle in cyanobacteria. Recently dynamics of this protein in solution as well as in hydrated powders has been studied by quasielastic neutron scattering and Molecular Dynamics simulation. We compare the latter results to data obtained on trehalose coated CPC samples. Experiments were performed on hydrated powder samples to investigate internal dynamics of the protein. Using different neutron scattering techniques dynamics between pico- and nanoseconds have been studied.

Neutron scattering experiments are sensible to the coherent and incoherent scattering cross sections of each atom present in the sample. In time-of-flight and backscattering experiments the incoherent scattering is investigated by measuring the dynamic structure factor. Using the difference between the scattering cross sections of protons and deuterons, one can hide certain parts of a sample by deuteration. We succeeded to deuterate the trehalose up to 80 %, so that its contributions in mixed samples can be minimized. In samples containing protonated protein, coated with deuterated trehalose and hydrated with heavy water the obtained signal is mainly due to contributions from the protein. In spin-echo measurements we used either the coherent scattering signal from completely deuterated samples or the

incoherent scattering from completely protonated samples.

We performed a study on concentrated aqueous trehalose solutions by time-of-flight and neutron spin-echo techniques. At short times the dynamics of the system could be described by a simple diffusion law, while a more complicated behaviour has been observed at longer times. Neutron spin-echo data at a ns-time-scale were described by a stretched exponential decay. The influence of the temperature on the relaxational behaviour has been studied. In the observed temperature range data can be plotted on a master curve with a unique stretching parameter β.

Interactions between trehalose and the CPC protein have been studied using hydrated powder samples of trehalose coated protein. Using this type of sample, long range transport can be neglected. One investigates the internal movements of the protein, for example dynamics of the backbone and the side-chains. The dynamics of trehalose coated protein is compared to that of the protein without trehalose.
Due to the fact, that the sample is a powder, the scattering signal shows an important elastic contribution with a small quasielastic broadening. This makes the analysis rather difficult.
Short time motions have been described by a simple localized diffusion. The geometry of this motion can be interpreted using a model of a particle diffusing inside a sphere. The addition of trehalose to the protein shows no effect on the geometry of the protein movements. The size of the sphere rests unchanged. Also the measurement of the atomic mean square displacements $< u^2 >$ show only very little variations in the amplitudes of atomic fluctuations when trehalose is added to the protein. The amplitudes decreases slightly with increasing trehalose content, but we can not distinguish if this effect is due to a slowing down of the motions or to a reduction of the amplitudes.

But when investigating the quasielastic broadening, especially on a ns-time-scale using neutron spin-echo techniques, one can observe a clear slowing down of the protein dynamics due to the presence of the disaccharide.
In literature two models for the molecular mechanism of the protecting effect of trehalose have been proposed. Our results favour the model of Green and Angell [8], who propose that the biomaterial is protected by being embedded in a glassy trehalose structure. So the structure of the biomolecules would be conserved and life and decay processes would be suspended.
When comparing experimental results with the two different models, one has to take into account the type of sample and the type of external stress applied to the sample. Evidence has been found, that when one dries membrane structures in the presence of trehalose, fusion of the polypeptidic chains is prevented by a direct binding of trehalose molecules to the polar head groups of the lipids [19].
We investigated a system containing a globular protein. In most of our experiments

the samples contained a certain amount of hydration water. Thus our approach is different to published experiments performed on completely dry samples. One should compare our results rather with experiments investigating the cryoprotective effect of trehalose at low temperatures [20, 21]. Here hydration water remains in the biomaterial and trehalose prevents the destruction of cellular material from the formation of ice crystals. In this case the protective mechanism might be due to similar interactions as those that we observed in our experiments. The high glass transition temperature of trehalose [8, 22] and the ability of trehalose to bind up to 11 water molecules per molecules of the sugar [107] should favour the formation of a protecting glass structure around the embedded biomolecule.
Our results show, that in our samples and under the applied conditions, the observed slowing down of the protein dynamics is due to an increase of the viscosity of the hydration layer around the protein when trehalose is added. We found no evidence for any direct interactions between the trehalose and the CPC molecules.

We analysed the obtained dynamic structure factors also in terms of the elastic incoherent structure factor. It could have been also interesting to investigate the Q-dependence of the relaxional behaviour of the trehalose coated protein measured in the spin-echo experiments. Similar to the analysis of the EISF, one should obtain information on the geometry of the observed movements. S.Dellerue performed this type of analysis for the intermediate scattering functions obtained from Molecular Dynamics simulation [10]. Unfortunately such an experiment would be very time consuming. At the present time, the spectrometer MUSES works with a single detector. The actual project for the development of a multidetector unit can be a great advantage in this kind of investigations.

To study individually motions of special parts of the protein, for example only side-chain motions, specific deuteration of only chosen amino acids of the protein would be necessary. It is nowadays also possible, to perform a complete synthesis of a protein, using chosen protonated or deuterated amino acids as basic units. These experiments would nevertheless be very expensive in view of the quantity one needs for a neutron scattering experiments using time-of-flight or spin-echo techniques to get a reasonable signal/noise ratio.

With our experiments, we cannot explain neither the reason, why trehalose is such a good bioprotecting agent nor the way trehalose is produced and used in nature. We point out, how trehalose molecules influence the dynamics of the C-phycocyanin protein in hydrated powder samples. The CPC is a small globular protein. Similar proteins should be influenced by trehalose in the same way, as we did not detect any evidence for preferential binding between trehalose and the CPC protein. Especially in the field of drug design, this information can be very helpful. To protect and store protein-based drugs trehalose solutions are already in use.

Specific informations on the interactions between the trehalose molecules and the proteins could help to improve these applications.

We used inelastic neutron scattering techniques to study dynamics in the complex biological system CPC/trehalose/water. Neutron scattering techniques are well appropriate to have a non-destructive view inside a sample. We were able to describe the interactions between the bioprotecting molecule trehalose and the CPC protein with regard of the two models proposed in literature. Our results favour the model of Green and Angell, that interprets the protective mechanism of trehalose via the embedding of the protected biomaterial in a glassy structure of aqueous trehalose, using the good glass-forming properties of trehalose.

Bibliography

[1] J. Crowe, L. Crowe and D. Chapman, "Preservation of membranes in anhydrobiotic organisms : the role of trehalose", *Science*, **223**, 701–703, (1984).

[2] K. Fox, "Putting proteins under glass", *Science*, **267**, 1922–1923, (1995).

[3] A. Rudolph, J. Crowe and L. Crowe, "Effects of three stabilizing agents - proline, betaine and trehalose - on membrane phospholipids", *Arch. Biochem. Biophys.*, **245**, Nr:1, 134–143, (1986).

[4] J. Crowe, L. Crowe, J. Carpenter and C. Aurel Wistrom, "Stabilization of dry phospholipid bilayers and proteins by sugars", *Biochem.J.*, **242**, 1–10, (1987).

[5] R. Payen, "Variations des teneurs en glycogene et en trehalose pendant le sechage de la levure", *Can.J Res.*, **27B**, 749–756, (1949).

[6] T. comission of the European Communities, "Commission decision of 25 sempember 2001", *Official journal of the European Communities*, **L269**, 17–19, (2001).

[7] D. Blakeley, B. Tolliday, C. Colaco and B. Roser, "Dry instant blood typing plate for beside use", *The Lancet*, **336**, 854–855, (1990).

[8] J. Green and C. Angell, "Phase relations and vitrification in saccharide-water solutions and the trehalose anomaly", *J.Phys.Chem.*, **93**, Nr:8, 2880–2882, (1989).

[9] K. Bradley, Chen.S.H., M.-C. Bellissent-Funel and H. Crespi, "The observation of structural transitions of a single protein molecule", *Biophys. Chemistry*, **53**, 37–44, (1994).

[10] S. Dellerue. *Structure er dynamique de protéines photosynthtíques étudiées par diffusion de neutrons et simulation par dynamique moléculaire.* PhD Thesis, Université de Paris-Sud, (2000).

[11] S. Dellerue, A. Petrescu, J. Smith and M.-C. Bellissent-Funel, "Radially softening diffusive motions in a globular protein", *Biophys. J.*, **81**, 1666–1676, (2001).

[12] J. Zaccai and C. Garrec. *Les macromolécules du vivant.* CNRS éditions, (1998).

[13] F. Volino and A. Dianoux, "Neutron incoherent scattering law for diffusion in a potential of spherical symmetry: general formalism and application to diffusion inside a sphere", *Mol.Phys.*, **41**, Nr:2, 271–279, (1980).

[14] J.-M. Zanotti and J. Bellissent-Funel, M-C.and Parello, "Hydration-coupled dynamics in proteins studied by neutron scattering and NMR: The case of the typical EF-hand calcium-binding paravalbumin", *Biophys. J.*, **76**, 2390–2411, (1999).

[15] L. Carpentier, M. Bee, A. Giroud-Godquin, P. Maldivi and J. Marchon, "Alkyl chain motions ins columnar mesophases, a quasielastic neutron scattering study of dicopper tetrapalmite", *Mol.Phys.*, **68**, Nr:6, 1367–1378, (1989).

[16] J. Rupley and G. Careri, "Protein hydration and function", *Adv. Prot. Chem.*, **41**, 37–173, (1991).

[17] K. Rector, J. Jiang, M. Berg and M. Fayer, "Effects of solvent ciscosity on protein dynamics: infrared vibrational echo experiments and theory", *J.Phys.Chem.*, **105**, 1081–1092, (2001).

[18] L. Cordone, M. Ferrand, E. Vitrano and G. Zaccai, "Harminic behaviour in trehalose coated carbon-monoxy-myoglobin at high temperature", *Biophys.J.*, **76**, 1043–1047, (1999).

[19] C. Lambruschini, A. Relini, A. Ridi, L. Cordone and A. Gliozzi, "Trehalose interacts with phospholipid polar heads in Langmuir monolayers", *Langmuir*, **16**, 5467–5470, (2000).

[20] J. Crowe, S. Leslie and L. Crowe, "Is vitrification sufficient to preserve liposomes during freeze-drying ?", *Cryobiology*, **31**, 355–366, (1994).

[21] J. Crowe, J. Carpenter and L. Crowe, "The role of vitrification in anhydrobiosis", *Annu.Rev.Physiol.*, **60**, 73–103, (1998).

[22] N. Karger and H.-D. Lüdemann, "Temperature dependence of the rotational mobility of the sugar and water molecules in concentrated aqueous trehalose and sucrose solutions", *Z. Naturforsch.*, **46c**, 313–317, (1991).

[23] S. Magazu, D. Majolino, H. Middendorf, P. Migliardo, A. Musolino, M. Scortino and U. Wanderlingh. "α,α-trehalose-water solutions: an important bioprotective liquid system. Diffusive motions as probed by dynamic light scattering and IQENS". In S. Cusack, Editor, *Biological Macromolecular Dynamics*, 155–159. Adenine Press, (1997).

[24] A. Elbein, "The metabolism of α,α-trehalose", *Adv.Carbohydr.Chem.Biochem.*, **30**, 227–256, (1974).

[25] J. Clegg and M. Filosa, "Trehalose in the cellar slime mould dictyostelium mucoroides", *Nature*, **192**, Nr:4807, 1077–1078, (1981).

[26] K. Madin and J. Crowe, "Anhydrobiosis in nematodes: carbohydrate and lipid metabolism during dehydration", *J.Exp.Zool.*, **193**, 335–342, (1975).

[27] S. Loomis, S. O'Dell and J. Crowe, "Anhydrobiosis in nematodes: control of the synthesis of trehalose during induction", *J.Exp.Zool.*, **221**, 321–330, (1980).

[28] M. H. B. Ltd, Editor. *A Dictionary of Biology.* Oxford University Press, (2000).

[29] A. Rudolph and J. Crowe, "Membrane stabilization during freezing: The role of two natural cryoprotectants, trehalose and proline", *Cryobiology*, **22**, 367–377, (1985).

[30] J. Carpenter, S. Hand, L. Crowe and J. Crowe, "Cryoprotection of phosphofructokinase with organic solutes: Characterisation of enhanced protection in the presence of divalent cations", *Arch.Biochem.Biophys.*, **250**, Nr:2, 505–512, (1986).

[31] J. Carpenter, L. Crowe and J. Crowe, "Stabilization of phosphofructokinase with sugars during freeze-drying: characterisation of enhanced protection in the presence of divalent cations", *Biochim.Biophys.Acta*, **923**, 109–115, (1987).

[32] J. Crowe, J. Carpenter, L. Crowe and T. Anchordoguy, "Are freezing and dehydration similar stress vectors ? A comparison of modes of interacting of stabilizing solutes with biomolecules", *Cryobiology*, **27**, 219–231, (1990).

[33] C. Colaco, S. Sen, M. Thangavelu, S. Pinder and B. Roser, "Extraordinary stability of enzymes dried in trehalose: simplified molecular biology", *Bio/Technology*, **10**, Nr:9, 1007–1011, (1992).

[34] T. Hottiger, C. de Virgilio, M. Hall, T. Boller and A. Wiemken, "The role of trehalose synthesis for the acquisition of thermotolerance in yeast II. Physiological concentrations of trehalose increase the thermal stability of proteins in vitro", *Eur.J.Biochem.*, (1994).

[35] M. Uritani, M. Takai and K. Yoshinaga, "Protective effect of disaccharides on restriction endonucleases during drying under vacuum", *J.Biochem.*, **117**, Nr:4, 774–779, (1995).

[36] L. Crowe, D. Reid and J. Crowe, "Is trehalose special for preserving dry biomaterials?", *Biophys.J.*, **71**, 2087–2093, (1996).

[37] S. Rossi, M. Buera, S. Moreno and J. Chirife, "Stabilization of the restriction enzyme EcoRI dried with trehalose and other selected glass-forming solutes", *Biotechnol.Prog.*, **13**, 609–616, (1997).

[38] M. Sola-Penna and J. Meyer-Fernandes, "Stabilization against thermal inactivation promoted by sugars on enzyme structure and function : Why is trehalose more effective than other sugars?", *Arch. Biochem.Biophys.*, **360**, 10–14, (1998).

[39] R. Bieganski, A. Fowler, J. Morgan and M. Toner, "Stabilization of active recombinant retroviruses in an amorphous dry state with trehalose", *Biotechnol. Prog.*, **14**, 615–620, (1998).

[40] J. Crowe, L. Crowe and S. Jackson, "Preservation of structural and functional activity in lyophilized sacoplasmic reticulum", *Arch. Biochem.Biophys.*, **220**, Nr:2, 447–484, (1983).

[41] J. Crowe, L. Crowe and D. Chapman, "Infrared spectroscopic studies on interactions of water and carbohydrates with a biological membrane", *Arch.Biochem.Biophys.*, **232**, Nr:1, 400–407, (1984).

[42] D. Johnston, E. Coppard, G. Valencia Parera and D. Chapman, "Langmuir film balance studys of the interactions between carbohydrates and phospholipid monolayers", *Biochemistry*, **23**, 6912–6919, (1984).

[43] L. Crowe, J. Crowe, A. Rudolph, C. Womersley and L. Appel, "Preservation of freeze-dried liposomes by trehalose", *Arch. Biochem.Biophys.*, **242**, Nr:1, 240–247, (1985).

[44] R. Mouradian, C. Womersley, L. Crowe and Crowe.J.H., "Degradation of functional integrity during long-term storage of a freese-dried biological membrane", *Cryobiology*, **22**, 119–127, (1985).

[45] E. Arnett, N. Harvey and E. Johnson, "No phospholipid monolayer-sugar interactions", *Biochemistry*, **25**, 5239–5242, (1986).

[46] I. Chandrasekhar and B. Gaber, "Stabilization of the bio-membrane by small molecules: interaction of trehalose with the phospholipid bilayer", *J.Biomol.Struct.Dyn.*, **5**, Nr:6, 1163–1171, (1988).

[47] T. Tsvetkov, L. Tsonev, N. Tsvetkova, R. Konynova and B. Tenchov, "Effect of trehalose on the phase properties of hydrated and lyophilized dipalmitoylphosphatidylcholine multilayers", *Cryobiology*, **26**, 162–169, (1989).

[48] T. Nishiwaki, M. Sakurai, Y. Inoue, R. Chujo and S. Kobayashi, "Increasing packing density of hydrated dipalmitoylphosphatidylcholine unilamellar vesicles induced by trehalose", *Chem.Letters*, 1841–1844, (1990).

[49] M. Nakagaki, H. Nagase and H. Ueda, "Stabilization of the lamellar structure of phosphatidycholine by complex formation with trehalose", *J.Membr.Science*, **73**, 173–180, (1992).

[50] P. Belton and A. Gil, "IR and Raman spectroscopy studies of the interaction of trehalose with hen egg white lysozyme", *Biopolymers*, **34**, 957–961, (1994).

[51] C. de Virgilio, T. Hottiger, J. Dominguez, T. Boller and A. Wiemken, "The role of trehalose synthesis for the acquisition of thermotolerance in yeast I. Genetic evidence that trehalose is a thermoprotectant", *Eur.J.Biochem.*, **219**, 179–186, (1994).

[52] M. Sakurai, H. Kawai, Y. Inoue, A. Hino and S. Kobayashi, "Effects of trehalose on the water structure in yeast cells as studied by in vivo ^{1}H-NMR Spectroscopy", *Bull. Chem. Soc. Jpn.*, **68**, 3621–3627, (1995).

[53] S. Hagen, J. Hofrichter and W. Eaton, "Protein reaction kinetics in a room-temperature glass", *Science*, **269**, 959–962, (1995).

[54] S. Hagen, J. Hofrichter and W. Eaton, "Geminate rebinding and conformational dynamics of myoglobin embedded in a glass at room temperature", *J.Phys.Chem*, **100**, Nr:29, 12008–12021, (1996).

[55] D. Gottfried, E. Peterson, A. Sheikh, J. Wang, M. Yang and J. Friedman, "Evidence for damped hemoglobin dynamics in a room temperature trehalose glass", *J.Phys.Chem.*, **100**, Nr:29, 12034–12042, (1996).

[56] G. Sastry and N. Agmon, "Trehalose prevents myoglobin collapse and preserves its internal mobility", *Biochemistry*, **36**, 7097–7108, (1997).

[57] H. Takahasi, H. Ohmae and I. Hatta, "Trehalose-induced destabilization of interdigitated gel phase in dihexadecylphosphatidycholine", *Biophys.J.*, **73**, 3030–3038, (1997).

[58] M. Adler and G. Lee, "Stability and surface activity of lactate dehydrogenase in spray-dried trehalose", *J. Pharm. Sci.*, **88**, Nr:2, 199–208, (1998).

[59] W. Sun and P. Davidson, "Protein inactivation in amorphous sucrose and trehalose matrices: effects of phase separation and crystallization", *Biochim.Biophys.Acta*, **1425**, 235–244, (1998).

[60] L. Cordone, P. Galajda, E. Vitrano, A. Gassmann, A. Ostermann and F. Parak, "A reduction of protein specific motions in co-ligated myoglobin embedded in a trehalose glass", *Eur. Biophys.J.*, **27**, 173–176, (1998).

[61] D. Lopes, J. Meyer-Fernandes and M. Sola-Penna, "Effects of trehalose and ethanol on yeast cytosolic pyrophosphate", *Z. Naturforsch.*, **54c**, 186–190, (1999).

[62] S. Wera, E. De Schriver, I. Geyskens, S. Nwaka and J. Thevelein, "Opposite roles of trehalose activity in heat-shock recovery and heat-shock survival in *saccharomyces cerevisae*", *Biochem. L.*, **343**, 624–626, (1999).

[63] P. Mariani, F. Rustichelli, L. Saturni and L. Cordone, "Stabilization of the monoolein Pn3m cubic structure on trehalose glasses", *Eur. Biophys. J*, **28**, 294–301, (1999).

[64] F. Librizzi, E. Vitrano and L. Cordone, "Dehydration and crystallization of trehalose and sucrose glasses containing carbonmonoxy-myoglobin", *Biophys. J.*, **76**, 2727–2734, (1999).

[65] A. Bonincontro, E. Bultrini, V. Calandrini, S. Cinelli and G. Onori, "Effect of trehalose on alkine transition of cytochrome-c", *J.Phys.Chem.B*, **104**, 6889–6893, (2000).

[66] B. Murray and H.-J. Liang, "Evidence for conformational stabilization of β-lactoglobulin when dried with trehalose", *Langmuir*, **16**, 6061–6063, (2000).

[67] J. Argüelles, "Physiological roles of trehalose in bacteria and yeast: a comparative analysis", *Arch Microbiol.*, **174**, 217–224, (2000).

[68] J. Schlichter, J. Friedrich, L. Herenyi and J. Fidy, "Trehalose effect on low temperature protein dynamics: fluctuation and relaxation phenomena", *Biophys.J.*, **80**, 2011–2017, (2001).

[69] J. Crowe, M. Whittam, D. Chapman and L. Crowe, "Interactions of phospholipid monolayers with carbohydrates", *Biochim.Biophys.Acta*, **769**, 151–159, (1984).

[70] M. Diehl, W. Doster, W. Petry and H. Schober, "Water-couples low-frequency modes of myoglobin and lysozyme observed by inelastic neutron scattering", *Biophys.J.*, **73**, 2726–2732, (1997).

[71] R. Winter and F. Noll. *Methoden der Biophysikalischen Chemie.* Teubner Studienbücher : Chemie, (1998).

[72] V. Reat, H. Patzelt, M. Ferrand, C. Pfister, D. Oesterhelt and G. Zaccai, "Dynamics of different functional parts of bacteriorhodopsin: H-^2H labeling and neutron scattering", *Proc.Natl.Acad.Sci. USA*, **95**, 4970–4975, (1998).

[73] H. Koch and R. Stuart, "A novel method for specific laballing of carbohydrates with deuterium by catalytic exchange", *Carbohydrate Res.*, **59**, C1–C6, (1977).

[74] H. Koch and R. Stuart, "The catalytic C-deuteration of some carbohydrate derivatives", *Carbohydrate Res.*, **67**, 341–348, (1978).

[75] H. Koch and R. Stuart, "The synthesis of per-C-deuterated D-glucose", *Carbohydrate Res.*, **64**, 127–134, (1978).

[76] G. Chittenden, "A new chemical synthesis of α-α-trehalose", *Carbohydrate Res.*, **9**, 323–326, (1969).

[77] A. de Bruyn, M. Anteunis and G. Verhegge, "^{1}H-NMR study of the di-glucopuranoses in D_2O", *Bull.Soc.Chim.Belg.*, **84**, Nr:7, 721, (1975).

[78] A. Glazer, "Light harvesting by phycobilisomes", *Ann.Rev.Biophys.Biophys.Chem*, **14**, 47–77, (1985).

[79] M. Duerring, G. Schmidt and R. Huber, "Isolation, Crystallization, crystal structure analysis and refinement of constitutive C-Phycocyanin from the chromatically adapting cyanobacterium fremyella diplosiphon at 1.66 Å Resolution", *J.Mol.Biol.*, **217**, 577–592, (1991).

[80] B. Stec, R. Troxler and M. Teeter, "Crystal structure of c-phycocyanin from *cyanidum caldarium* provides a new perspective on phycobilisome assembly", *Biophys.J.*, **76**, 2912–2921, (1999).

[81] T. Schirmer, W. Bode and R. Huber, "Refined three-dimensional structures of two cyanobacterial c-phycocyanins at 2.1 and 2.5 Å resolution", *J.Mol.Biol.*, **196**, 677–695, (1987).

[82] M.-C. Bellissent-Funel, J. Lal, K. Bradley and S. Chen, "Neutron structure factors of in vivo deuterated amorphous protein C-phycocyanin", *Biophys.J.*, **64**, 1542–1549, (1993).

[83] M.-C. Bellissent-Funel, A. Filabozzi and A. Chen, "Dynamics of a deuterated C-phycocyanin protein studied by coherent inelastic neutron scattering", *Biological Macromolecular Dynamics*, 143–146, (1996).

[84] M.-C. Bellissent-Funel, A. Filabozzi and Chen.S.H., "Measurement of coherent Debye-Waller factor in in vivo deuterated C-phycocyanin by inelastic neutron scattering", *Biophys. J.*, **72**, 1792–1799, (1997).

[85] M.-C. Bellissent-Funel, J. Teixeira, K. Bradley and S. Chen, "Dynamics of hydration water in protein", *J. Phys. I France*, **2**, 995–1001, (1992).

[86] M.-C. Bellissent-Funel, J.-M. Zanotti and S. Chen, "Slow dynamics of water molecules on the surface of a globular protein", *Faraday Discuss.*, **103**, 281–294, (1996).

[87] S. Dellerue, A. Petrescu, J. Smith, A. Longeville and M.-C. Bellissent-Funel, "Collective dynamics of a photosynthetic protein probed by neutron spin-echo spectroscopy and molecular dynamics simulation", *Physica B*, **276-278**, 514–515, (2000).

[88] S. Dellerue and M.-C. Bellissent-Funel, "Relaxational dynamics of water molecules at protein surface", *Chem.Phys.*, **258**, 315–325, (2000).

[89] M. Debreczeny. *Comparison of the rate constants for energy transfer in the light-harvesting protein, C-phycocyanin, calculated from Förster's theory and experimentally measured by time-resolved fluorescence spectroscopy.* PhD Thesis, Lawrence Berkeley Laboratory, University of California, (1994).

[90] G. Squires. *Thermal neutron scattering.* Cambridge University press, (1978).

[91] M. Bée. *Quasielastic neutron scattering.* Adam Hilger, (1988).

[92] L. van Hove, "Correlations in space and time and Born approximation scattering in systems of interactions particles", *Phys.Rev.*, **95**, 249–262, (1954).

[93] ILL. "Yellow Book". technical report, ILL, (2001).

[94] F. Mezei, "Neutron spin echo: a new concept in polarized thermal neutron scattering", *Z.Physik*, **255**, 146–160, (1972).

[95] R. Gähler and R. Golub, "Neutron resonance spin echo, bootstrap method for increasing the effective magnetic field", *J.Phys.France*, (1988).

[96] R. Gähler, R. Golub and T. Keller, "Neutron resonance spin echo - a new tool for high resolution spectroscopy", *Physica B*, (1992).

[97] R. Gähler, R. Golub and T. Keller, "Possible improvements in high resolution spectroscopy", *Physica B*, (1989).

[98] T. Keller, P. Zimmermann, R. Golub and R. Gähler, "Demonstration of a bootstrap method for neutron resonance spin echo (NRSE) spectrometry", *Physica B*, (1990).

[99] M. Köppe, P. Hank, J. Wuttke, W. Petry and R. Gähler, R. amd Kahn, "Performance and future of a neutron resonance spin echo spectrometer", *J.Neutron Research*, **4**, 261–273, (1996).

[100] W. Besenböck, R. Gähler, P. Hank, R. Kahn, M. Köppe, C.-H. de Novion, W. Petry and J. Wuttke, "First scattering experiment on MIEZE: a Fourier transform time-of-flight spectrometer using resonance coils", *J. Neutron Research*, **7**, 65–74, (1998).

[101] M. Köppe, M. Bleuel, R. Gähler, R. Golub, P. Hank, T. Keller, S. Longeville, U. Rauch and J. Wuttke, "Prospects of resonance spin echo", *Physica B*, **266**, 75–86, (1999).

[102] G. Wang and A. Haymet, "Trehalose and other sugar solutions at lower temperature: Modulated differential scanning calorimetry (MDCS", *J.Phys.Chem. B*, **102**, 5341–5347, (1998).

[103] C. Duda and E. Stevens, "Trehalose conformation in aqueous solution from optical rotation", *J.Am.Chem.Soc.*, **112**, 7406–7407, (1990).

[104] M. Sakurai, M. Murata, Y. Inoue, A. Hino and S. Kobayashi, "Molecular-dynamics study of aqueous solution of trehalose and maltose: Implication for the biological function of trehalose", *Bull.Chem.Soc.Jpn.*, **70**, 847–858, (1997).

[105] G. Bonanno, R. Noto and S. Fornili, "Water interaction with α-α-trehalose : molecular dynamics simulation", *J.Chem.Soc.,Faraday Trans.*, **94**, 2755–2762, (1998).

[106] H. Kawai, M. Sakurai, Y. inoue, R. Chujo and S. Kobayashi, "Hydration of oligosaccharides : anomalous hydration ability of trehalose", *Cryobiology*, **29**, 599–606, (1992).

[107] S. Magazu, P. Migliardo, A. Musolino and M. Sciotino, "α,α-trehalose-water solutions. 1. Hydration phenomena and anomalies in the acoustic properties", *J.Phys.Chem.B*, **101**, 2348–2351, (1997).

[108] M. Elias and A. Elias, "Trehalose+water fragile system : properties and glass transition", *J.Mol.Liquids*, **83**, 303–310, (1999).

[109] G. Batta, K. Köver, K. Gervay, M. Hornyak and G. Rpberts, "Temperature dependence of molecular conformation, dynamics, and chemical shift anisotropy of α,α-trehalose in D_2O by NMR-relaxation", *J.Am.Chem.Soc.*, **119**, 1336–1345, (1997).

[110] S. Magazu, G. Maisano, P. Migliardo, E. Tettamanti and V. Villari, "Transport phenomena and anomalous glass-forming behaviour in α,α-trehalose aqueous solutions", *Mol. Physics*, **96**, Nr:3, 381–387, (1999).

[111] C. Branca, S. Magazu, G. Maisano, P. Migliardo and E. Tettamanti, "On the bioprotective effectiveness of trehalose: ultrasonic technique, Raman scattering and NMR investigations", *J. Mol. Structure*, **481-481**, 133–140, (1999).

[112] E. Iannilli, E. Tettamanti, L. Galantini and S. Magazu, "An intagrated quasi-elastic light-scattering, pulse-gradient-spin-echo study on the transport properties of α,α-trehalose, sucrose and maltose deuterium oxide solutions", *J.Phys.Chem*, **105**, 12143–12149, (2001).

[113] S. Magazu, G. Maisano, D. Majolino, P. Migliardo, A. Musolino and V. Villari, "Diffusive properties of α,α-trehalose-water solutions", *Prog. Theor. Ph. Supplement*, **126**, 195–200, (1997).

[114] S. Magazu, G. Maisano, P. Migliardo and V. Villari, "Experimental simulation of macromolecules in trehalose aqueous solutions : A photon correlation spectroscopy study", *J. Chem.Phys.*, **111**, Nr:19, 9086–9092, (1999).

[115] M. Donnamaria, E. Howard and J. Grigera, "Interaction of water with α-α-trehalose in solution ; molecular dynamics simulation approach", *J.Chem.Soc.Faraday Trans.*, **90**, Nr:18, 2731–2735, (1994).

[116] Q. Liu, R. Schmidt, B. Teo, P. Karplus and J. Brady, "Molecular dynamics studies of the hydration of α,α-trehalose", *J.Am.Chem.Soc.*, **119**, Nr:33, 7851–7862, (1997).

[117] A. Engelsen and S. Perez, "Unique similarity of th asymetric trehalose solid-state hydration and the diluted aqueous-solution hydration", *J.Phys.Chem. B*, **104**, 9301–9311, (2000).

[118] S. Magazu, G. Maisano, P. Migliardo, A. Musolino and V. Villari, "Fragile-like behaviour and H-bond interactions of the glass-forming water-trehalose system", *Phil. Magazine B*, **77**, Nr:2, 655–661, (1998).

[119] C. Branca, S. Magazu, G. Maisano and P. Migliardo, "α,α-trehalose-water solutions. 3. Vibrational dynamics studies by inelastic light scattering", *J.Phys.Chem.B*, **103**, 1347–1353, (1999).

[120] S. Magazu, V. Villari, P. Migliardo, G. Maisano and M. Telling, "Diffusive dynamics of water in the presence of homologous disaccharides: a comparative study by quasi elastic neutron scattering. IV.", *J.Phys.Chem.B*, (2001).

[121] C. Branca, S. Magazu, G. Maisano, P. Migliardo, V. Villari and A. Sokolov, "The fragile character and structure-breaker role of α,α-trehalose: viscosity and Raman scattering findings", *J.Phys.: Condens.Matter*, **11**, 3823–3832, (1999).

[122] C. Branca, M. Magazu, G. Maisano, G. Migliardo, P. Migliardo and G. Romeo, "α, α-trehalose/water solutions. 5. Hydration and viscosity in dilute and semidilute disaccharide solutions", *J.Phys.Chem.*, **105**, 10140–10145, (2001).

[123] L. L. B. (CEA/CNRS). "Equipement Experimentaux", (1995).

[124] M.-C. Bellissent-Funel. "privat communications". .

[125] S. Magazu, G. Maisano, H. Middendorf, P. Migliardo, A. Musolino and V. Villari, "α,α-trehalose-water solutions. II. Influence of hydrogen bond connectivity on transport properties", *J.Phys.Chem.B*, **102**, 2060–2063, (1998).

[126] Q. Liu and J. Brady, "Anisotropic solvent structuring in aqueous sugar solutions", *J.Am.Chem.Soc.*, (1996).

[127] G. Palazzo, A. Mallardi, A. Hochkoeppler, L. Cordone and G. Venturoli, "Electron transfer kinetics in photosynthetic reaction centers embedded in trehalose glasses: Trapping of conformational substates at room temperature", *Biophys.J.*, **82**, 1–11, (2002).

[128] R. Austin, K. Beeson, L. Eisenstein and H. Frauenfelder, "Dynamics of ligand binding to myoglobin", *Biochemistry*, **14**, Nr:24, 5355–5373, (1975).

[129] A. Ansari, C. Jones, E. Henry, J. Hofrichter and W. Eaton, "The role of solvent viscosity in the dynamics of protein conformational changes", *Science*, **256**, 1796–1798, (1992).

[130] A. Ansari, C. Jones, E. Henry, J. Hofrichter and W. Eaton, "Conformational relaxation and ligand binding in myoglobin", *Biochemistry*, **33**, 5128–5145, (1994).

[131] F. Librizzi, C. Viappiani, S. Abbruzzetti and L. Cordone, "Residual water modulates the dynamics of the protein and of the external matrix in trehalose coated MbCO: an infrared and flash photolysis study", *J.Chem.Phys.*, **116**, Nr:3, , (2002).

[132] W. Doster, S. Cusack and W. Petry, "Dynamical transition of myoglobin revealed by inelastic neutron scattering", *Nature*, **337**, 754–756, (1989).

[133] G. Zaccai, "How soft is a protein ? A protein dynamic force constant measured by neutron scattering", *Science*, **288**, 1604–1607, (2000).

[134] G. Cottone, L. Cordone and G. Ciccotti, "Molecular dynamics simulation of carboxymyoglobin embedded in a trehalose-water matrix", *Biophys.J.*, **80**, 931–938, (2001).

[135] M.-C. Bellissent-Funel, "Hydration in protein dynamics and function", *J. Mol. liquids*, **84**, 39–52, (2000).